Expression of flavin-containing monooxygenases in the human brain

Marie Antoinette Bootman

A thesis submitted in partial fulfilment for the degree of Doctor of Philosophy in the University of London.

Department of Biochemistry and Molecular Biology
University College London.

July 1999

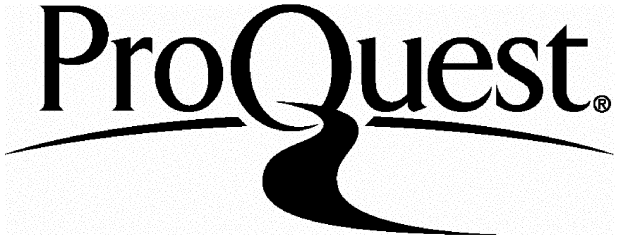

Abstract

Flavin-containing Monooxygenases (FMOs) were found in the human brain *basal-ganglia*, an area affected by neurodegenerative disorders. Full length radiolabelled cDNA probes encoding each of the five known FMOs were used in northern blot hybridisation. FMO3 and FMO4 mRNAs were detected in thalamus, substantia nigra, subthalamic nucleus and corpus callosum regions. *In-situ* hybridisation analysis of brain sections from normal and Parkinson's disease individuals was carried out using cRNA FMO3 and FMO4 probes. Both mRNAs were detected in dopaminergic neurons of the substantia nigra and red nucleus, neurons of the subthalamic nucleus, neurons of the thalamus and pyramidal cells of Ammon's horn. Neither mRNA was found in the crus cerebre, internal capsule or superior colliculus of mid brain, or the internal capsule, putamen, dentate gyrus of the hippocampus. FMO3 was detected in higher levels than FMO4. Immunocytochemistry confirmed FMO3 is present in the same neuronal types as its mRNA. To confirm expression in human brain (and not other cross-reacting FMO mRNAs), RT-PCR of RNA from the thalamus of human subjects was undertaken. Each of the five known FMO DNA sequences were amplified using specific primers. Neither FMO1 or FMO2 sequences were amplified. The PCR product for FMO3 was of the expected size. Restriction digestion analysis and Southern blotting confirmed FMO3 is expressed in human brain. FMO5 gave a positive result which was an RT-PCR of RNA from human subthalamic nucleus. Due to the species difference in FMO expression it was of interest to see if other primates express FMO3 in brain. Substantia nigra, thalamus, midbrain and central brain regions were dissected from Orang-utan and Gorilla brain and RNA prepared. Each FMO sequence was amplified using RT-PCR reactions. No amplification products were observed for FMO1, FMO2 or FMO5. However, FMO3 amplification products were detected and a faint amplification product for FMO4 was observed.

Table of Contents

List of Tables

List of Figures

Abbreviations

1 BnTIQ	1Benzyl tetrahydroisoquinoline
1 MeTIQ	1 Methyl tetrahydroisoquinoline
%	Percentage
°C	Degrees centigrade
3.3X XL Buffer	r*T*th DNA polymerase chain reaction buffer
3-D	Three dimensional
4-PP	4-Phenyl pyridine
Å	Angstroms
α-[^{32}P]-dCTP	Cytosine 5'-triphosphate-[^{32}P]
α-[^{35}S]-UTP	Uridine 5'-[α-thio]triphosphate-[^{35}S]
AP	Alkaline phosphatase
APS	Ammonium peroxodisulphate
ATP	Adenosine triphosphate
Bis	*N,N'*-methylene-bis-acrylamide
bp	Base pairs
BSA	Bovine serum albumin
C	Cytosine
C-6	6-Carbon ring
C-7	7-Carbon ring
$CaCl_2.2H_2O$	Calcium dihydrochloride
CCC	Codon for Proline
cDNA	Complementary DNA
Ci/mmol	Curies per millimolar
CNS	Central nervous system
CO_2	Carbon dioxide
Cpm	Counts per minute
cRNA	Complementary RNA
CTC	Codon for Leucine
D-19	Kodak developer
D_2	Dopamine D2 receptor
DAB	Diaminobenzadine
dATP	Deoxyadenosine triphosphate
dCTP	Deoxycytidine triphosphate
dGTP	Deoxyguanosine triphosphate
DMEM	Dulbecco's minimum essential medium
DMF	Dimethyl formamide
DMSO	Dimethylsulfoxide
DNA	Deoxyribonucleic acid

DNAse	Deoxyribonuclease
dNTP	Deoxynucleoside triphosphate
DTT	Dithiothreitol
dTTP	Deoxythymidine triphosphate
E.*coli*	*Escherichia coli*
e.r.	Endoplasmic reticulum
EDTA	Ethylenediaminetetraacetic acid di-sodium salt
EMEM	Eagles minimum essential medium
FBS	Fetal bovine serum
FMO	Flavin-containing monooxygenase
g	Grams
HCl	Hydrochloric acid
HEPES	*N*-2-hydroxyethylpiperazine-*N*'-2-ethanesulphonic acid
HLFMO-D	Human Liver Form Monooxygenase D
I3C	dietary indole-3-carbinol
IgG	Immunoglobulin G
kb	Kilobase
KCl	Potassium chloride
L	Litre
LB	Luria-Bertani
L-DOPA	L-3-4-dihydroxyphenylalanine
M	Molar
MAO	Monoamine oxidase
MAO-A	Monoamine oxidase A
MAO-B	Monoamine oxidase B
µCi	Microcurie
MFOs	Mixed function oxidases
mg	Milligram
µg	Microgram
$Mg_2(OAc)$	Magnesium acetate
Mg_2Cl	Magnesium chloride
$MgSO_4$	Magnesium sulphate
ML	Millilitre
µl	Microlitre
mM	Millimolar
µM	Micromolar
µmoles	Micromoles
MOPS	3-[*N*-morpholino] propane-sulfonic acid
MPDP	*N*-methyl-1,2,3,6-dihydropyrididium
MPP	*N*-methyl-4-phenylpyridinium

MPTP	*N*-methyl-1,2,3,6-tetrahydropyridine
mRNA	Messenger RNA
MuLV RT	Moloney murine leukemia virus reverse transcriptase
NaCL	Sodium chloride
NADP+	Nicotinamide adenine dinucleotide phosphate
NADPH	Nicotinamide adenine dinucleotide phosphate (reduced)
$NaH_2PO_4.H_2O$	Sodium dihydrogen orthophosphate buffer
NaOH	Sodium hydroxide
NEAA	Non essential amino acids
ng	Nanogram
NH_3	Ammonia
nm	Nanometre
nmoles	Nanomoles
NT2 (Ntera2/D1)	Human teratocarcinoma cell line
NTB-2	Autoradiography emulsion type 2 (Kodak)
OD	Optical density
OH	Hydroxyl group
OPA	One phor all buffer
P450	Cytochrome P450
pB	pBluescript
PBS	Phosphate buffered saline
PCR	Polymerase chain reaction
PFA	Paraformaldehyde
p*I*	Isoelectric point
PK	Proteinase K
pmoles	Picomoles
PMSF	Phenylmethanesulfonylfluoride
PNS	Peripheral nervous system
RNA	Ribonucleic acid
RNAse	Ribonuclease
RP	Random primer
rpm	Revolutions per minute
RQ1	RNA free DNAse
RT	Room temperature
RT-PCR	Reverse transcriptase polymerase chain reaction
r*Tth*	Recombinant Thermus thermophilus DNA polymerase
S	Substrate
SDS	Sodium dodecyl sulphate
SDS-PAGE	Polyacrylamide gel electrophoresis

T3	T3 bacteriophage RNA polymerase specific for T3 promoter
T7	T7 bacteriophage RNA polymerase specific for T7 promoter
TAE	Tris-borate EDTA
TBE	Tris-acetate EDTA
TBS	Tris buffered saline
TE	Tris EDTA
TEMED	*N,N,N',N'*-tetramethylethylenediamine
TIQ	Tetrahydroisoquinoline
Tm^{o}C	Melting temperature
TMA	Trimethylamine
TMANO	Trimethylamine *N*-Oxide
Tris Base	Tris(hydroxymethyl)aminomethane
Tris-HCL	Tris(hydroxymethyl)aminomethane hydrochloride
Triton-x-100	Octyl phenoxy polyethoxyethanol
tRNA	Transfer RNA
TTBS	Tween-20 tris buffered saline
Tween-20	Polyoxyethylene sorbitan monolaurate
TXF	Tamoxifen
U-87 MG cell line	European Collection of Cell Cultures N^{0}:89081402
UV	Ultraviolet
V/V	Volume to volume
W/V	Weight to volume

Acknowledgements

There are a number of people that I wish to thank for their help throughout the duration of this research.

Firstly I would like to thank The Wellcome Trust for awarding me a Toxicology Scholarship, which enabled me to embark upon this programme of research.

I would also like to thank my supervisor, Professor Elizabeth Shephard. Firstly on a professional level for her support and guidence during the course of this research and, secondly, on a personal level for her support and understanding throughout the course of my pregnancy.

I would also like to take the opportunity to give a special thanks to Dr Azara Janmohamed for her continuing support and help.

I wish to thank Anne Kingsbury and Louise Bray at the Parkinson's Disease Brain Bank for their help with histology, and Dr Mina Edwards for her help with tissue culture. I would also like to thank the members of lab 402.

Last but not at all least. I reserve a **big** thanks to my immediate family, *Carl, Hugh and Ellie*, for putting up with me during the course of this research, with its ups and downs, particularly in these last few weeks.

Chapter One

Introduction

Introduction to Metabolism

Metabolism is the physiological process by which living systems are able to procure and utilise the free energy required for inter and intra-cellular chemical reactions while maintaining a steady-state. Living systems are able to maintain this steady-state by metabolic control involving a series of related pathways and enzyme systems.

Metabolism of xenobiotics in mammalian systems can take a number of different routes, including reactions involving, oxidation and reduction, *(N-)* and *(O)* dealkylation, methylation, sulphonation and glucosidation as well as conjugation. Such reactions act to detoxify foreign chemicals leading to their elimination from the organism.

Drug metabolism can be divided into two phases consisting of phase I *functionalisation* reactions, and phase II *conjugative* reactions. However, phase I and phase II reactions do not function independently, but rather represent a system of dynamic interaction in metabolism. Phase I reactions are considered a preparatory stage in drug metabolism, while phase II reactions act as recipients of phase I prepared xenobiotics. Phase II enzymes therefore, are said to represent the "true" chemical pathway for detoxification(**1**). It is thought that the oxidation-reduction, hydrolysis-hydration reactions which are characteristic of phase I activity "functionalises" the drug by either, producing a chemical reactive group or by uncovering such a group so that phase II conjugative reactions can occur. Phase I reactions involve the addition of one atom of oxygen into the substrate, resulting in a more lipophilic structure. This is achieved by exposure of negative, or the creation of reactive, chemical groups such as -OH, -SH, $-NH_2$ and COOH resulting in the compound being in the precise chemical condition to be

manipulated by phase II enzymes. Phase II metabolism in fact therefore, results in the detoxification of drugs and xenobiotics leading to final end products which are largely water soluble and easily excreted. Phase II conjugation reactions involve a range of enzymes and result in the formation of a product that is excreted through the kidneys or in the bile. These reactions tend to have a universal requirement for an activated intermediate either a co-factor such as NADPH or an activated drug.

Both phase I and phase II metabolising enzymes are able to metabolise a variety of substrates, both exogenous (e.g.) drugs, foodstuffs and other foreign chemicals as well as endogenous compounds. Substrates for this liver microsomal oxidative enzyme activity range from organic chemicals as found in foods to therapeutic drugs, such as phenobarbital, clofibrate and phenothiazines **(2, 3, 4)**. Steroid and thyroid hormones, and prostaglandins, are metabolised by phase I enzymes, while phase II enzymes are largely involved in methylation and acetylation of endogenous compounds such as acetylation of serotonin and aminoacid conjugation of bile acids. Phase II enzymes like phase I enzymes, are also involved in the metabolism of many steroids **(5)**. Phase I reactions are catalysed by either mixed function oxidases (MFOs), such as the cytochromes P450 or by flavoproteins like microsomal Flavin-containing Monooxygenases (FMOs) **(6, 7, 8)**. Phase II reactions are catalysed by glutathione transferases, sulfotransferases, and UDP-glucuronyl transferases **(1)**.

Much of the data available on drug metabolism has been gathered from experiments involving liver perfusion, microsomal fractions and hepatocyte cell cultures **(9, 10, 11)**, in conjunction with isolated enzymes. The drug metabolism reactions which have yielded the most data have used the sub-cellular fractions, endoplasmic reticulum (e.r.) and cytosol. Oxidative enzymes involved in phase I metabolism have been located in the e.r. fraction while phase II enzymes, (except UDP-glucuronosyl-transferases), are located in the cytosol **(5)**. Liver microsomes

are one of the major centres for the NADPH-dependent oxidation of xenobiotic compounds (**12**).

MFO's act by consuming one molecule of oxygen for each molecule of substrate utilised. They insert one atom of oxygen into their substrates, while catalysing the reduction of the second atom to water. This addition can lead to further rearrangements and/or decomposition reactions of the first stage product to produce a final phase I product. Monooxygenases as a group have been subdivided into categories which compartmentalise internal and external monooxygenase activity. Monooxygenases are defined as internal if two reducing equivalents from the substrate (SH) are extracted, resulting in the reduction of one atom of the dioxygen to water. External monooxygenases however, comprise those that require the additional support of an external reductant such as NADPH, before any form of reduction can occur. This type of monooxygenase represents the group to which microsomal monooxygenases have been assigned and the basic reaction they catalyse can be represented as follows (**13**) .

$$SH + O_2 + NADPH + H^+ \rightarrow SOH + H_2O + NADP+$$

[where *S* = substrate]

The role of Microsomal Flavin-containing Monooxygenases (FMO) in drug metabolism

Microsomal flavin-containing monooxygenases (FMOs) are a family of enzymes that catalyse the NADPH-dependent oxygenation of nucleophiles such as phosphorus, nitrogen, sulphur and selenium(**14, 15, 16, 17**).The proteins are bound to the endoplasmic reticulum fraction of the cell, and are involved in the oxidative metabolism of xenobiotics, drugs and pesticides(**18**). Evidence shows that these enzymes metabolise a variety of important pharmacologically active compounds such as tricyclic anti-depressants and neuroleptic drugs **(19,20)**. FMOs have a very broad substrate specificity and tissue distribution(**21, 22, 23**).

Mammalian FMOs, like the mixed function monooxygenase system cytochromes P450, are involved in phase I metabolism. However, unlike other phase I monooxygenases, FMOs are the only known mammalian flavoprotein hydroxylases which have the unusual catalytic mechanism that FMOs exhibit. One of the most distinctive features of these enzymes is the order of substrate binding with regard to their catalytic mechanism. The basic chemical reaction governing FMOs can be interpreted as two separate half reactions(**24**) consisting of an initial reductive step whereby the flavin is reduced. This reduction occurs by utilising two electrons from a pyridine nucleotide. The second step can be represented as the oxidative step. Here the reduced flavin ring interacts with oxygen and substrate so as to bring about oxygenation. Characteristic of FMOs is the fact that throughout catalysis the pyridine nucleotide is bound tightly, and released last, in the reaction sequence. From these and other investigations including rapid-reaction kinetics(**25, 26**) all FMOs studied form the C(4α)-hydroperoxyflavin moiety. When substrate is absent, FMOs are able to form a relatively stable C(4α)-hydroperoxyflavin intermediate. The ease at which this occurs means therefore,

that these monooxygenases exist mainly in their reactive hydroperoxide form, where stabilisation of the C(4α)-hydroperoxyflavin results from the binding of NADP. Therefore, in cells, FMO is actually present as the highly reactive C(4α)-hydroperoxyflavin moiety. This means that dioxygen reduction by NADPH is not dependent upon the oxygenatable substrate presence **(27, 28)**. This is in stark contrast to all other monooxygenases comprising of prosthetic groups, including flavin's of the non-phenolic hydroxylase type such as luciferase and those that contain haem **(29)**. The very fact that FMO is present in the cell in its reactive form means that contact between itself and any nucleophile results in the substrate being immediately oxidised **(30)**. The peroxyflavin intermediate is capable of oxygenating nucleophilic compounds including both *N*- and *S*- containing xenobiotics devoid of an anionic group.

Compounds containing an anionic group are excluded from the enzyme's active site. It has been suggested that ionic groups normally found on cellular nucleophiles are the determining force preventing the oxidation of normal physiological cellular nucleophiles **(31, 16)**. This steric constraint effectively serves to inhibit oxidation of endogenous cellular nucleophiles that have more than one negatively charged group and as such prevents their oxidation. This strongly suggests that product formation via substrate reduction requires only transient contact between the hydroperoxyflavin's terminal oxygen and the substrate **(32)**. As a result, this property of FMOs facilitates their ability to catalyse the oxidation of extremely dissimilar compounds, since the energy required to induce metabolism of compounds is already present in the enzyme prior to contact.

Much of the work surrounding the kinetics of FMO catalysis has been carried out using model organic nitrogen and sulphur substrates such as trimethylamine and methimazole respectively. Initial kinetic data suggested that the catalytic

mechanism employed by FMOs was consistent with an ordered Ter-Bi mechanism **(33, 34).** This mechanism essentially establishes that the enzyme uses three substrates in a series of oxido-reduction reactions. Ziegler and Poulson maintain that the organic substrate is added last, while NADPH and oxygen represent the first and second substrates respectively. It can be concluded from analysis of data from a series of substrate binding studies that NADPH reduces the flavin, while in its absence oxygen and the substrate are unable to interact with the flavoprotein. Spectral studies by Ball and Bruice **(28)**, confirm the role of molecular oxygen in the catalytic process. They demonstrated that in the absence of substrate, and when in its reduced state, the flavoprotein monooxygenase reacts with oxygen to form an enzyme bound 4α-hydroperoxyflavin. The catalytic mechanism of FMO is given in figure 1.**(35).**

While for the FMOs, the more basic amines are the preferred substrates **(36)**, less basic amines are predominately metabolised by enzymes of the MFO system such as the cytochrome P450 monooxygenases **(37, 38)**. For example cytochrome P450 catalyses the *C*-oxidation of amines while the action of NADPH-dependent cytochrome P450-reductase results in *N*-dealkylation **(39)**. Studies using crude tissue preparations treated with organic nitrogen and sulphur nucleophiles showed that differences between known FMO isoforms and their subsequent metabolism of a substrate, resides in access to the 4α-hydroperoxyflavin **(40)**. It seems that the overall size of the substrate nucleophile is the predominant factor which determines accessibility to the 4α-hydroperoxyflavin **(41)**. Using five thiocarbamide analogues, with different surface areas, Guo *et al* (1992) found that the oxidation of these chemically synthesized analogues within different tissues, and between different species, demonstrated a dependency upon substrate size **(42)**

For example, rat liver, rat kidney and rabbit liver microsomes could not catalyse the oxidation of thiocarbamides larger than 1,3-diphenylthiourea. Rabbit lung

microsomes only catalysed the oxidation of substrates smaller than 1,3-diphenylthiourea. However, chicken, pig and guinea pig microsomes were able to oxidise larger thiocarbamides. This variation between microsomes, isolated from different species and different tissues, can be explained by the differential FMO species patterns of expression **(43-50)**, (see later).

FMO isoforms are capable of metabolising small substrates such as *N,N*-dimethylamine or methimazole **(51)**, (figure 2), while larger substrates, such as phenylthiourea are unable to form a point of contact with all FMOs **(52,53)**. More evidence has emerged which confirms the specificities of FMO as being partly substrate-size dependent amongst species and between tissues, and this has been a major contributory factor in the early definition of isoforms. For example, while FMO form A (now known as FMO 1) catalyses the oxidation of the five thiocarbamides; thiourea, phenylthiourea, 1,3-diphenylthiourea, 1,3-bis-(3,4-dichlorophenyl)-2-thiourea and 1,1-dibenzyl-3-phenyl-2-thiourea, FMO E (now known as FMO4), will only metabolise substrates which are smaller than phenylthiourea **(54)**. Similarly, Poulson *et al* **(53),** established that rabbit and rat isoforms D and E (now known as FMO 3 and 4 respectively) will not metabolise 1,3,-diphenylthiourea, and are inefficient in the *N*-oxygenation of impramine, and other tricyclics. It seems that in these compounds the side-chain nitrogen is within 3 Å of the tricyclic ring system, near to the nucleophilic heteroatom, which appears to be the optimal distance for substrate metabolism. However, more recent studies of a human liver HLFMO-D, (now known as human FMO 3), has demonstrated that when this protein is expressed in bacteria its substrates were tertiary amines such as chlorpromazine but not imipramine **(55)**. Tricylics are good models for use in assessing monooxygenase activity. These compounds have a tertiary amine centre which is selectively *N*-oxygenated by FMOs **(56)**. Tricylics act by inhibiting the cellular re-uptake of amines. A distinction to make between tricylics like chlorpromazine and imipramine is that while the former is a

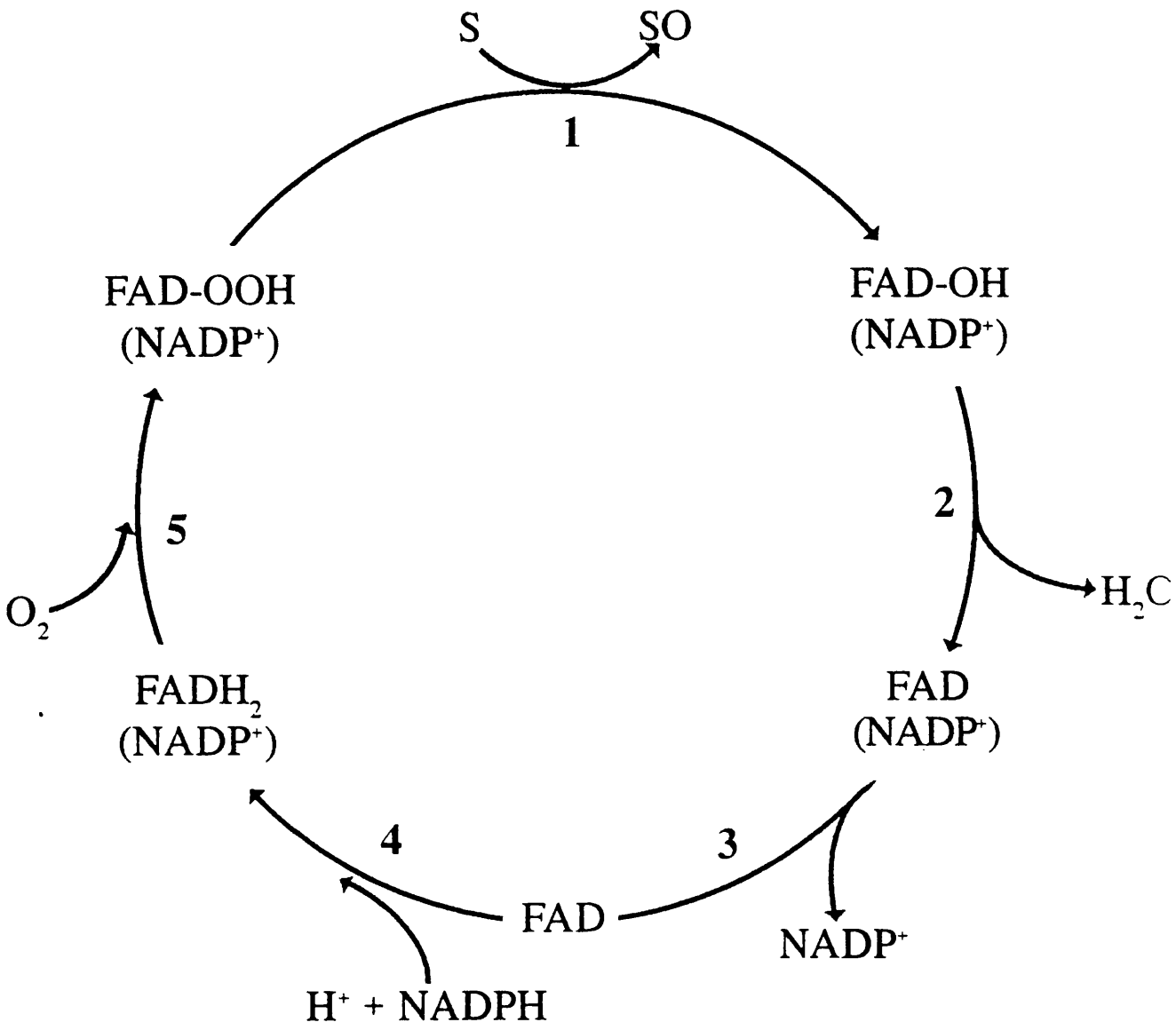

Figure 1.1 Catalytic cycle of FMO. Step 1. consists of a nucleophilic attack by the substrate (S) on the terminal oxygen of the hydroperoxyflavin (FAD-OOH) to produce formation of the oxygenated product (FAD-OH). Step 2. produces the heterolytic cleavage of the peroxide, and release of H_20. NADP+ is then released (Step 3). The flavin (FAD) is now reduced by NADPH (step4) to produce $FADH_2$, before oxygen is added (step 5) thus completing the cycle by regenerating the enzyme bound oxygenating agent. (see text for details).

neuroleptic, essentially anti-psychotic drug, imipramine is an anti-depressant. FMO mediated drug metabolism has been associated with a number of diverse substrates ranging from primary and tertiary amines including imipramine and chlorpromazine **(19,20)** to substrates such as dimethylaniline **(56,19,48)**.

Experimental work by Lomri *et al* **(54)** using substituted phenothiazines as substrates for pig liver FMO-A (FMO1), rabbit pulmonary FMO (FMO2) and human liver HLFMO-D (FMO3), determined (like Guo *et al* previously) that substrate size conditioned FMO activity. It was found that pig liver (FMO1) catalyses the *N*-oxygenation of secondary and tertiary amines, while (FMO3) from guinea pig liver *N*-oxygenates primary aliphatic alkylamines as well as secondary and tertiary amines. All the substituted phenothiazines in their studies proved to be substrates for pig liver (FMO1), while for rabbit pulmonary (FMO2), only phenothiazine tertiary amines with C-6 and C-7 alkyl side chains were confirmed as substrates. The fact that the rate of substrate catalysis and the ability of different isoforms to metabolise different substrates decreases in proportion to increasing substrate size, seems to be linked to the hydroperoxyflavin of the active site of different FMO species. Lomri has shown that the active site of the 4α-hydroperoxy form of mammalian FMOs, such as in rabbit lung FMO (FMO2), resides 6-8 Å below the surface of the enzymes substrate binding channel. In pig liver (FMO1) however, the binding channel is more open. As such pig liver (FMO1) admits larger substrates. Similarly, in human liver (FMO3) the substrate binding channel which leads to the active site hydroperoxyflavin is much more restricted. Therefore larger substrates like imipramine are not admitted to the active site and so *N*-oxygenation does not appear to occur. Differences in the catalytic properties of FMO have been observed between a number of species. For instance it has been shown that rabbit FMO1 is capable of metabolising imipramine and chlorpromazine and is activated by primary aliphatic amines **(40)**.

Dimethylaniline

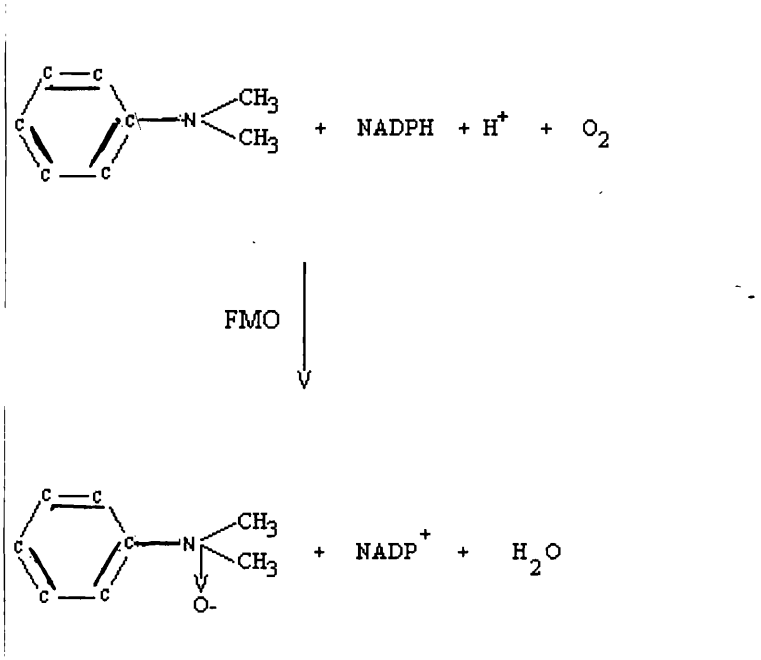

Figure 1.2a. FMO metabolism of model substrate *N,N,*-Dimethylaniline. Oxygenation occurs at the -*N* position.

Methimazole

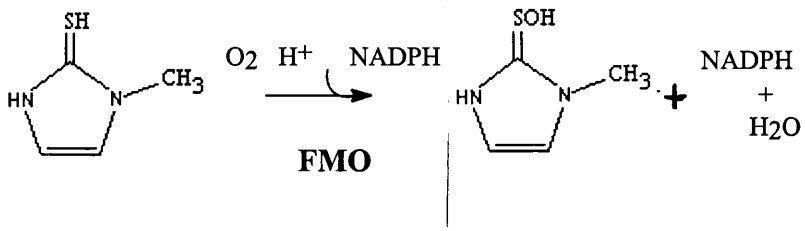

Figure 1.2b. Structure of FMO model substrate methimazole. Oxygenation takes place at the -*S*H site.

FMO2 however, is unable to metabolise chlorpromazine and imipramine but does metabolise primary aliphatic amines, as does FMO1, such as *n*-octylamine. Again, differences in isozyme behaviour between different species is evident, where it is suggested that FMO3 has a lower affinity for chlorpromazine than FMO1 **(40)**, but a greater affinity for primary amines **(56)**. These differences seem to suggest that metabolism of primary amines is species specific representing a species conditioned relationship in the metabolism of primary amines and the activities of FMO isoforms **(41)**.

Chlorpromazine:

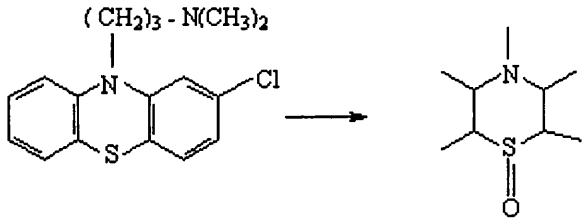

Imipramine:

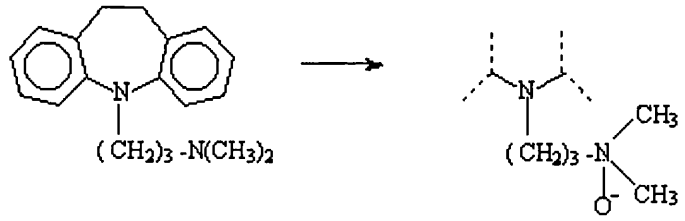

Figure 1.3. Structure of therapeutic type Phenothiazines: chlorpromazine and imipramine both of which are substrates for FMO. Chlorpromazine undergoes *S*-oxidation , while imipramine undergoes *N*-oxidation.

Regulation of FMO gene expression

It has been shown that FMO exists in multiple forms in mammalian tissues(**49, 50, 53,57,58**).Early work by Philpot *et al* **(6)** and Poulson *et al* **(33)** had suggested the possibility of multiple forms of FMO. Using the rabbit as a model Ozols *et al* were able to establish that there are multiple forms of FMO enzyme in this species(**59, 60**). This was confirmed by screening cDNA libraries of rabbit liver where a number of cDNA sequences were isolated, one of which encoded a protein of 533 aminoacids(**59**). Each cDNA encoded proteins containing putative pyrophosphate binding domains (**61**). The finding that a number of distinct forms of FMO exist revealed that FMO constitutes a small gene family (see table 1).

The studies relating to expression patterns of FMOs in a number of different species, have suggested that the level and rate at which FMO expression occurs is determined by particular physiological conditions (**62, 63**). In mammals, although FMO, unlike P450s, is considered to be un-inducible by foreign chemicals, there is evidence to suggest that FMO activity is affected by developmental and hormonal changes(**64, 65, 66**). Early studies showed that changes occured in the activity of FMO when test animals were subjected to hormonal stimulation and/or repression(**67, 68, 69, 70**).For example Coecke *et al* **(71)** have found that differences in FMO expression exist in the rat in relation to gender. Using a primary hepatocyte cell culture system, Coecke *et al* are able to demonstrate that males show a higher activity in hepatic expression of FMO than females. This work suggests that the male / female differences observed are a product of steroid hormonal activity, in particular the role of testosterone and 17-β-estradiol. This group has found that administration of sex hormone 17-β-estradiol to gonadectomized rats at birth lead to a 50% inhibition of FMO activity. However, the administration of the male sex

New Nomenclature Protein & mRNA / Genes & cDNA		Previous Nomenclatures of FMOs amongst different species
FMO 1	*FMO 1*	Pig liver FMO and orthologs in Rabbit [FMO 1A1 or form 1], Human [FMO 1], Rat [RFMO1]
FMO 2	*FMO 2*	Rabbit lung FMO1B1 and its orthologs in Guinea-pig [FMO 1B1]
FMO 3	*FMO 3*	FMO form 2 [FMO 1D1]from Rabbit liver and its orthologs in Humans [HLFMO II] / [FMO 3]
FMO 4	*FMO 4*	Human FMO 2 and its orthologs in Rabbit [FMO 1E1]
FMO 5	*FMO 5*	FMO 1C1 from Rabbit [also known as FMO 3]

Table 1. FMO Isoforms within the mammalian species. Adapted from M P Lawton 1994

hormone testosterone, had no discernable effect on FMO activity. This clearly indicates a gender-dependent modulation of FMO in rats which seems to be primarily determined at the neonatal period of development. Hormonal regulation/induction of FMO in rabbits has also been noted. Lee *et al* **(61)** have demonstrated that FMO in rabbit is under the control of both developmental and hormonal constraints. Using pregnant rabbits this group has found that there are increased levels of FMO1 and FMO2 protein in rabbit liver and lung respectively, in mid to late gestation. Their research suggests that expression of FMO1 and 2 during development is both gender and tissue dependent. They also show that administration of the steroid hormones progesterone, and dexamethasone, leads to induction of FMO2 **(67)**. In pregnant rabbits FMO2 protein was induced in maternal lung, increasing with increased gestational time, sharply decreasing at postpartum to levels found in non-pregnant rabbits. Although progesterone levels were high throughout the pregnancy reaching their peak at day 15 of pregnancy, plasma cortisol levels peaked at day 31. This suggests that both these steroids have a role in the induction of pulmonary FMO2. Lee *et al* **(61)** also conclude that during late pregnancy and postpartum, FMO1 is induced in rabbit liver by progesterone and cortisol, suggesting that the timing of this surge corresponds to initiation of parturition, thus implicating this hormone in the late induction of liver FMO1. This evidence suggests therefore, that FMO may well be modulated to a certain degree by endogenous factors. Differences in the concentration and enzyme activity of FMO for males and females has been noted in rats, mice and rabbits **(71, 72, 73)**. The difference here seems to be related to the down regulation of FMO via testosterone **(72, 74, 75)**. Also it has been demonstrated, in studies using rabbit as a model, that in late gestation, hormonal changes lead to an increase of FMO activity in lung but not in liver **(76, 77)**. Research relating to nutritional status and FMO activity have implicated diet in the observed changes in FMO activity. Lack of ascorbic acid in the diet of guinea pigs has been shown to lead to a 50%+ reduction in the activity of liver FMO **(72,73)**. A similar loss of FMO activity in rat liver has also been noted for rats on modified diets **(80,81)**. Similarly, work by Larsen-Su *et al* **(82)** has shown that

in the rat, FMO expression and activity is inhibited by the administration of dietary indole-3-carbinol (I3C). Treatment of male rats with I3C leads to induction of hepatic levels of cytochromes P450 CYP1A1 and CYP1A2, CYP2B1/2, and CYP3A1/2 as well as resulting in a alteration of steroid metabolism. However FMO1, in rat liver and intestine, is completely inhibited resulting in an 8-fold reduction in expression of FMO. I3C has recently been found to be a cancer preventative agent and is undergoing human trials for use in oestrogen-related cancers. As such, given its effect on an important metabolising enzyme system, its use could have unforeseen consequences within mammalian metabolism. However, this area is still largely unclear, unlike the now established hormonal conditioning and modulation of FMO.

Much of the work characterising FMO expression has been carried out using rabbit lung and liver **(83-86, 21, 23, 35).**There are differences in the expression pattern of FMO isoforms in liver and lung between different species **(87, 88).** Differences were initially identified by Devereux *et al* (1977) **(87)**, in relation to the activity of FMOs, and were further established by Williams *et al* **(86).** The evidence cited by Williams *et al* and others**(83, 87, 21)**acknowledges the fact that differences in FMO function, exhibited amongst different tissues for example pulmonary and hepatic, are not just a factor of enzyme concentration, however, but are a consequence of tissue specific expression of FMOs. Likewise, FMO expression in the same tissue type but of a different species may well be a consequence of species dependent FMO expression **(89, 87).** Studies have been able to distinguish between the different isoforms of the enzyme so that a clear picture of mammalian FMO expression can be seen **(88, 89, 56)**,(tables2a/2b).

FMO	Kidney	Liver	Lung
FMO 1	+++	++	-
FMO 2	-	-	-
FMO 3	-	+	+
FMO 4	constitutive	constitutive	constitutive
FMO 5	-	-	-

Table 2a. Tissue distribution of human FMO mRNAs (Foetal)

FMO	*Brain	Intestine	Kidney	Liver	Lung	Placenta	Skin
FMO 1	-	++	+++		-	-	++
FMO 2	-	-	-	-	+++	+++	+
FMO 3	++	-	+	+++	+	-	++
FMO 4	constitutive	constitutive	constitutive	constitutive	constitutive	constitutive	constitutive
FMO 5	-	-	-	++	-	-	+++

Table 2b. Tissue distribution of human FMO mRNAs (Adult) *[refers to unpublished work] (+) represents relative abundance of FMOs. Constitutive represents basal level in cells (i.e.) low level expression in all above tissue types.

FMO proteins have now been isolated, purified and sequenced from a number of different species. Five distinct forms have been determined in rabbit and man(**45, 46, 47**).As a consequence of this, data have been gained regarding aminoacid similarity, molecular weight comparison substrate and catalytic specificities and mammalian species similarities between the FMOs (**90, 91, 92**) (see tables 3 and 4). As such a systematic nomenclature of naming these genes of FMO has been determined (see table 1).

SPECIES	FMO 1	FMO 2	FMO 3	FMO 4	FMO 5
Guinea Pig		86 %			
Pig	88 %				
Rabbit	86 %	87 %	83 %	84 %	85 %
Rat	82 %				
Mouse	83 %		82%		84 %

Table 3. Percentage identity between the amino acid sequence of FMOs from various species in relation to humans. Adapted from Phillips *et al* (44) and Falls *et al* (105)

	FMO 1	FMO 2	FMO 3	FMO 4	FMO 5
Molecular weight	60306	60903	60047	63338	60225
Number of amino acids	532	535	532	558	533
p*I*	6.9	8.9	8.3	9.1	8.6

Table 4. Physical characteristics of the Human FMO protein family

The Flavin Containing Monooxygenase Family

FMO1

FMO1 was initially purified from pig liver by Ziegler *et al* **(16)** and was shown to catalyse the NADPH oxygenation of the model substrates methimazole and dimethylaniline **(92,93)**. The sequencing of a rabbit FMO1 by Ozols **(94)** indicated a number of similarities with FMO1 cDNA isolated from pig liver by Gasser *et al* **(46).** The two FMO1 sequences have an 87% amino acid sequence similarity **(43)**. The interspecies tissue distribution patterns of FMO1 orthologues are different. Where FMO1 has been shown to be present in the liver and kidney of mammals such as pig and rabbit **(91,39,41,43)**. In humans, FMO1 seems to be predominately expressed in foetal liver, but not to any significant level in the adult liver. It is also expressed in adult kidney. This between species difference in hepatic expression is significant. The reason for FMO1 expression during early development, in human liver is not known. FMO may have different roles to play in relation to gross physiological development as well as more specific cell based expression **(95)**. Studies on the rabbit *FMO1* gene have determined that it comprises 9 exons and 8 introns **(96)**. The 5' flanking sequence of the rabbit *FMO1* gene carries a consensus sequence for a glucocorticoid response element **(97,70)**. This supports evidence for involvement of hormones in the modulation of FMO1 expression.

FMO2

FMO2 was initially isolated from rabbit lung **(95,21)** where it has been shown to be expressed at high levels and has subsequently come to be recognised as the major lung form of rabbit FMO. In terms of comparisons with FMO1, it has been demonstrated that rabbit FMO2 shows variation from FMO1 in both its substrate specificity and activities **(21,41,98)**. Evidence suggests that FMO1 *N*-

oxygenates tertiary amines with short side chains such as phenothiazines **(55)**. In contrast however, FMO2 tends to be involved in the metabolism of primary amines **(41)**. These differences are largely indicative of variation in the accessibility to the enzymes' active site. Indeed, studies have shown that differences between FMO1 and FMO2 isoforms in terms of substrate specificity lies within the size of their respective binding channels **(32)**.

In humans, Dolphin e*t al* **(99)** have shown that FMO2 can be detected at the mRNA level, but it is not expressed at the protein level. FMO2 in humans carries a mutation which gives a truncated protein. This suggests that FMO2 mRNA may be producing a non-functional protein in humans, but not necessarily in other primates. Evidence from Yueh *et al* **(100)** detected an FMO in adult rhesus macaque lung and liver that cross reacts with a rabbit FMO2 antibody and which has a similar expression pattern to rabbit FMO2. FMO2 in rabbit is fully functional and its expression is regulated on the basis of age and sex **(101)**. This group have found that rabbit FMO2 protein and mRNA are expressed in rabbit fetal and neo-natal lung, indicating, they suggest, that FMO2 may be involved in the protection of the fetus and neonate from toxic chemicals.

FMO3

The FMO3 isoform is the most highly characterised of the FMO family so far. Initial data regarding FMO3 was provided through work by Ozols **(102,49)** using the rabbit as a model and by Lomri *et al* **(53)** and Burnett *et al* **(76)** who isolated a human FMO3 cDNA. FMO3 is thought to be the major isoform expressed in human liver **(42,44,54)**. Rabbit and human FMO3 share an amino acid sequence similarity of approximately 80%. Each of the FMO3 orthologues consists of 533 amino acid residues, with an approximate molecular mass of 60000 Daltons. While FMO3 is the predominant form in human liver, in other species FMO1 is the predominant liver form expressed. It is thought that

hepatic FMO3 is involved in the detoxification of nucleophilic heteroatom-containing chemicals. These compounds from exogenous sources for example, diet or xenobiotic chemicals, are altered by FMO3 to a more polar lipophilic oxygenated metabolite that is easily excreted. FMO3 cDNA has been expressed in several expression systems. The expressed protein metabolises primary and tertiary amines **(103,104)**.

In the case of mice regulation of FMO3 expression is controlled differently between the sexes **(105)**. Studies have shown that hepatic expression of FMO3 isoform in the male mouse is under hormonal control **(74,75,78)**, while its expression in the lung is not **(105)**. In addition Falls *et al* (1997) showed that adult male mouse liver does not actually express FMO3, but does express high levels of FMO1 **(69)**.

Recent studies on FMO3 and FMO5 using liver microsomal extracts and monospecific antibodies have suggested that the concentration of FMO3 isoform in adult human liver is greater than FMO5 **(106)**. *S*-oxidation of the model substrate methimazole by liver microsomes was entirely due to FMO3. FMO5 exhibits little, if any, activity towards methimazole.

FMO4

FMO4 was initially isolated by Dolphin *et al* **(107)** and found to have 52% identity with other members of the FMO family. Both rabbit and human FMO4 are different from the remaining FMO isoforms in a number of important ways. For instance, the predicted molecular mass of the protein is 63000 Daltons encoding a protein of 558 amino acids in length. This represents an increase of 25 amino acid residues in relation to the other isoforms **(108,56)** (see table 3). FMO4 mRNA has been detected in adult human liver but at very low levels. Protein expression however, has not so far been detected due to the

lack of an antibody. Although FMOs have been expressed in a number of different heterologous systems, little success has been achieved with FMO4 expression **(109,110)**. It seems that the tertiary structure of FMO4 contains a sequence adjacent to the upstream start codon which tends to inhibit translation initiation. Generally the sequence ACCATGG is most favoured for translation initiation and as such is found in most vertebrate mRNA sequences. The sequence that Dolphin *et al* found was TNNATG **(107)**. This is interesting as it is a sequence which is known to be "associated" with the presence of start codons located upstream which are non-functioning. The continuing inability to express functional FMO4 has led to difficulties in characterising the isoform. Experimental work conducted with both rabbit and human orthologues has given inconsistent results, and although FMO4 for each of these species has been cloned and sequenced, expression of the isoform remains difficult **(44,58)**. It seems that only by modification of FMO4 so that a stop codon is introduced, 81 bases to the 5'end of its original position, can expression be achieved. Using this shortened version of FMO4, Itagaki *et al* **(111)** have been able to express a fully functional enzyme. Why this difference in expression in FMO4 occurs is unknown at present and as such, remains an active area of research.

FMO5

FMO5 was initially identified in the rabbit by Atta-Asafo Adjei *et al* **(112)** FMO5 shares an amino acid sequence similarity of 55% with other members of the rabbit FMO family. More recently, a human FMO5 cDNA has been isolated and sequenced **(113).** This isoform encodes a protein of 533 amino acids like the rabbit, and shares 82-87% amino acid sequence identity with FMO5. In the rabbit and pig. Evidence suggests that although FMO4 RNA is located in the human adult liver, the major FMOs expressed in adult human liver are FMO3 and FMO5 **(106,114,115)**. FMO5 has only recently been fully

expressed and characterised and like FMO4, FMO5's role in metabolism has yet to be elucidated.

The Human FMO family

cDNA clones encoding five members of the human FMO family have been isolated,**(44, 116, 117).**The deduced amino acid sequences show a similarity of approximately 51% to 57% to each other. However, each of the FMOs has 82% to 87% identity with its orthologous protein in other mammalian species,**(118, 49)** (see table 3). Recently, a sixth FMO sequence (FMO6) has been identified by the Human Genome Sequencing programme **(119)**. All six *FMO* genes have been mapped to the long arm of chromosome1**(120, 46, 44)** and FMOs 1-4 and 6 further located to a position at chromosome 1q23-q24,**(121, 119)**indicative of a gene cluster. FMO5 is located in the region 1q21 **(122, 122a)**. FMOs 1-6 are encoded by single genes. The deduced aminoacid sequences from cDNA clones encoding human FMOs show that FMOs 1, 2, 3 and 5 contain between 532 and 535 amino acid residues, and that these proteins have molecular masses of between 60000 and 61000 Daltons**(123)**. Human FMO 4 however, is slightly longer and contains a further 25 residues at its carboxy terminus**(111)**; FMO 4 thus has an increased relative molecular weight (see table 4) . It has been suggested that a point mutation in the FMO4 stop codon is the cause of the extra carboxy region of this protein. Each FMO has a FAD and a NADPH binding site at the equivalent positions. The putative FAD binding site is located at the *N*-terminus between residues 9-14, while that of NADPH lies between residues 191 and 196 **(123, 47).**

As in other mammalian species it seems that human *FMO* genes exhibit both developmental and tissue-specific expression patterns**(124, 125).** Where expression in different tissues is determined by age**(126)**. For example, FMO1 mRNA is undetectable in adult liver, but is detected in foetal liver **(127)**. The *FMO1* gene is also expressed in foetal and adult kidney **(129)** and in skin **(130)**. FMO2 mRNA has been detected in human adult lung**(99)**. However, although

the mRNA is expressed the protein is not. It seems protein expression is retarded by a sequence variation in the FMO2 coding region Dolphin *et al* (1998). The human FMO2 lacks a 64 aminoacid residue stretch at the carboxy terminus. This truncation occurs at a region corresponding to codon 472. The truncated FMO2 is catalytically inactive due to a C-T transitonal shift at codon 472 which actually produces an in-frame TAG translational termination codon in replace of the CAG codon at similar positions in other FMO4 orthologues such as in the rabbit, rhesus macaque and chimpanzee **(43,58,100)**. Analysis of mRNA which encodes FMO3 shows that it has a low level of expression in foetal liver and lung, as well as in adult kidney and lung **(105)**. However, FMO3 mRNA has been detected at high levels in adult liver. FMO4 mRNA is found only in low abundance in a number of foetal and adult tissues **(127)**, and seems to be expressed constitutively **(111)**, while FMO5 exhibits relatively high levels of expression in adult liver and lung **(113, 127)**. These findings suggest that expression of FMO genes (*FMO1* and *FMO3* in particular), is selectively increased and / or decreased in different tissues during different developmental stages, (see tables 2a and 2b).

Role of FMO in known clinical conditions

Trimethylamine (TMA) is an aliphatic amine and is a chemical compound derived from a variety of foods such as red meat, eggs, soya and fish. TMA is a breakdown product of choline and lecithin. Bacteria in the gut cleave off the TMA grouping which is then transported to the liver for detoxification by FMO3. TMA produces the pungent odour associated with rotting fish. In the liver this compound is rendered odourless through *N*-oxidation by FMO which results in TMA being processed to TMA-*N*-Oxide **(131,132)**. In humans it is FMO3 that is responsible for the conversion of TMA to its *N*-oxide in normal individuals **(133)**. However, when an individual is unable to convert 65% or more of TMA to TMAO they are deemed to suffer from primary Trimethylaminuria, known more colloquially as "fish odour syndrome" **(134,135)**. Characteristically, individuals suffering from this condition excrete un-metabolised TMA in their urine, sweat and other body fluids, producing a fishy odour **(136,137)**. This inevitably produces socio-emotional consequences for the individual which can be devastating **(138)**. Evidence by Al-Waiz *et al* **(137)** suggested that the condition trimethylamininuria is a autosomal recessive genetic response to TMA metabolism. Dolphin *et al* (1997) identified a mutation in the codon sequence in exon 4 of the *FMO3* gene. This changes CCC (proline-153) in normal individuals, to CTC (leucine-153) in individuals suffering from trimethyaminuria **(139)**. This point mutation at position proline-153, leads to a significant reduction in the catalytic activity of FMO3 and so disrupts the *N*-oxygenation of TMA to the inoffensive TMAO. Similar work by Treacy *et al* **(140)** has confirmed FMO3 mutation as the cause of fish odour syndrome. Recent studies have indicated that TMA metabolism to TMAO can be achieved by FMO1, FMO5 and truncated FMO4. However, FMO3 has the greatest turnover rate and a K_M of 28 μmolar providing the most efficient means of TMAO formation, while the other FMOs had turnover rates at least thirty times lower than FMO3 **(141)**. Due to the fact that FMO3 represents the major FMO isoform expressed in adult human liver, carriers of the mutation

may well be unable to metabolise other common FMO3 substrates such as phenothiazines which may result in other as of yet unknown conditions or susceptibilities. The consequences of polymorphisms in the FMO3 gene **(139)**, that may encode proteins with altered activities is also not known.

Recent research has demonstrated the possibility that FMOs perform an important intermediary detoxification role in the metabolism of the antioestrogenic-anticancer drug Tamoxifen (TXF). TXF is a drug used in the treatment of breast cancer and is subject to extensive biotransformation in both rodents and humans **(142)**. It has been suggested that compared with cytochromes P450, FMO may be more involved in the metabolism of TXF than previously thought **(143)**. TXF has a potent anti-oestrogen activity, undergoing metabolism in the liver to its *N*-oxide producing mono-*N*-desmethyl and 4-hydroxy-phenyl intermediates. Mani *et al* **(144)** have demonstrated that the formation of *N*-oxide of TXF in liver microsomes of rat and human is mediated by FMO. However, while formation of mono-*N*-desmethyl and 4-hydroxy-phenyl intermediates seem to be due to the activity of P450 and FMO respectively, this does not represent the final product of TXF metabolism **(144)**. However, unlike TMA metabolism, evidence of a definitive role for FMO in the metabolism of TXF is less clear.

Chapter Two

Flavin containing monooxygenases in the human brain

Role of FMOs in the human brain ?

Of the major organs involved in detoxification, the expression of FMO mRNAs is greatest in the liver, lung and kidney. The brain is a highly specialised organ, which on occasion is exposed to many organic chemicals such as pesticides, the phenothazine based psychoactive drug chlorpromazine and the anti-depressant imipramine. These compounds are known substrates for FMOs. A possible role for FMOs in the brain is the localised metabolism and detoxification of such compounds.

There are five major divisions in the brain: telencephalon, diencephalon, mesencephalon, metencephalon and myelencephalon. The telencephalon (end brain) consists of two cerebral hemispheres which are connected by a large bundle of commissural fibres known as the *corpus callosum*. This forms the largest part of the human brain. Each hemisphere has a thin superficial layer of grey substance heavily folded into *gyri* forming *fissures* and *sulci*, known as the *cerebral cortex*. Within the interior of each cerebral hemisphere lies a cavity referred to as the *lateral ventricle* as well as a large mass of white matter, including several large nuclei known as the *basal ganglia*. The basal ganglia refers to the two telencephalic nuclei, the *caudate* and *lentiform nuclei*, as well as some closely related brainstem nuclei which have a special significance in control of movement. Telencephalic subcortical structures also include the *caudate nucleus* and *putamen* known together as the *striatum* as well as the *amygdaloid body* **(145,146)**.

Basal ganglia refers to the combination of the caudate nucleus, putamen, globus pallidus, subthalamic nucleus and substantia nigra. Bridges of grey matter which stretch across the internal capsule between the putamen and the caudate nucleus in conjunction with the lentiform nucleus, form a loop called the *corpus striatum* **(147)**. The corpus striatum has a major subdivision known as the striatum. The globus pallidus forms the medial part of the lenticular

nucleus and is comprised of an external and internal (lateral and medial) division. The medial part of the globus pallidus is closely connected to the substantia nigra *pars reticulata*. Connections of the basal ganglia and thalamus form a loop-like "circuit" from the cortical areas to the corpus striatum, through the globus palladus via ventral thalamic nuclei and then return to one of the multiple cortical areas. This is an area which is involved in both initiation and control of movement. Thus disease of, or lesions in, the basal ganglia leads to a number of characteristic dysfunctional motor symptoms such as akinesia, rigidity and tremor which accompanies Parkinson's disease and chorea-athetosis of Huntingtons disease as well as Hemiballism **(148,149)**.

It is now known that ventral parts of the basal ganglia are intimately connected with two other basal forebrain systems, that of the basal nucleus of Meynert and the extended amygdala. The basal nucleus of Meynert contains cholinergic neurons projecting into the cerebral cortex which become impaired as a consequence of old age. These overlapping different anatomical systems, in conjunction with other forebrain regions, have been found to be involved in many of the neuropsychiatric disorders such as Alzheimer's disease and schizophrenia. Indeed, the cholinergic neurons of the nucleus of Meynert show extensive loss in innervation of the cortex in Alzheimer's patients, thus implicating this area strongly in this disorder **(150)**. While in the midbrain, basal ganglia damage is associated with Parkinsonian patients. The corpus striatum forms the largest part of the basal ganglia but is unable to affect motor neurons directly. The corpus striatum influences movement by affecting the activity of motor areas of the cerebral cortex through a series of linked processes as outlined above. Thus the only way it is able to play a role in movement control is by influencing one or more of the descending pathways, such as the corticospinal or rubrospinal tracts. As such, the basal ganglia influences movement by influencing output from the cerebral cortex to the brainstem and the spinal cord. Three other categories of connections of the basal ganglia are also involved in affecting movement. The interconnections of the substantia nigra with the striatum, subthalamic nucleus with the globus

pallidus and the thalamic intralaminer nuclei with the corpus striatum. The basal ganglia are informed at all times about most aspects of cortical function. The substantia nigra projects to all areas of the striatum by way of fine axons that use dopamine as their neurotransmitter. Destruction of this nigrostriatal pathway is the major factor causing Parkinsons disease **(151,152)**. Destruction of subthalamic nuclei or lesions herein, leads to pronounced movement disorders such as hemiballism. Movement disorders associated with all basal ganglian nuclei are in fact related to the condition of the subthalamic nucleus. Disturbances in metabolic pathways in the basal ganglia, can disrupt fine movement and control (see figure 2.1). The subthalamic nucleus is pivotal to the smooth functioning of the basal ganglia circuitry. It receives major input from cortical motor areas of the cerebral cortex which itself gives a massive input to the basal ganglia. It also receives major input from the external segment of the globus pallidus, which enables the subthalamic nucleus to influence directly the two output structures of the basal ganglia; that of the internal pallidal segment and the substantia-nigra pars reticular. The reticular part receives inputs from the striatum and subthalamic nucleus. The pigmented neurons of the compact part of the substantia nigra, which use dopamine as their neurotransmitter, project in an organised fashion into the caudate nucleus and putamen. These projections represent dopaminergic endings in the striatum which ultimately determine / modulate the output from the globus pallidus in conjunction with subthalamic activity. Defects in this influence can result in movement disorders such as bradykinesia and hypokinesia. Neurons in the subthalamic nucleus are thought to be glutaminergic and have an excitatory effect on the two basal ganglia output structures (as mentioned above). These two structures in turn have an inhibitory effect in their thalamus and brain stem targets. Damage to the subthalamic nucleus leads to a loss of subthalamic input to the basal ganglia output structures, which results in a dis-inhibition of their thalamic and brain stem targets. Such lack of inhibition of output in these areas is one explanation of the hyperkinetic movements in hemiballismus, and to some extent the involuntary movements in Huntingtons chorea.

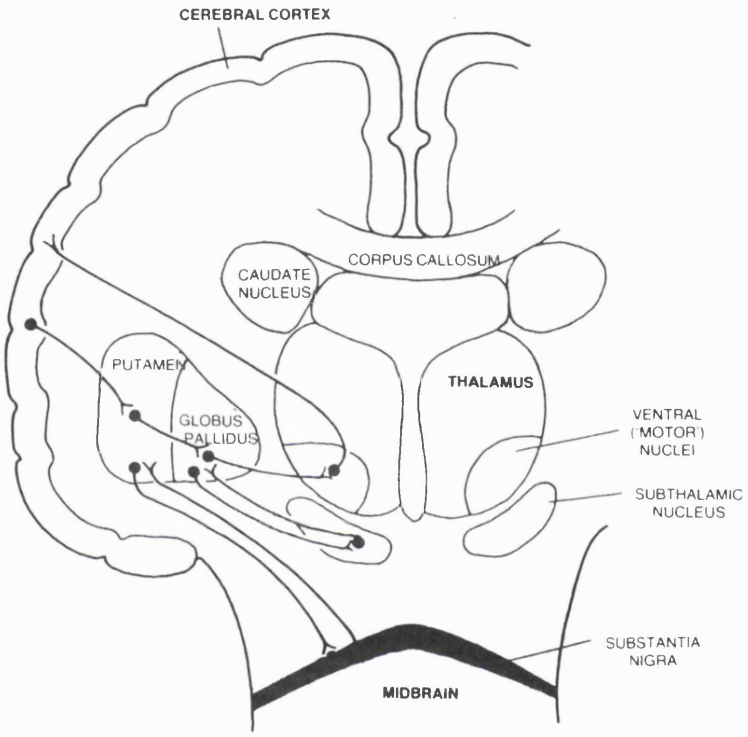

Figure 2.1 Schematic diagram of the brain to show mid brain and basal ganglian regions. Adapted from England and Wakely "A Colour Atlas of the Brain and Spinal Cord".

In Parkinson's disease, inhibition by basal ganglian output structures may be exacerbated by subthalamic action. Experimental evidence has shown that by reducing the excitatory impact from the subthalamic nucleus leads to reduced akinesia in primates with experimental Parkinsons disease **(153,154)**. Removal of dopaminergic input to the striatum, as occurs in Parkinson's disease and hypokinesia, results in increased activity in the subthalamic region (see figure 2.1). Parkinson's disease is a result of the decrease in dopamine levels in the striatum which can occur naturally or as a side effect of drugs that act as antagonists, such as phenothiazines, where it is known as drug-induced Parkinson's disease **(155)**.

FMOs in the brain

FMOs are a family of enzymes responsible for metabolising a wide variety of substrates including a number of theraputic drugs. An important aspect of drug:drug interactions is the effect these exert on enzyme activity. For example, drugs used in the treatment of disruptive psychological, emotional and physiological conditions, which exert their effects on the brain are candidates for *N*-oxygenation by FMO **(156)**. Although there have been some indications of possible FMO presence in mammalian brain such as the rat **(157)**, it is only recently that FMO activity has been confirmed in this tissue. Research of mammalian brain has revealed the presence of FMO and cytochromes P450 in specific areas **(158,159,160,161,162)**. Although cytochromes P450 and the FMOs share a number of common substrates, the metabolism of the substrate can be quite different. For instance in the metabolism of amines, generally cytochromes P450 catalyse the *C*-oxidation while FMOs catalyse the *N*-oxidation and *S*-oxidation of amines **(4,37,39)**. FMO metabolism in relation to the brain is a complex and a largely undefined area of research. It has been reported that FMO activity detected in rat brain using a number of substrates including *N,N*-dimethylaniline and methimazole, was actually higher than that found in the liver **(162,163)**. Similarly, it has been suggested that rat brain microsomes reacted with antisera to rabbit lung FMO and not pig liver FMO **(164,165)**. In terms of FMO activity in human brain the evidence has been contradictory and confusing. For instance, work by Bhagwat *et al* **(166,167)** has suggested that human brain microsomes contain FMO2. These workers used antisera to rabbit lung FMO (FMO2 orthologue in man). However, in man this isoform of FMO is not expressed at the protein level **(168,100)**. The results of Bhamre *et al* have so far not been confirmed by others in the field. Using an RT-PCR approach Blake *et al* (1995)**(168)** detect only FMO4 expression in rabbit brain.

Substrates which are metabolised by FMO include a number of tertiary amines which are known to exert their effects on the brain. One such substrate is *N*-methyl-1,2,3,6-tetrahydropyridine (MPTP) **(169)**. MPTP is a highly selective neurotoxin which has been implicated in the development of a Parkinsonism-like syndrome in humans and primates **(170,171,172,173)**. The neurotoxic effects of this substance are linked to its biotransformation to the dihydropyridium intermediate $MPDP^+$ which is further oxidised to the quaternary amine *N*-methyl-4-phenylpyridinium (MPP^+) by Monoamine oxidase A and B (MAO). MAO is an enzyme which functions primarily to break down endogenous neurotransmitter, and is responsible for the metabolism of endogenous catecholomines. MAO can also metabolise exogenous amines of similar structure and dietary exogenic amines such as tyramine (found in cheese and alcohol) to their corresponding aldehyde. The MAOs are found in the mitochondria of the liver as well as in the mitochondria nerve endings.

Biotransformation of MPTP by MAO can be blocked by the substance 4-phenyl pyridine (4-PP), which is found in peppermint, spearmint and cigarette smoke **(174,175)**. In studies using mice, 4-PP acts as an antagonist to the dopamine depleting effects of MPTP **(175,176)**, and seems to give partial protection. Metabolism of MPTP by liver microsomes results in its *N*-oxidation from MPTP to MPDP **(177)** (see figures 5 and 6). Research by Chiba *et al* **(178)** on mice, revealed that hepatic FMO was the major pathway for metabolism of MPTP. Chiba *et al* **(178)** pre-treated mice with an alternative substrate for the flavin-containing monooxygenase, *N*-methylmercapto-imidazole. Their results showed that this alternate substrate, increases the amount of MPTP delivered from the peripheral nervous system to the CNS. This is assumed to occur via inhibition of MPTP oxygenation mediated via hepatic FMO, because the alternative FMO substrate *N*-methylmercaptoimidazole competes with or is a better substrate than MPTP for FMO in the liver, resulting in its blocking or binding with FMO. The use of this substrate leads to a significant increase in

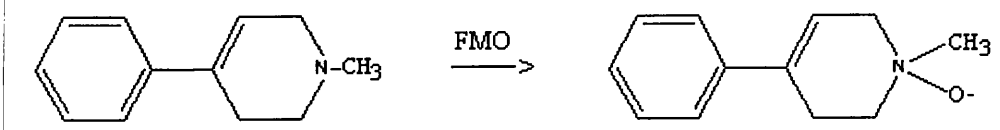

Figure 2.2 MPTP *N*-oxygenation by hepatic FMO. One pathway of metabolism which attenuates the neurotoxic effects of MPTP in the brain by preventing this compound passing through the blood-brain barrier and so breaking the cycle which would otherwise lead to the formation of neurotoxin MPP^+. Other related pathways include cytochrome P450 *N*-demethylation of MPTP to 4-phenyl-1,2,3-6-tetrahydropyridine (PTP) in the liver **(169)**.

MPDP MPP+

Figure 2.3 Intermediate and end products of the biotransformation of MPTP, which occurs in the mitochondria of neurons.

the plasma concentration of MPTP. This suggests that increased metabolism of MPTP by hepatic FMO would attenuate the neurotoxic effects of MPTP by reducing the brain concentration of MPTP available to interact with the monoamine oxidases situated in the brain such as MAO-B. Since the hepatic metabolism of this MPTP seems to be the predominant route for detoxification, it would seem that FMO has, even at this hepatic level, a role in attenuating the neurotoxic effects of MPTP. More recent research by Chiba *et al* **(179)** has confirmed the role of hepatic-form FMO in the mouse brain as a pathway for in-vivo detoxification. Research by Hoe *et al* **(180)** suggests that MPTP-induced neurotoxicity in the rodent is decreased by the presence of dimethylthiourea. Similarly in human and rodent liver, FMO is able to block MPTP induced toxicity in the brain by forming the *N*-oxide of the neurotoxic substrate. MAO inhibition prevents neurotoxicity of MPTP to MPP^+ **(181)**, and it seems that many of the inhibitors of MAO-A and MAO-B are actually substrates for the flavin-containing monooxygenases **(182)**. It seems that inhibitors of MAO-B such as deprenyl can protect against neurotoxicity of MPTP, while MAO-A, although with a lower affinity for MPTP, is inhibited by clorgyline **(183,184)**. Evidence such as this has produced interesting results which show that pretreatment of Parkinson's disease patients with deprenyl is effective in delaying the need to use L-DOPA therapy, which is self limiting **(185,186)**.

Substrates such as deprenyl (selegiline), a tertiary amine is used as a therapeutic agent for the treatment of Parkinson's disease. It would seem that clorgyline and deprenyl together are capable of suppressing OH- radical formation by MPP^+ after biotransformation of the neurotoxin MPTP by MAO-B. This results in retardation of development of idiosyncratic Parkinson's disease, and a retardation in the exacerbation of Parkinson's disease **(187,188)**. These relationships and links regarding substrates and inhibitors for FMO and MAO-B/A would seem to suggest a certain degree of interplay between the respective roles of these enzymes. More research in this area is needed to define whether or not such an interplay exists. Evidence, however, hints at some kind of relationship between these substrates and enzyme systems. Other

substrates involved in neurotoxicity and neurodegenerative symptoms like those caused by MPTP, centre around neuronal cell death in the mitochondria via inhibition of complex I of the electron-transport chain **(189,190)**. Although it is unlikely that FMO in brain is there to metabolise exogenous/xenobiotic toxins by chance, it would seem that the existence of endogenous compounds in the brain leading to the induction of Parkinson's disease by a mechanism similar to that of MPTP exists in the form of tetrahydroisoquinoline (TIQ) **(191,192,193)** see figure 2.4b. These metabolites are present in a specific area of the human brain, the frontal lobe and caudate nucleus in individuals. However, Niwa *et al* **(192)** have shown that methylated tetrahydroisoquinoline in human brain was significantly reduced in concentration in Parkinson's disease patients suggesting that it has a protective role. Recently it has been reported that biosynthesis of the compound TIQ is inhibited by deprenyl **(194)**. Deprenyl it seems, leads to a decrease in the endogenous Parkinson's inducing compound TIQ in rodents **(195)**. In relation to this, it has been reported that mouse FMO1 is able to metabolise TIQ **(196)**. This presents an exciting area of research as it introduces the possibility that FMO does have a "natural" detoxification role in the brain. Clearly, much work is required in this developing area.

The information surrounding FMO and its role in the brain, specifically the human brain, follows a central theme of inhibition of neurotoxins, but links are tenuous with regard to the contribution of these proteins to particular neurodegenerative disorders. It seems safe to suggest that FMO mediated metabolism of drugs acting on the brain is likely to play an important role in the pharmakinetic modulation of neurotoxic and/or psychoactive drugs in the brain but to what degree this may occur can only remain speculative at this stage. Recent research by Cashman *et al* (1999) suggests that FMO3 may have clinical consequences for humans in terms of detoxification. Cashman reports that *N*-oxygenation of amphetamine hydroxylamine to phenylpropanone oxime, and metabolism of methamphetamine represents a detoxification

a.

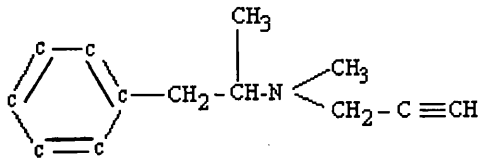

b.

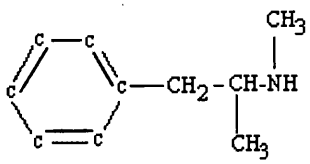

Figure 2.4 Structure of FMO substrate, MAO-B inhibitor, and theraputic agent for the treatment of Parkinson's disease, deprenyl (a). Structure (b) shows one of the final products produced by the metabolism of deprenyl, that of metamphetamine. Metamphetamine is a compound identified by Cashman *et al* where metabolism by FMO3 represents an alternative route in its detoxification pathway **(197)**.

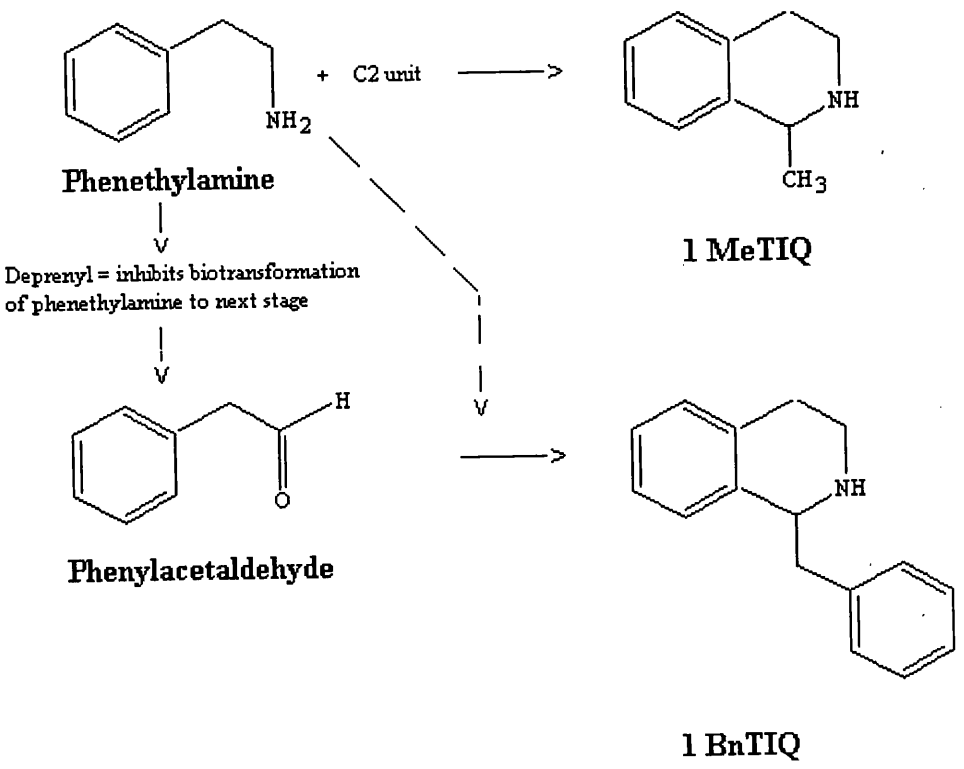

Figure 2.4a Possible pathways of 1Bn TIQ and 1 MeTIQ as outlined by Kotake *et al* **(195)**. They suggest that 1BnTIQ is formed when Phenethylamine is metabolised to phenylacetaldehyde by MAO-B, then subsequently to 1BnTIQ. Deprenyl acts as an inhibitor of this process. The above pathways are still not completely defined at present and the overall scheme represents only a possible series of stages.

pathway **(197)**. These drugs like MPTP, although non-clinical, can have a detrimental physiological and psychological effect on individuals, leading to psychosis due to the release of increased levels of neurotransmitters such as dopamine. Such compounds are known as indirect receptor agonists and are able to displace neurotransmitter from storage vesicles so that it leaks into the synaptic cleft. In the case of dopamine, it is not destroyed in the cytoplasm in the normal way by the action of MAO because amphetamine and these amphetamine based compounds are reversible inhibitors of MAO. As such this leads to the blocking of MAO action. As such, removing them from the body system is important. It seems that human FMO3 was able to metabolise these amphetamines to their *N*-oxide and so clear them out of the system. Substrates alone suggest such a link. Substrates such as phenothiazine chlorpromazine and the antidepressant imipramine, as well as therapeutic drugs such as selegiline and madopar, are all good substrates for FMO and are used extensively in treatment of psychotic and neurodegenerative disorders respectively. Tricyclics are good substrates for FMO and many of these drugs can induce Parkinson's syndrome. The action of such phenothiazine based tricyclics is via competitive blockade of the post-synaptic dopamine D_2 receptor in the striatum. However, the nigrostriatal system is able to compensate for a loss of up to 80% of striatal dopamine at which point clinical Parkinson's disease becomes apparent. It has been noted that up to 60% of patients using psychoactive drugs for the treatment of brain disorders like schizophrenia, acquire drug-induced Parkinson's syndrome **(198)**. This suggests that induced susceptibility is an important area in the determination of drug-induced Parkinson's disease. If so, genetic variance in drug metabolism may be a contributory factor.

Aims

The aims of this research project are:

- To determine using northern blot hybridization analysis the FMOs expressed in the human brain.
- To identify the cellular location of FMO3 and FMO4 mRNAs using *in situ* hybridization of human brain sections and antisense FMO mRNA probes.
- To compare the expression profiles of FMO3 mRNA and protein in the basal ganglia.
- To confirm by PCR, and sequence determination of the amplification product, that FMO3 (and not an as yet unknown FMO) is expressed in the human brain.
- To compare the expression patterns of FMO3 and FMO4 mRNAs in brain tissue-sections from male and female, normal individuals and those diagnosed with Parkinsons' disease.
- To determine if *FMO3* is expressed in the brain of other primates such as the gorilla and orang-utan.

Main findings of experimental procedures

The main findings of the experimental work described in this thesis are:

- FMO3 and FMO4 mRNAs are expressed in the basal ganglia region of the human brain. This region is a centre of motor function and control.
- Results from *in-situ* hybridisation studies showed that FMO3 and FMO4 mRNA expression was restricted to pyramidal cells, granular cells in the hippocampus and the small neurones of the thalamus. The evidence also suggests that FMOs are expressed in motor neurones.
- Western blot analysis demonstrated expression of FMO3 at the protein level in both human and non-human primate brain samples.
- RT-PCR followed by Southern blotting and sequence determination confirmed that FMO3 (and not another closely related isoform) is expressed in the human brain.
- FMO5mRNA is expressed in the human subthalamic nucleus. This mRNA was detected only when RT-PCR was carried out on poly A+ mRNA of this brain region.

Chapter Three

Materials and Methods

3.1 Bacterial cultures

Solutions

Ampicillin: A stock solution of ampicillin was prepared in water, at a concentration of 50mg/ml. The solution was filter sterilised using a 0.22μm gauge nitrocellulose sterile filter (Millipore), aliquoted out and frozen at -20^{0}C. Ampicillin from the stock solution was added to the sterile liquid agar media immediately prior to use, resulting in a final concentration of 100μg/ml. When adding antibiotic to liquid media, a final concentration of 50μg/ml was used.

Luria-Bertani (LB) bacterial growth medium (pH 7.5):(Bio 101, INC.)
Capsules of dried LB medium were placed in a Duran bottle and distilled water was added to give a solution of 10g bactotryptone, 5g bacto-yeast extract and 10g NaCl per litre. The solution was autoclaved and cooled to between 50-55^{0}C prior to the addition of required antibiotics. Alternatively, the solution was stored at room temperature without addition of antibiotics, until future use.

SOB bacterial medium (pH 7.5):(Bio 101, INC.)
Capsules of dried SOB medium were added to distilled water to give a solution containing: 20g bacto-tryptone, 5g bacto-yeast extract, 0.58g NaCl and 20mM $MgSO_4$ per litre. The SOB solution was autoclaved and then cooled to between 50-55^{0}C prior to the addition of antibiotics. Alternatively, the medium was stored at room temperature without the addition of antibiotics, until required.

LB-Agar:(Bio 101, INC.)
Capsules of dried LB-Agar were added to distilled water to give a solution consisting of: 20g bacto-tryptone, 5g bacto-yeast extract, 0.58g NaCl and 15g Agar per litre (for plates). The LB-Agar solution was autoclaved.
All autoclaving took place at a temperature of 121^{0}C (15 Ib), for 15 minutes.

3.1.1 Preparation of glycerol stocks

Solutions

LB Medium, required antibiotics, glycerol (BDH)

Protocol

10ml of LB medium, containing the appropriate antibiotic for the bacterium in use, were inoculated with a bacterial colony picked from an agar plate of freshly cultured cells. A sterile platinum wire loop was used to pick and transfer the colony in to the LB medium which was then incubated at 37^{0}C overnight with shaking. 4 ml of overnight culture were added to glass bottles containing 1ml of autoclaved glycerol. The resulting solution was gently mixed giving a final concentration of 20% (v/v) of glycerol and stored at -70^{0}C.

3.1.2 Inoculation of cultures

Solutions

LB medium, required antibiotic, glycerol stock

Protocol

Cultures were inoculated by picking a single colony from an agar plate using a sterile pipette and placing it in 10 ml of liquid medium, or by scraping the tip across the surface of a glycerol stock. The culture was then grown overnight at 37^{0}C in a shaking water bath. Large cultures were prepared by first inoculating 10 ml of culture as above and leaving it at 37^{0}C for approximately 8 hours before transferring it to a larger volume of medium, approximately 100 ml, and growing it overnight at 37^{0}C.

3.1.3 Preparation of agar plates

Solutions

Agar, water, required antibiotic at [5mg/ml]

Protocol

Agar containing capsules were placed in a Duran bottle containing a magnetic stirrer and the appropriate amount of distilled water and then autoclaved. The resulting mixture was then placed on a stirring plate to dissolve the agar and then cooled to approximately 55^{0}C before adding specific antibiotics to a final concentration of 5μg/ml. The agar was poured into sterile 8cm Petri dishes and covered until set. The plates were dried in a 37^{0}C oven prior to use.

3.1.4 Alkaline Lysis of plasmid DNA

This method is based on a procedure described in Sambrook *et al.* **(199)**.

Solutions

1x Tris-EDTA (TE) buffer (pH 8.0):

10mM Tris-Cl (Tris[hydroxymethyl] aminomethane), (Sigma) (pH 8.0), 1mM EDTA (diaminoethanetetra acetic acid disodium salt), (pH 8.0) (BDH) 70% ethanol; 100% ethanol, LB broth, ampicillin [10mg/ml], phenol liquidified *washed in tris buffer* (Fischer Scientific), buffered phenol/chloroform, 1% sodium dodecyl sulphate (SDS);(BDH), glacial acetic acid (BDH), glucose (BDH), NaOH (BDH), 3M potassium acetate (Sigma), sterile distilled water.

Solution 1:

50mM glucose, 10mM EDTA (pH8.0), 25mM Tris-Cl (pH8.0). The solution was autoclaved and stored at 4^{0}C.

Solution 2:

0.2M NaOH, 1% w/v SDS. Prepared immediately before use.

Solution 3:

3M potassium, 5M acetate preparation. The solution was prepared by adding 60ml of 5M potassium acetate solution to 11.5ml of glacial acetic acid and mixing with 28.5ml of distilled water. The solution was autoclaved and stored at 4^{0}C.

Protocol

5ml of LB-broth containing ampicillin [10μg/ml] was inoculated with a single bacterial colony and incubated at 37^{0}C overnight with shaking. 1.5ml of culture was poured into an Eppendorf tube, centrifuged for 1 minute. The remainder of the culture was stored at 4^{0}C. The supernatant was removed and the bacterial pellet dried via aspiration. The pellet was resuspended by adding 100μl of ice-cold solution 1, vortexed and left at room temperature for 5 minutes. 200μl of fresh solution 2 was added and the contents mixed by inverting rapidly. The mix was then stored on ice for a further 5 minutes. 150μl of ice-cold solution 3 was added and the sample vortexed, inverted, for 10 seconds and stored on ice for 5 minutes. The sample was centrifuged for 5 minutes in an Eppendorf 5414S bench centrifuge. The supernatant was transferred to a fresh Eppendorf tube and an equal volume (1:1 ratio) of buffered phenol/chloroform was added and the solution vortexed (20 seconds). The solution was centrifuged for 3 minutes and the supernatant transferred to fresh Eppendorf tubes. Two volumes ~900 ml of ethanol were added, the solution vortexed (10 seconds) and left to stand for 2 minutes at room temperature. It was then centrifuged for 5 minutes. The supernatant was removed and discarded, tubes were inverted to drain excess ethanol, and left to stand. 1 ml of 70% ethanol was added and the tubes vortexed for ~5 seconds then centrifuged for 5 minutes. The supernatant was removed and the pellet dried briefly for approximately 5 minutes in a vacuum desiccator. The pellet was resuspended in 10 ml of 1x TE (pH 8.0), and heated for ~5 minutes in a pre-heated heating block at 65^{0}C to remove endogenous nucleases. The resulting DNA suspension was frozen at -20^{0}C.

3.1.5 Plasmid DNA Purification: Maxi-Prep [Qiagen]

Solutions

P1 solution: 100μg/ml RNase A, 50mM Tris.Cl (pH 8.0), 10Mm EDTA (pH 8.0). Store at 4^{0}C until required.

P2 buffer: 200mM NaOH, 1% SDS. Store at room temperature.

P3 buffer: 3M potassium acetate (pH 5.5). Store at 4^{0}C until required.

QC buffer: 1M NaCl, 50mM MOPS, 15% (v/v) ethanol (pH 7.0).

QF buffer: 1.25M NaCl, 50mM Tris. Cl, 15% (v/v) ethanol (pH 8.5).

QBT buffer: 750mM NaCl, 50mM MOPS, 15% (v/v) ethanol, 0.15% Triton X-100 (pH 7.0).

QC, QF, QBT buffers were stored at room temperature until required.

Ethanol, Isopropanol (BDH).

Protocol

5ml of LB-broth containing ampicillin [100μg/ml] was inoculated with a single bacterial colony or with a single bacterial colony taken from a previously streaked agar/ampicillin plate comprising of colonies containing the insert of interest.

The culture was grown for eight hours at 37^{0}C with shaking. This 8 hour culture was re-inoculated into 100ml LB culture to which 100μl of ampicillin, from a stock of 50mg/ml, was added. The culture was then incubated overnight at 37^{0}C with shaking. The culture was divided between two 50ml centrifuge tubes and centrifuged at 4^{0}C at 6000rpm in a Sorvall GSA or GS3 or a Beckman JA-10 centrifuge for 10-15 minutes. The supernatant was removed by inverting the centrifuge tube and the pellet resuspend in 10 ml of P1 buffer. The solution was transferred to Qiagen elution tubes where 10 ml of P2 buffer was added. The solution was mixed gently 4-6 times by inversion to avoid shearing of genomic DNA, and incubated at room temperature for 5 minutes. 10 ml of chilled P3 buffer was added and the solution was mixed gently 5-6 times by inverting. It was then incubated on ice for 20 minutes to avoid localised precipitation of the potassium-dodecylsulphate. The solution was transferred to corex glass tubes and centrifuged in a Sorvall SS34 machine at 16000 rpm, at 4^{0}C for 30 minutes. The supernatant was removed. [If the supernatant is cloudy, re-centrifuge at 4^{0}C for 15 minutes at ~ 15000 rpm]. During this period the Qiagen-tip 500 column was equilibrated with 10 ml of QBT buffer, allowing the column to empty by gravity flow into a waste tray. After 30 minutes the supernatant was removed and remaining solution applied

immediately onto the Qiagen column, allowing it to enter the resin by gravity flow. The procedure was continued and the column washed twice with 30 ml of QC buffer. [Stage when DNA binds the column]. A glass corex tube was placed under the column and the DNA eluted using 15ml of QF buffer. The column was drained without application of pressure and the sample collected (~15ml). The DNA was precipitated using 0.7 volumes of Isopropanol [previously kept at room temperature]. The solution was then centrifuged using the Sorvall SS34 or Beckman JS-13 at 9500rpm for 30 minutes at 4^0C. The supernatant was carefully removed.

The DNA was washed briefly using 15ml of ice cold 70% ethanol and centrifuged at 9500rpm in a Sorvall SS34 for 15 minutes at 4^0C. The ethanol supernatant was removed carefully and the pellet air dried for 10 minutes. The pellet was redissolved in approximately 20µl of TE buffer and the amount of DNA recovered was calculated by measuring the Optical density (O.D.) at 260nm (method 3.3)

3.1.6 Preparation of total RNA

From Human and Primate brain tissue using Ultraspec™ RNA solution

Solutions

Ultraspec™ solution (Biotecx Laboratories Inc.), chloroform, isopropanol, 75% ethanol, sterile distilled water.

Protocol

Frozen brain tissue:

200-300 mg of tissue was used to extract total RNA. For each 100mg of tissue 1ml of Ultraspec™ solution was used. The tissue was weighed in the frozen state and transferred to a glass homogenizer. Ultraspec™ was added and the tissue was subject to crushing by gentle plunging strokes. The resulting liquid mix was transferred to sterile Eppendorf tubes and incubated on ice for

approximately 5 minutes. After this time 0.2 volumes of chloroform was added and the solution mixed by shaking. It was transferred back on to ice for a further 5 minutes. The mix was centrifuged at 9000 rpm at 4^{0}C for 15 minutes.

The resulting aqueous phase was transferred to a clean Eppendorf tube and the RNA was precipitated by the addition of an equal volume of isopropanol. This solution was vortexed and then incubated on ice for 10 minutes. Precipitated RNA was recovered by centrifugation at 7500 rpm for 10 minutes at 4^{0}C. The supernatant was removed and the pellet washed with 75% ethanol (1ml) by vortexing and then re-centrifugation at 7500 rpm for 5 minutes at 4^{0}C. Ethanol was removed and the pellet dried before re-suspending in 20µl of sterile distilled water. The RNA was stored at -20^{0}C. The condition and integrity of the RNA was checked by agarose gel electrophoresis (method 3.2.3), and RNA concentration was determined by measuring the optical density at 260nm (method 3.3).

3.2. Restriction enzyme digests

Solutions

10 x One-Phor-All (OPA) buffer (Pharmacia): 100mM Tris-acetate (pH 7.5), 100mM magnesium acetate, 500mM potassium acetate. RNAase A [50µg/ml], (Boehringer Mannheim), restriction enzymes (Pharmacia) concentrations were dependent upon the particular restriction enzyme used ranging from 5000 units/ml to 15000 units/ml. DNA sample, sterile distilled water.

Protocol

The reaction was carried out in a final volume of 20µl and contained:

10x (OPA) buffer, 0.5-20µg of DNA, 5% RNAse A at [10µg/ml] per 5µg DNA, restriction enzyme(s), water to make the volume to 20µl. The restriction enzyme buffer was added to the digest mix at 1x or 2x concentration depending on the enzyme(s) to be used, and the volume of the restriction digest mix was

made up with water. The digest was mixed by gently vortexing, centrifuged briefly, then incubated for between 2 and 24 hours at 37^{0}C. The resulting digest was then loaded on to an agarose gel.

3.2.1 Precipitation of DNA and RNA

Solutions:

Ethanol (100% and 80%), 3M sodium acetate, sterile distilled water.

Protocol:

DNA was precipitated out of solution by adding two volumes of absolute ethanol and 0.1 volume of sodium or ammonium acetate at 3M concentration. The sample was mixed by vortexing and then left on dry ice for 10 minutes. The samples were centrifuged in an Eppendorf centrifuge: 5414 S at 7500 rpm, for 10 minutes at room temperature. The supernatant was removed with fine tipped pipettes. The resulting pellet was washed with 80% ethanol by vortexing and then re-centrifuged in a Eppendorf 5414 S centrifuge for 5 minutes at room temperature . The supernatant was discarded and the pellet air dried. The DNA pellet was resuspended in 20µl of water and stored at -20^{0}C.

3.2.2 DNAse treatment of RNA samples

Solutions

RNAse free-DNAse 5000 units/50µl (Pharmacia), buffered Phenol (pH 5.0), chloroform, sterile distilled water.

Protocol

To approximately 50µl (30µg) of RNA 1µl of RNAase-free-DNAase was added. The sample was incubated for one hour at 37^{0}C. The RNA was then precipitated as follows:

Phenol/chloroform extraction: Equal volumes of buffered phenol (pH5.0) and chloroform were added to the Eppendorf containing the RNA sample. The mix was vortexed for approximately 20 seconds. The samples were centrifuged in a

bench Eppendorf centrifuge 5414 S 7500 rpm for 5-10 minutes at room temperature. The top layer was removed and transferred to fresh sterile Eppendorf tubes. RNA was precipitated and recovered as described in (method 3.2.1).

3.2.3 Gel electrophoresis of restriction enzyme digests I

Solutions

10 x TBE buffer: 0.89M Tris.borate, 0.89M Boric acid, 0.02M EDTA:

55g Boric acid, 9.3g EDTA and 108g tris-base were dissolved in distilled water and the final volume adjusted to 1 litre. The solution was autoclaved and stored at room temperature.

Running buffer:

10 x TBE was diluted in a ratio of 1:9 with distilled water to make a working solution of 1 x TBE

Loading buffer:

0.25% (w/v) bromophenol blue, 30% (v/v) glycerol.

The above components were dissolved in distilled water and then filter sterilised using a 0.45μm nitrocellulose filter and stored in 1ml aliquots at -20^{0}C

Tris-EDTA (TE) buffer (pH 8.0):

10mM Tris-Cl at pH 8.0, 1mM (EDTA) at pH 8.0

The solution was autoclaved and stored at room temperature.

Agarose Type I: low EEO,(BDH); Ethidium bromide [10mg/ml], (Sigma); 10x (OPA) buffer; water. Molecular weight standards used were the 1Kb Ladder from GibcoBRL. A working solution was prepared by mixing 100μl of 1Kb stock solution with 800μl of sterile water and 100μl loading buffer.

Protocol

Agarose gels (e.g.1% gel) were prepared by dissolving 0.5 grams of agarose in 50 ml of 1 x TBE. The buffer and agarose were placed in a glass beaker with a metallic stirrer and the agarose was dissolved by heating in a microwave oven

for ~2 minutes. The beaker was removed from the microwave and placed on a magnetic stirrer in a fume cupboard. When cool (~50^{0}C), 2.5 µl of ethidium bromide was added to give a concentration of 0.5µg/ml. The agarose solution was poured into a gel-casting apparatus with the appropriate gel comb. Once set, the comb was removed, and the gel was removed from its casting sheath and placed in an electrophoresis tank. A buffer composed of 1 x TBE was then poured into the tank covering the gel until the wells created by the comb were filled.

DNA samples were prepared as in (method 3.2.).

Samples were electrophoresed at ~100 volts. Depending on the separation required, electrophoresis was continued until the loading dye was approximately 1-2 cm from the end.

3.2.4 Gel electrophoresis of restriction digests II (low melting point gels)

Solutions

50 X TAE buffer:

40mM Tris-acetate, 2mM EDTA pH 8.0

242 grams of Tris base and 100 ml of 0.5M EDTA (pH 8.0) were mixed together with 57.1 ml of glacial acetic acid and dissolved in distilled water to make a working solution of 1 litre. The solution was autoclaved and stored at room temperature.

Running buffer: 50 x TAE diluted 1:49 to give 1x TAE.

Agarose: Low melting point agarose, (GibcoBRL).

Loading buffer.

Protocol

The gel was prepared as for a general agarose gel (method 3.2.3) with the exception that the buffer used is 1x TAE rather than 1x TBE. Similarly, the running buffer used for low melting point agarose gels was 1x TAE containing ethidium bromide at 5µg/ml. Electrophoresis was carried out at ~50 volts.

3.2.5 DNA extraction from low melting point agarose gel slices

Solutions

20mM Tris-Cl, 1mM EDTA (pH 8.0), buffered phenol (pH 8.0), chloroform, buffered phenol / chloroform in a 1:1 ratio, 10M ammonium acetate, absolute ethanol, 75% ethanol, 1x TAE buffer, water, ethidium bromide [5mg/ml], low melting point agarose (BDH), 1Kb ladder (GibcoBRL).

Protocol

After electrophoresing the DNA sample on a low melting point agarose gel (usually a 1.5% or 2% agarose gel), the gel was visualised briefly using a UV hand lamp so as not to nick the DNA in any way. The appropriate band was cut out from the gel using a sterile scalpel blade. The gel slice was placed in an Eppendorf tube and frozen at -20^{0}C or used for DNA extraction at once.

DNA extraction was performed as follows:

Five volumes of 20mM Tris-Cl /1mM EDTA (pH 8.0) were added to the gel slice. The sample was incubated for 5 minutes at 65^{0}C. The mix was cooled to room temperature and an equal volume of buffered phenol (pH 8.0) was added. The mix was vortexed for ~20 seconds. The aqueous phase was recovered by centrifugation using an Eppendorf® 5414S bench centrifuge at room temperature for 10 minutes. The recovered aqueous phase was transferred to a clean Eppendorf tube and an equal volume of buffered phenol / chloroform (1:1 dilution) was added. The mix was vortexed for ~20 seconds and the centrifugation step repeated. The aqueous phase was removed and transferred to a clean Eppendorf tube. An equal volume of chloroform was added to the tube and the centrifugation step repeated. The final aqueous phase was transferred to a fresh Eppendorf tube and 0.2 volumes of cold 10M ammonium acetate, and 2 volumes of absolute ethanol added. The sample was inverted several times and left at room temperature for 10 minutes.

DNA was recovered by centrifugation in a Sorvall GSA at 6000 rpm for 20 minutes at 4^{0}C. If the DNA pellet was absent, the sample was recentrifuged at 6000 rpm for a further 10-15 minutes, re-spin in bench centrifuge for ~10-15

minutes. The DNA pellet was washed in 70% ethanol (~100µl) by vortexing and recovered by centrifugation in an Eppendorf® bench centrifuge 5414 S, for 10 minutes at room temperature. DNA pellets were dried in a vacuum desiccator for 5-10 minutes. DNA was dissolved in sterile water (up to 10 µl).

3.3 Measurement of DNA and RNA concentration

Measurement by use of optical density readings

DNA concentration was determined using a Phillips PU 8720 UV/Vis scanning spectrophotometer set at 260nm. The absorbance of an aqueous solution of DNA or RNA at λ_{260}nm (A_{260}) can be assumed to be proportional to the amount of DNA or RNA present within the sample Sambrook *et al* **(199)**. Therefore, the optical density as measured by a spectrophotometer can be used to calculate the concentration of a given sample for experimental use.

Double stranded DNA:

50 x A_{260} x dilution factor of the sample in [mg/ml]

Single stranded DNA:

37 x A_{260} x dilution factor of the sample in [mg/ml]

RNA:

40 x A_{260} x dilution factor of the sample in [mg/ml]

3.4 Ligation & sub-cloning of DNA fragments into pBluescript KS II

The FMO cDNAs used in sub-cloning experiments were taken from glycerol stocks prepared from full length clones isolated by CT Dolphin *et al* **(99,107,129)**. The cDNA fragments used in these experiments were generated by restriction digest of a small section located in the 3' non-coding area of the

FMO3 and 4 cDNAs. This part of the clone was chosen as it represented the most diverse sequence of all five FMOs.

pBluescript KS II is a high copy number ColE 1 based phagemid 2961 basepairs in length. It has a polylinker that has two orientations. In the KS type its polylinker is oriented so that *lacZ* transcription occurs in the direction from restriction site *Kpn*I to *Sac*I. It has a multiple cloning site from 657-759 base pairs containing 21 unique restriction sites, flanked by T3 and T7 RNA promoters. The main advantage of using pBluescript KS II (+) as a cloning vector is its versatility, and its T3 and T7 RNA polymerase promoters which make it ideal for in-vitro transcription of RNA. The main advantage of using pBluescript KS II(+) as a cloning vector is its versatility, and its T3 and T7 promoters which make it ideal for in-vitro transcription of RNA.

The combination of having a multiple cloning site containing restriction enzyme sites which complemented those flanking the 5' and 3' ends of the cDNA fragment to be sub-cloned and the T7 and T3 promoters, made it a good choice for sub-cloning.

Restriction enzymes used for ligation and sub-cloning were Sma I and Pst I (FMO3) and BamH I and Sac I (FMO4). These particular enzymes were chosen for sub-cloning FMO3 and FMO4 into pBluescript KS II as these restriction sites (or compatible sites) were located at the 5' and 3' ends of the fragments extracted from FMO cDNA, and so complemented those at the 5' and 3' ends in the cloning vector.

Solutions

10x (OPA) buffer, restriction enzymes, vector (pBluescript KS II, 60ng/ml), cDNA insert (100ng/ml), T4 DNA ligase 5000 units/ml (Stratagene)

Protocol

(Based on a method by Sambrook *et al* (**199**))

pBluescript KS II vector was digested with Sma I (10 000 units/ml) for ~4 hours at 30^0C and then Pstl(10 000 units/ml) at 37^0C overnight. Sma I was incubated at 30^0C before PstI as the enzyme activity of Sma I is heat

inactivated at temperatures above 30^{0}C. Pst I restriction enzyme was added after Sma I as this enzyme requires a temperature of 37^{0}C for efficient activity.

1 µl Sma I (10 000 units/ml)

1 µl Pst 1 (10 000 units/ml)

1 µl vector (60ng/µl), (at molar ratio of size of ~2:1 in favour of insert)

2 µl 1x (OPA) buffer

15 µl distilled water

Test controls for each restriction enzyme:

1 µl vector (60ng/µl)

2 µl 1x (OPA) buffer

16 µl distilled water

1 µl of Pst 1 and Sma I (separately) with Pst 1 at 37^{0}C and Sma I at 30^{0}C overnight.

Ligation vector mixes were prepared as above for FMO4, using restriction enzymes BamH I (10 000 units/ml) and SacI (15 000 units/ml), in replace of Sma I. Both BamH I and Sac I sites can be restricted at 37^{0}C. Test controls of BamH I and Sac I digestion were also set up. Following digestion of pBluescript with restriction enzymes, the restrictions for Sma I and Pstl and BamH I and Sac I were frozen at -20^{0}C.

Ligation:

Restriction enzymes were heat inactivated at 65^{0}C for 5 minutes.

The ligation reaction contained the DNA insert of FMO3 or FMO4 and consisted of the following components:

4 µl 5mM ATP

2 µl 10x OPA buffer

10 µl digested pBluescript (60ng/µl)

3 µl of a fragment of either FMO 3 or FMO 4 cDNA (100ng/µl)(in a ~2:1 ratio insert to pBluescript KS II vector)

1 µl T4 DNA Ligase (5000 units/ml).

The sample was incubated at room temperature overnight.

3.4.1 Transformation of DH5α cells & Sub-cloning of FMO DNA fragment into pBluescript KS II

Solutions

Transformation buffer: 10mM potassium acetate, 45mM $MnCl_2.4H_2O$, 10mM $CaCl_2.2H_2O$, 100mM KCL, 3mM hexaminecobalt chloride, 10% glycerol. The solution was filter sterilised using a 0.45μm nitrocellulose filter. Store at 4^0C.

LB medium, SOB, LB-agar plates, ampicillin, ligation mix, distilled water.

Bacterial strain: E.*coli* strain DH5α: *sup* E44 Δ*lac* U169,(Φ 80 *lac* Z ΔM15) *hsd R*17 *rec*A1 *end*A1 *gyr* A96 *thi*-1 *rel*A1, **(200)**.

Bacterial strain: E.*coli* strain JM109: *rec* A1 *sup* E44 *end*A1 *hsd R*17 *gyr* A96 *rel* A1 *thi* Δ (*lac-pro* AB) F' [*traD* 36 *pro* AB^+ $lac/^q$ *lac*Z DM15], **(201)**.

Protocol

E.*coli* DH5α cells in 10 ml of LB-medium (without ampicillin) were grown overnight at 37^0C with shaking.

The optical density of the overnight culture was determined using LB-medium as the blank. The reading should be between 0.6 and 0.8 absorbance units at A_{550} nm. If the reading was above 0.8 then 1 ml of culture was diluted with 9 ml of fresh LB-medium and incubated at 37^0C for ~1 hour with shaking. The culture was used when the absorbance reached ~0.6 to 0.8.

The bacterial culture was removed from the 37^0C water bath and transferred to 50 ml Falcon tubes. It was then placed on ice at ~4^0C for 10 minutes. The Falcon tubes containing the culture were centrifuged at 2500 rpm in a MSE 18 centrifuge at room temperature for 10 minutes. The resulting pellet was resuspended in 8 ml of ice-cold transformation buffer. The solution was placed on ice at ~ 4^0C for 10 minutes. The solution was centrifuged at 2500 rpm at room temperature for 10 minutes. The pellet was resuspended in 2 ml of transformation buffer. To the following five mixes 200 ml of transformed cells were added:

Ligation mix (method 3.4)

Un-cut pBluescript KS II plasmid (ligation control)
Restriction digest of pBluescript KS II (restriction enzyme test), (method 3.4)
control of transformed cells.

The sample mixes were left on ice at ~ 4^0C for 30 minutes. The cells were heat shocked for 90 seconds at 42^0C. The samples were transferred to 10 ml Falcon transformation tubes containing 1 ml of SOB. The samples were left for ~1 hour at 37^0C with shaking.
Agar ampicillin plates were prepared in duplicate (method 3.2.3). Each of the five samples were plated out (in duplicate) on to the agar plates at volumes of 200 µl and 1ml. One control sample for transformed cells was plated on to an agar plate without ampicillin. The plates were left to dry before placing in an incubation oven at 37^0C overnight. Colony counts were performed to check efficiency of transformation. Resulting colonies from the overnight incubation were picked and standard Alkaline lysis (method 3.1.4) was performed to recover ligation positives containing DNA insert. Plasmid DNA purification was performed using the Qiagen plasmid prep procedure (method 3.1.5).

3.5 Salmon-sperm DNA preparation

Solutions

70% Ethanol, phenol, buffered phenol/chloroform, 1M NaCl, sterile distilled water, salmon sperm DNA [10mg/ml](Stratagene)

Protocol

One gram of salmon sperm DNA was dissolved into 100 ml of sterile distilled water to give a concentration of [10mg/ml]. To 30 ml of the solution 3.5 ml of 1M NaCl was added. Sterile water was added to give a final volume of 35 ml with a concentration of 0.1M NaCl. The solution was split into two Falcon tubes and an equal volume of phenol was added. The solution was vortexed and centrifuged in an Eppendorf centrifuge 5414 S for 5 mins. The aqueous layer was recovered and phenol /chloroform buffered solution was added in a (1:1)

ratio. The solution was vortexed and centrifuged for 5 minutes. A 19 G sterile needle was passed into the salmon sperm genomic layer and the layer removed. It was transferred into fresh Falcon tubes and the DNA sheared by passing it through the needle approximately 12 times. The DNA was precipitated at room temperature with two volumes of absolute ethanol. The solution was centrifuged in a Sorvall RC-2B at 9000 rpm at 4^0C for 30 minutes. The supernatant was discarded. The pellets were washed in 70% ethanol at room temperature. The resulting pellets were air dried and resuspended in sterile distilled water to give a volume of [10mg/ml].

The solution was boiled for 10 minutes and frozen at -20^0C.

3.5.1 Preparation of deionised formamide

100 ml of Formamide was de-ionised by stirring with 30g of AR mixed-bed resin (AG-501-X8 (D) 20-50 mesh (BioRad), in a fume cupboard for approximately one hour. Beads were removed by filtration through a sintered glass filter. The solution was sterilised by filtration through a 0.45μm (millipore) filter. De-ionised formamide was stored at -20^0C.

3.6 RNA dot blots

Solutions

Denaturation solution: 500μl deionised formamide, 162μl (37% v/v) formaldehyde, (3-[N-Morpholino]propane-sulfonic acid), (MOPS)(Sigma). 100μl (MOPS) buffer: 0.2 MOPS/0.5M sodium acetate, 0.01 M EDTA (pH 7.0) 2x SSC, 10x SSC, 20x SSC, water, RNA sample, Nylon membrane (BDH).

Protocol

RNA from human liver at a concentration of [3μg / μl] was used as a control. To the RNA sample, denaturation solution was added at three times the volume of RNA . The solution was placed on ice at ~ 4^0C.

The nylon membrane was soaked in water. The membrane was placed in 10x SSC to saturate it before placing it on filter paper. To 12μl of denaturation solution 4μl of RNA sample was added. The solution was placed on a pre-heated heating block at 65^0C for 5 minutes. After denaturation one volume of cold 20x SSC (~16 ml) was added to the solution. The saturated nylon membrane was placed on Whatman 3MM filter paper and the RNA sample mix was pipetted on to membrane in 2μl aliquots. A second piece of filter paper was moistened with SSC and the blots placed on top. The blots were baked in a vacuum oven at 80^0C for 15 minutes to bind RNA to membrane. The blot was covered in cling-wrap and stored at -20^0C.

3.6.1 Preparation and radio labelling of cDNA probes

In northern blot analyses, cDNA probes encoding FMOs 1, 2, 3, 4 and 5 were radiolabelled with [α^{32}P]-dCTP using the random primer method **(201)**. Probes were labelled to an average specific activity of $7x10^8$ cpm/μg cDNA giving a final working concentration of 1-$2x10^6$ cpm/μl. As a control for RNA loading the brain northern blot was hybridised to100ng of human β-actin cDNA. FMO probe controls were human adult liver RNA dot blots, and human fetal liver RNA dot blot. Each dot of RNA was approximately 15μg.

Solutions:

20mM Dithiothreitol (DTT), 5mM deoxyribonucleoside triphosphates dATP, dGTP, dTTP (dNTP's) (Pharmacia), Random hexamer primers (GibcoBRL), [α^{32}P]-dCTP at 3000Ci/mmol, 10μCi/μl (NEN); Klenow fragment of E.Coli

DNA polymerase I (5000 units/ml) (Pharmacia), DNA sample, sterile distilled water.

10x Random primer buffer (RP) buffer: 900mM *N*-2-Hydroxyethylpiperazine-*N'*-2-ethanesulphonic acid (HEPES), (adjust to pH6.6 with 4N NaOH) 100mM $MgCl_2$ di-sodium hydrogen orthophosphate buffer 0.5M Na_2HPO_4 (pH 7.0), radioisotope counting medium: scintillation fluid, Whatman DE-81 paper

Protocol

Labelling mix:

The reaction was carried out in a final volume of 20µl and contained the following components:

1 µl 20mM dithiothreitol (DTT)

1 µl 5 mM dNTP mix

1 µl 10x RP buffer

5 µl [α P^{32}]-d CTP at a concentration of 10 µCi/µl

1 µl DNA at a concentration of 50 ng/µl

1 µl Random hexamer primers at a concentration of 75 ng/µl

1 µl (5 units) of DNA polymerase (Klenow)

Distilled water to give a final volume of 20 µl.

A labelling mix was prepared by adding (in 1µl volumes) the DTT, dNTPs and 10x RP buffer to a sterile 0.5ml Eppendorf tube. 5µl of [α^{32}P]-dCTP at a concentration of 10 µCi/µl was added to the labelling mix. The random primers and DNA were mixed together in a 2 µl volume and boiled for 3 minutes. The solution was snap-cooled on ice for 1 minute before adding to the Eppendorf tube containing the labelling mix. DNA polymerase was added to the mix and the contents of the Eppendorf tube mixed by gently tapping. The labelling mix was incubated for ~3 hours at room temperature.

The percentage incorporation of radiolabel was analysed by spotting 1µl of the labelling mix on to DE 81 paper for both control (total radioactivity) and probe (incorporated radioactivity). The DE 81 Whatman paper for only one of the

samples was washed. Washes were carried out at room temperature. DE 81 paper was placed in a small Tupperware container and covered with 0.5M Na_2HPO_4 buffer (pH 7.0) for ~3 minutes each time (x6), distilled water ~1 minute (x2), 95% ethanol 1 minute (x2). The DE 81 filter paper was dried at room temperature. Both DE 81 filters were put into separate vials containing 1ml of scintillation fluid and the radioactivity was measured by scintillation counting.

3.6.2 Northern blot analysis

Solutions

20x SSPE: 3.6M NaCl, 0.02M, EDTA, 200mM Sodium phosphate (pH6.8).The solution was adjusted to pH 7.4 with 10 M NaOH and made up to 1 litre with distilled water. The solution was autoclaved and stored at room temperature.

100x Denhardt's solution: 2% (w/v) BSA fraction V(Sigma), 2% (w/v) Ficoll 400000, (Sigma), 2% (w/v) Polyvinylpyrrolidone 400000 (Sigma), stored at -20^{0}C. Salmon sperm DNA [100mg/ml], SDS, sterile distilled water.

Prehybridisation and hybridisation solutions:

5x SSPE, 2% SDS,

10x Denhardt's solution

deionised formamide

salmon sperm DNA [100mg/ml]

[α^{32}P]-dCTP* labelled DNA probe **(hybridisation solution only)**

Wash solutions:

2x SSPE, 0.05% SSPE, 0.1% SDS, 0.1% SSPE,

Probe stripping:

0.05% SDS in sterile distilled water, 2x SSPE

Protocol

Northern blot hybridisation analysis was performed **(202)**, using a MTB blot of Poly A^+ RNA from 7 different regions of the human brain and a whole brain sample. (PT 1200-1 Clontech).

RNA was from: *Amygdala, Caudate nucleus, Corpus Callosum, Hippocampus, Whole brain, Substantia nigra, Subthalamic nucleus and Thalamus*. RNA had been immobilised on a charged modified nylon membrane using a 0.8% denaturing formaldehyde agarose gel. Each sample consisted of ~ 2μg of poly A^+ RNA. 10 ml of prehybridisation solution was pre- heated to 42^0C in a water bath. The northern blot was placed into an open ended plastic pouch back to back with control blot, using gauze to separate the two membranes. Three sides of the pouch were sealed, and the 10 ml of prehybridisation solution was added, making sure all air bubbles were expelled. The fourth side was then heat sealed. The pre-hybridisation solution consisted of 5x SSPE, 10x Denhardt's solution, 100μg/ml of denatured salmon sperm DNA, 2% SDS and 50% deionised formamide. The bag was immersed in a water bath set at 42^0C and incubated for between 6 and 18 hours.
The pre-hybridisation solution was removed and replaced with 10ml of hybridisation solution, prepared as follows:

The 10ml of hybridisation solution was prepared without salmon sperm DNA. This was heated to 42^0C in a water bath. The DNA probe was added. The amount, of which, depended on the specific activity achieved. On average a specific activity of ~$4.5x10^8$ cpm/μg was obtained and a concentration of 1-$2x10^6$cpm/μl was used in hybridisation reactions. 100μg/ml of salmon sperm DNA was added to the labelled DNA probe. The DNA was then denatured by boiling for 10 minutes. The sample was briefly centrifuged and snap-cooled on ice for 1 minute. The DNA probe mix was then added to the previously warmed hybridisation mix. The blot was hybridised at 42^0C for between 18 and 24 hours.
Blots were removed from the plastic bag and the probe mix and excess radioactivity washed off. The membrane was rinsed in 2x SSPE, then washed three times for 10 minutes, with 2x SSPE/0.05% SDS at room temperature. The blot was agitated during the wash procedures. The membrane was then washed for 2x 20 minute intervals with 0.1x SSPE/0.1 % SDS at 50^0C.

Control blots consisted of approximately 15μg of RNA from human liver and human lung (method 3.6). RNA from these tissues was used as a control because each of the five FMO cDNAs will hybridise to either lung or liver RNA.

A Geiger counter was used to check approximate level of probe binding and distribution on the blot / background. The blots were then placed separately on cling-wrap and covered. These were taped to Whatman 3MM paper. The orientation of the blots was marked with [^{35}S]-labelled radioactive ink. In a dark room, the blots were placed in a developing cassette with film. Cassettes were put at -70^{0}C for between 2 and 7 days. The blot was stripped (see method 3.6.3) and the hybridisation procedure was repeated for each of the five FMO cDNAs.

3.6.3 Probe stripping

Solutions

0.5% SDS, sterile distilled water,

Protocol

In sterile water a solution of 0.5% SDS was prepared and heated to between 90 and 100^{0}C.

To remove any bound radioactive probe, the blots were placed in a small heat resistant plastic container adding approximately 500ml of this heated solution. The temperature of the solution was maintained at approximately 80^{0}C in a shaking water bath for 10 minutes. After this time the box containing the blots was removed from the water bath and cooled for 10 minutes at room temperature. The blots were then removed and rinsed in 2x SSPE. The blots were vacuum sealed in a plastic pouch and stored at -20^{0}C.

3.7.0 cDNA template for FMO ribo-probes

FMO3

Templates for antisense and sense (negative control) cRNAs were generated by cloning a 120 basepair Rsa1/Pst1 fragment of the FMO3 cDNA into the plasmid p.Bluescript KS II. The fragment contains part of the 3' non-coding region of the FMO3 cDNA. The cDNA was subjected to standard restriction digestion (method 3.2.4) using a 1.5% low melting point agarose gel. The 120 basepair fragment was extracted from the gel slice and the purified product cloned into the multiple cloning site of vector pBluescript KS II between the Sma1 and Pst1 sites **(199)**. Transformation of E.*coli* DH5-α cells with pBluescript constructs was performed (method 3.4.1).

Plasmid was isolated from several colonies using Maxi-prep plasmid purification (method 3.1.5). The orientation of the fragment subcloned into the plasmid vector was known, as the fragment was flanked with different overhangs at the 5'and 3' ends, each corresponding to a unique site in pBluescript plasmid. The linearised construct was transcribed with the appropriate RNA polymerase to produce either antisense or sense RNA probes.

Solutions

cDNA sample, restriction enzymes, (OPA) buffer, SDS, buffered phenol/chloroform, ethanol, 3M sodium acetate, sterile distilled water.

Protocol

Template for sense (A) and anti-sense (B) probes were prepared as follows. Each reaction was carried out in a final volume of 200μl and contained the following:

To a sterile Eppendorf tube the following components were added:

(A) 30 μg of plasmid DNA containing insert	40 μl
Pst 1 enzyme (5000 units/μl)	5 μl
OPA 10x buffer	20 μl

Water (filter sterile) 135 µl

(B) As above but using the enzyme Bam HI (5000 units/µl) in place of Pst1.

The restriction digest was left overnight at 37^{0}C, in a water bath, to linearise plasmid DNA. Following linearisation standard gel electrophoresis was performed using an 0.8% agarose gel in 1x TBE buffer for each restriction digest (A) and (B) above. 10 µl of each digest was loaded on to the gel to see if enzymes have linearised the plasmid (method 3.2.3). If successful, proteinase K digestion was carried out on the linearised template (method 3.7.1).

FMO4

A template for antisense and sense (negative control) cRNAs was generated by cloning a 206 base pair Sac1/BamH1 fragment of the FMO4 cDNA into the plasmid p.Bluescript KS II. The fragment contains part of the 3' non-coding region of the FMO4 cDNA. The cDNA was subjected to standard restriction digestion (method 3.2.4) using a 1.5% low melting point agarose gel. The 206 basepair fragment was extracted from the gel slice and the purified product cloned into the multiple cloning site of vector pBluescript KS II between the Sac1 and BamH1 sites. Transformation of E.coli DH5-α cells with pBluescript constructs was performed (method 3.4.1). Colonies were selected and plasmid isolated and analysed by electrophoresis. The appropriate plasmid was linearised with either Sac1 or BamH1. If digestion was successful the templates were treated with proteinase K.

3.7.1 Proteinase K digestion

Templates for sense (A) and anti-sense (B) probes were prepared (as in method 3.7.0) for both FMO3 and FMO4. For FMO3 samples (A) and (B) represent plasmid DNA containing insert restricted with Pst1 enzyme (A), while sample

(B) was incubated with BamH1. For FMO4 sample (A) was incubated with restriction enzyme Sac1 while sample (B) was incubated with BamH1.

Solutions

Proteinase K [20mg/ml], (Boehringer Mannheim), SDS, buffered phenol, chloroform, ethanol, sodium acetate, sterile distilled water.

Protocol

The remaining 190 µl from samples (A) and (B) were incubated for 30 minutes at 37^{0}C with 2 µl of 20 mg/ml proteinase K and 20 µl of 10% SDS. An equal volume of buffered phenol-chloroform was added to each sample and the mix vortexed. The mix was centrifuged in an Eppendorf bench centrifuge (5414 S) at room temperature for 10 minutes. The aqueous layer was transferred to a sterile Eppendorf tube. This step was repeated. Linearised plasmid, containing DNA insert, was precipitated using $2^{1/2}$ volumes of absolute ethanol and 3M sodium acetate at $^{1/10}$ th of final volume. The mix was left overnight at -20^{0}C. The resulting precipitate was centrifuged as above for 15 minutes. The liquid was discarded and the pellet washed with 75% ethanol. The solution was centrifuged as above for ~10 minutes. The ethanol was discarded and the pellet resuspend in 20 µl of filter sterile distilled water. The absorbance was read at 250 nm and the sample was diluted with sterile water to give a concentration of 0.1 mg/ml.

This procedure was carried out for both sense and anti-sense templates.

3.7.2 *In-vitro* transcription:

labelling of cRNA riboprobe with [S^{35}] α-UTP:

In vitro synthesis of high specific activity radiolabelled cRNA probes for FMOs 3 and 4 was carried out using [α^{35}S]-UTP label at a final concentration

of ~20μM in a reaction volume of 10μl **(203)**. In-vitro transcription was carried out using the linearised DNA templates for FMO3 and (method 3.7.0).

Solutions

5x cRNA transcription buffer:

200mM Tris-Cl (pH 8.0), 40mM $MgCl_2$, 10mM spermidine (BDH), 250mM NaCl, 0.75M DTT, cold ribonucleotides: (rATP/rCTP/rGTP at 10mM each, Pharmacia) [α^{35}S]-UTP at 400-800 Ci/mmol [10μCi/μl]. RNAse guard (40,000 units/ml), RQ1-RNAse free DNAse (10,000 units/ml), RNA polymerase T3/T7 (50,000 units/ml) (Pharmacia).

Protocol

In two separate Eppendorf tubes labelled (A) and (B)10μl of [α^{35}S]-UTP was pipetted. The tubes were placed in a vacuum desiccator for ~20 to 30 minutes to give a pellet of UTP. To the dried radioactive pellets the following constituents were added (thus giving a final concentration of radioactive probe of ~20μM per 10μl):

The resuspension mix contained the following components:

1 μl 5x cRNA transcription buffer

1 μl 0.75M DDT

2 μl ribonucleotides of [2.5 mM] each of ATP, CTP and GTP

1 μl Linearised DNA at 100 ng each for (A)-anti-sense or (B)-sense probes

1 μl (10 units) of either RNA Polymerase T3 or T7

1 μl RNAse inhibitor (40 units)

water up to a final total volume of 10 μl.

This was incubated for one hour at 37^{0}C. The DNA template was removed from the samples by adding RQ1 RNAase-free DNase to a final concentration of 1 unit/μg of DNA. This was then incubated for between 30 minutes and 1 hour at 37^{0}C. It was then frozen at -20^{0}C.

For FMO3, T7 polymerase was used to transcribe antisense probe, T3 polymerase transcribing a sense probe.

For FMO4, T7 polymerase was used to transcribe antisense probe, T3 polymerase transcribing a sense probe.

3.7.3 Preparation of tRNA for *in-situ* hybridization

Solutions

tRNA (Bovine calf thymus), (Boehringer Mannheim). TE (pH 7.6) containing 0.1M NaCl, buffered phenol, chloroform, absolute ethanol, sterile distilled water.

Protocol

Prepared as a 10 ml stock of 25mg/ml:

tRNA was dissolved in TE (pH 7.6) containing 0.1M NaCl. The solution was phenol extracted with an equal volume of buffered phenol (pH 8.0) and the aqueous layer transferred to a sterile Eppendorf tube. This step was repeated again. The aqueous layer was removed and transferred to a sterile Eppendorf tube. The solution was chloroform extracted. The extraction was repeated with chloroform before final precipitation. The RNA was precipitated with 2.5 volumes of absolute ethanol at room temperature. RNA was recovered by centrifugation in an Eppendorf centrifuge (5414 R) at 7500 rpm for 15 minutes at 4^0C. The pellet was redissolved to give a solution of 10mg/ml in sterile TE (pH 7.6) and stored at -20^0C.

3.7.4 *In-Situ* Hybridisation:

Solutions

cRNA sample, 4% PFA/PBS, 1x PBS, ethanol.

Hybridisation solution: 20x Sodium citrate (SSC): 3M NaCl, 0.3M $Na_3Citrate.2H_2O$. The pH of the solution was adjusted to (pH 7.0) with 1 M

HCl and made up to 1 litre with distilled water. The solution was autoclaved and stored at room temperature. Deionised formamide, 50x Denhardt's solution, 100μg/ml salmon sperm DNA, 25mg/ml tRNA (Bovine, calf thymus), (Boehringer Mannheim), 25mg/ml poly A (Boehringer Mannheim), 0.1M DTT, dextran sulfate (Sigma).

Protocol

In-Situ hybridisation was performed using cRNA probes. The probes were produced using cDNA fragments from FMO3 and FMO4 which had been subcloned in to pBluescript. The cRNA[α^{35}S]-UTP sense and anti-sense probes for FMO3 were generated by in-vitro transcription using Pst1 and BamH1 linearised plasmid cDNA and T3 and T7 RNA polymerase respectively as described in (method 3.7.3).

In-situ hybridisation: (Based on a modified method described by Sambrook *et al* (1989).

Brain sections were removed from storage at -70^{0}C and fixed at room temperature in a 4% PFA/PBS solution. Sections were washed in PBS for 3x 1 minute and dehydrated in graded ethanol washes: 70%, 80%,95% for 2 minutes each time. The sections were then air dried.

Hybridisation:

20 ml of hybridisation solution was prepared and the following components were added to make a solution with a final volume of 20ml: 50% deionised formamide, 4% SSC, 50x Denhardt's solution,100μg/ml salmon sperm DNA, 25mg/ml tRNA, 25mg/ml poly A, 0.1M DTT, 2g dextran sulfate. The solution was stored in 2ml aliquots at -20^{0}C. Hybridisation was carried out for approximately 16 hours at 37^{0}C in a humid box. Each of the sections were treated with 200μl of hybridisation solution containing 4.9x10^5 cpm of [α^{35}S]-UTP labelled cRNA probe. After hybridisation, the sections were washed briefly in 1x SSC at room temperature. The sections were covered with 1x SSC and heated to 55^{0}C and placed in a shaking water bath for 15 minutes. This step was repeated three times. The sections were removed from the water bath and covered with 1x SSC and left at room temperature for 30 minutes. This step was repeated once. The sections were washed in distilled water

briefly. They were then washed in 70% industrial methylated spirits for ~30 seconds. The sections were then air dried prior to emulsion coating.

3.7.5 Emulsion coating:

Solutions

Kodak NBT-2 emulsion, 600mm sodium acetate, sterile distilled water.

Protocol

A dark room was prepared for autoradiography by fitting it with a Whattan #4 lamp. Kodak NBT-2. Emulsion was pre-warmed in a water bath at 45^{0}C before dilution with pre-warmed ammonium-acetate in a ratio of 1:1. All vials and emulsion-bearing items were covered with a double wrapping of tin foil to reduce the risk of premature exposure. The diluted emulsion mix was left for ~15 minutes at 45^{0}C. The emulsion mix was poured in to a foil-wrapped coating chamber. A blank microscope slide was slowly dipped into the solution to dispel bubbles. Tissue sections attached to microscope slides were slowly dipped into the emulsion solution (twice). The slides were placed vertically in a drying rack and allowed to dry for 1-2 hours in a light-tight container. The slides were transferred to light tight boxes containing desiccant The boxes were sealed and covered with foil. The boxes were placed at 4^{0}C for between 2 and 4 weeks.

3.7.6 Development of slides:

Solutions

Kodak D-19 developer, Kodak fixer, 20% acetic acid solution, sterile distilled water, ethanol, Xam mounting solution (BDH), Gurr certistain: Cresyl violet (BDH), Gurr certistain: Toluidine blue (BDH),

Protocol

Tissue sections were developed in Kodak D-19 developer at room temperature for 3.5 minutes. They were then dipped in STOP solution (20% acetic acid) for 30 seconds and fixed with Kodak Fixer for 3.5 minutes. The sections were then bathed in distilled water for 5 minutes before staining with cresyl violet or toluidine blue. Staining was carried out for between 5 and 7 minutes. The sections were rinsed in water and dehydrated in a series of graded ethanol washes: 50%, 70%, 80%, 95%. The sections were then subjected to a final xylene wash of 3 minutes. The sections were air dried, covered with Xam mounting solution and mounted under coverslips. Corresponding sense strand probe treated sections were used as controls. All washes and incubations were performed simultaneously under the same conditions but separate glass ware and boxes were used for anti-sense treated slides to avoid cross contamination of probe.

3.8 Human brain tissue:

Human brain tissues were obtained at autopsy from known Parkinson's disease patients and non-Parkinson's disease individuals. Tissues were immediately flash-frozen prior to sectioning on to glass slides. The sections were taken from (a) Midbrain and (b) coronal sections of the cerebral hemisphere encompassing the basal-ganglia.

Of the nine individuals from which brain tissue was obtained, four were clinically diagnosed as having Parkinson's disease, while the remaining five had no known neurological disorders. The interval between death, autopsy and flash-freezing ranged between 4 hours and 28 hours. Of the Parkinson's diagnosed group, 2 were female and 2 were male, whereas in the group of patients exhibiting normal brain function, 3 were female. Ages of the patients ranged from 65 years to 88 years with an average age of 73.3 years. Following autopsy, designated areas were prepared as 5μm thick sections on to pre-treated

glass microscope slides. The prepared tissue sections were stored at -70^{0}C prior to experimental analysis.

Solutions

Phosphate buffered saline (PBS), (pH 7.4); paraformaldehyde (PFA), 10N NaOH, sterile distilled water.

Protocol

Preparation of specimens

Slides of human brain tissue used in Immunocytochemistry and *in-situ* hybridisation experiments were fixed in a freshly prepared solution containing 4% paraformaldehyde in phosphate buffered saline (PBS), (pH 7.4). To 200 ml of distilled water 16g of paraformaldehyde was added. The solution was heated to ~60^{0}C and approximately 100µl of 10N NaOH was added to clear the solution. The solution was cooled and 200 ml of 1x PBS was added. The solution was stored at 4^{0}C and used fresh. Specimens from primary cell culture experiments were fixed as above but using 3.5% paraformaldehyde in replace of 4% as this proved less harsh on cultured cells.

3.8.1 Immunocytochemistry

Solutions

Triton-X-100 (Octylphenoxy polyethoxyethanol) (Sigma), 1x PBS, primary antibody: IgG-Rabbit-anti-Human [15mg/ml] (JRCashman Seattle Biochemistry Research Institute USA). Primary antibody: IgG-anti-Rabbit FMO3 using recommended dilution of 1/3000 (RM Philpot), Xam mounting medium, (BDH). From Vector laboratories an immunoperoxidase staining kit was used (Vectorstain® *Elite* ABC Kit), consisting of the following: Normal blocking solution (goat), crystalline grade BSA, biotinylated secondary antibody, avidin-biotin complex.

Colour development:3',3'-diaminobenzidine (DAB) substrate kit (refer to manufacturers instructions).

Fixative: 4% PFA/PBS.

Protocol

All incubations were carried out at room temperature in a covered humid box with minimal agitation.

Immunocytochemistry **(204)**, was performed on human brain tissue specimens which were fixed as for *in-situ* hybridisation, (method 3.7). The brain sections were incubated with primary antibody (FMO3) consisting of anti-Human Rabbit-IgG at a concentration of 15µg/ml in PBS containing 0.1% crystalline grade BSA. BSA was added to the antibody solution to prevent adsorption of the antibody to its storage container once diluted.

The fixed slide sections were washed in 1x PBS three times for 2 minutes each time. The cells were permeablised using 0.2% Triton-X 100 in PBS, for 5 minutes. This step was carried out to unmask the antigen in the cell so that antibody binding would be more effective.

The sections were rinsed in 1x PBS twice for 5 minutes. The sections were incubated with normal blocking solution for 30 minutes to 1 hour. The blocking solution consisted of 150µl normal goat serum in 10ml of PBS. Excess solution was drained from the sections and the sections were incubated with primary antibody for approximately 1 hour. Sections were washed in 1x PBS for 5 minutes. Incubation with biotinylated secondary antibody diluted in 1x PBS was for 30 minutes.

The ®ABC-*Elite* substrate was prepared and left at room temperature for 30 minutes prior to use. The biotinylated secondary antibody treated sections were washed in 1x PBS for 5 minutes. The sections were incubated with the ®ABC-*Elite* reagent for 30 minutes. Sections were washed in 1x PBS for 5 minutes. The treated sections were incubated with colour substrate (DAB) for 10-15 minutes. The color reaction was stopped by placing slide sections in water for 5 minutes. The sections were coated with Xam and covered with a glass coverslip **(205)**.

Control experiments consisted of:

a) omission of primary antibody, b) omission of primary and secondary antibodies and c) omission of secondary antibody. These were carried out concurrently.

3.9 Preparation of whole cell homogenates from human and primate brain tissue.

Solutions

Homogenisation buffer:

10mM Sodium phosphate buffer (pH7.25): 1M di-sodium hydrogen orthophosphate buffer (Na_2HPO_4); sodium di-hydrogen orthophosphate buffer (1M $NaH_2PO_4.H_2O$), pH the solution by adding 1M $NaH_2PO_4.H_2O$ to the 1 molar Na_2HPO_4 buffer until pH7.25 is reached, 1mM EDTA (pH 8.0), PhenylMethylSulfonylFluoride (PMSF) [0.2mM] (Sigma) giving a 4mM final concentration. 20% glycerol. Distilled water.

Protocol:

All procedures were carried out on ice. Brain tissue was kept at -70^{0}C. Tissue samples were homogenised by adding an equal volume of homogenisation buffer to sample. The tissue was placed in a chilled sterile beaker and cut up into small pieces. The tissue was transferred to a chilled sterile glass homogenisation tube. Initially, half the buffer was added to the homogenisation tube and the tissue was subjected to a series of gentle plunging movements by depressing and raising the glass rod. The remaining buffer was added to the homogenisation tube and the tissue was further ground up until a smooth constituency was achieved. The homogenate was transferred to a chilled sterile Eppendorf® and stored at -70^{0}C. The concentration of protein in the homogenate extracts was determined by a two point assay using the method of Lowry *et al* **(206)**.

3.9.1 Measurement of protein concentration

The method of Lowry *et al* (1951) using BSA Standard

Solutions

Reagent A: 2% Na^+/K^+ tartrate (w/v), 1% copper sulphate (w/v)(Sigma), 2% sodium carbonate made up in 0.1M NaOH (w/v). Mixed in a ratio of 1:1:100

Reagent B: Folin Ciocalteau phenol reagent 2.0N (Sigma), diluted in a ratio of 1:1.5 (v/v) with distilled water

BSA[1.23µg/µl], protein samples, 1 ml plastic cuvettes (Sarstedt), 4ml Rohren tubes (Sarstedt).

Protocol

BSA standard: Ten 4ml tubes were labelled 1 to 10, and a series of BSA-protein concentrations were set up from a stock solution at 1.23µg/µl. The concentration of the BSA protein in the samples ranged from: 0µg, 2µg, 4µg, 6µg, 10µg, 20µg, 30µg, 40µg, 50µg and 60µg. Distilled water was added to each Rohren tube to bring the final volume of the tube contents up to a maximum of 200µl. Standards were prepared in triplicate.

Within a 20 minute period 1ml of reagent A was added to each 200µl sample. After reagent A had been added to all samples they were then vortexed for a few seconds. The solutions were left to stand for the remainder of the 20 minutes. A timer was restarted and set for a period lasting 45 minutes. To each sample, 100µl of reagent B was then added. The Rohren tubes containing the samples were immediately vortexed. The samples were transferred to plastic cuvettes and left in the dark for the remainder of the 45 minutes. The cuvettes containing the samples were then placed in a Spectrophotometer and the absorbance was read at 700nm. A standard curve for BSA protein concentration against absorbance was drawn so that the concentration of protein in the homogenate samples could be ascertained.

Protein samples

Duplicate protein samples were prepared as for BSA standard. The concentration was determined by a two-point assay:

1 µl protein homogenate added to 199 µl water x 2 per sample

2 µl protein homogenate added to 198 µl water x 2 per sample

The assay was carried out at the same time as the BSA standard curve.

3.9.2 Protein analysis: Western blotting

Sodium dodecyl sulphate polyacrylamide gel electrophoresis (SDS-PAGE)

Solutions

Buffers:

1M Sodium phosphate buffer: (pH 7.25) (method 3.9), autoclave.

0.2/0.25M PMSF: Dissolve 1.742g of PMSF in to 50ml of ethanol (using a 37^{0}C water bath), aliquot into 1ml tubes and store at -20^{0}C.

pH8.8 Buffer (4x stock): 1.5M Tris, 0.4% SDS. pH the solution using HCl and autoclave. Store at room temperature.

pH6.8 Buffer (4x stock): 0.5M Tris, 0.4% SDS. pH the solution using HCl and autoclave. Store at room temperature.

Protein loading buffer (2x): 1% SDS, 10mM EDTA, 10mM sodium phosphate buffer (pH 7.25), 1% β-mercaptoethanol (BDH), 15% (v/v) glycerol, 0.01% Bromophenol blue (BioRad), 4mM PMSF at a final concentration of 0.2M. The solution was filter sterilised using a 0.45µm nitrocellulose filter and stored at -20^{0}C.

Electrophoresis running buffer: (1.5 litres) 21.62g glycine, 4.54g Tris base, 1.5g SDS, water.

Stacking gel (3%) acrylamide:

2ml of protogel (National Diagnostics): 30% (w/v) acrylamide, 0.8% (w/v) Bis-acrylamide stock solution. 5ml pH 6.8 buffer, 200µl 10% ammonium peroxodisulphate (APS), (BDH) made up in distilled water, 12.78ml water, 20µl Temed. Amount of protogel to be used was calculated according to manufacturer's instructions: Vp = (% gel) x (volume of solution in ml) / 30%.

For a 20ml solution:

2ml of protogel was poured into a glass beaker containing a magnetic stirrer, to which 5ml of pH 6.8 buffer and 12.78ml of water was added. 200µl of 10% (APS) was then added to the solution and 20µl of Temed. The solution was then stirred. The solution was immediately poured into a protein gel-casting apparatus to a marked position 1cm from the base of the teeth of the comb. The gel was overlaid with 0.1% SDS to prevent drying out.

Separating gel (10%) acrylamide:

16.67ml of Protogel, 12.5ml of pH8.8 buffer, 0.5ml 10% (APS), 20.28ml water, 50µl Temed. (Prepared as for 3% above).

Prestained SDS-PAGE Standards (Broad Range) (BioRad).

Protocol

A vertical gel casting system (BioRad), was assembled. Two glass plates separated by 1.5mm spacers were used for casting a 10% separating gel. Combs were placed between each set of glass plates. A distance of 1cm below the teeth of the comb was marked on the outer side of the plates. The combs were removed and the separating gel was prepared and poured in to the gel apparatus up to the mark indicated on the outer side of the glass plate. The gel solution was overlaid with 0.1% SDS, covered in cling-film and left to set. Once set the SDS overlay was poured off and the stacking gel was prepared (as above). The gel was poured into the casing system on top of the separating gel and the comb was manoeuvred so that it was central to the gel. The gel was left for approximately 1 to $1^{1}/_{2}$ hours until ready for use. Once the stacking gel is set, the gel case is immersed in running buffer up to one inch above the foot of the gel casting apparatus. The remaining buffer was poured into the top of the gel case covering the electrodes and comb. The comb was removed allowing the buffer to enter the spaces and the wells were washed out with running buffer using a 10ml syringe.

Preparation of samples

Protein homogenates were removed from the -70^{0}C freezer and diluted to the desired concentration with distilled water in a sterile Eppendorf. The sample

was then diluted 1:1 with 2x protein loading buffer. Samples were mixed by gentle vortexing and then centrifuged, briefly, in an Eppendorf bench centrifuge. The lid of the Eppendorf tubes were pierced with a needle and the samples were boiled for 3 minutes. The samples were removed from the heat and 3µl β-mercaptoethanol added to each tube. The tubes were centrifuged in a bench centrifuge for a few seconds before loading on to the gel. Molecular weight markers were prepared by adding 5µl of protein standards to 5µl of water and 10µl of 2x loading buffer for a 20µl total volume. Control samples consisted of FMO3 protein expressed in E.*coli* cells. The molecular weight markers and control samples were boiled along side the protein samples and treated in the same way. The gel was electrophoresed at 50mA (stacking) until the samples had passed through the stacking portion of the gel into the separating section. The current was then increased to give 75mA (for separation), until the dye was approximately 1cm from the end.

3.9.3 Staining of protein (SDS-PAGE) gels using Coomassie Brilliant Blue

Solutions

Coomassie stain (BDH): 0.2% (w/v) brilliant blue R. 10% (v/v) glacial acetic acid, 45% (v/v) water, 45% (v/v) methanol. Brilliant blue R. stain was dissolved in a solution consisting of a 1:1 volume of methanol and water. Glacial acetic acid was added and the solution was stirred. The stain was stored at room temperature.

Coomassie destain: 10% (v/v) glacial acetic acid was added to a solution of 45% (v/v) methanol and 45% (v/v) water. The solution was stored at room temperature.

Protocol

The gel to be stained was transferred from the gel running apparatus to a plastic storage container. The Coomassie stain was poured over the gel and the container sealed. The gel was left to soak overnight before pouring off the stain and replacing it with the destain solution. The box containing the gel was placed on an orbital shaker at room temperature. When the destain solution became saturated it was replaced with fresh solution. This procedure continued until only the protein bands in the gel were visible. The gel was later photographed for reference.

3.9.4 Transfer of proteins to a nitrocellulose membrane

Solutions

Transfer buffer: (3 litres) 42.42g glycine, 9.09g tris base, 600ml methanol, water. Hybond nitrocellulose membrane (BDH), Whatman 3MM paper.

Protocol

Transfer buffer was made up and poured into two lunch-box type containers. Hybond nitrocellulose filter paper, and 4 pieces of Whatman 3MM paper (per gel), were cut to fit the size of the gel. The membrane and Whatmann paper were immersed in the transfer buffer in one of the lunch-box containers. The second container was used to soak four Scotch blotting pads to be used in the overnight transfer. Once fully soaked two blotting pads were removed and placed on top of a perforated plastic hinged case (BioRad Transfer Blot Cell System). Two pieces of the Whatman paper were placed on top of the pads. During this time the gel case was dismantled. The top glass plate was carefully removed and the gel was positioned over the Whatman paper. The gel was gently transferred on to the Whatman paper and then the nitrocellulose membrane was placed on top of the gel. Air bubbles were removed by placing a 10 ml pipette on top of the membrane and employing a gentle rolling action. The remaining two sheets of saturated Whatman paper were placed on top of the membrane. The remaining scotch blotting pads were placed on top. The plastic transfer case was closed and placed in the transfer tank (BioRad), such

that the nitrocellulose membrane was closest to the anode for protein transfer. The tank was filled with the remaining buffer and a current of 100mA was set for overnight transfer. After 24 hours the current was increased to 200mA for one hour before removal of the gel and membrane **(207)**.

3.9.5 Probing a Western blot and visualisation of antibody binding using BioRad Immuno-blot Assay Kit

Solutions

5x TBS (pH7.5): 200mM Tris, 5M NaCl, were added to ~800 ml of distilled water. The pH of the solution was adjusted using HCl and autoclaved. The solution was diluted 1/5 with distilled water for a working solution of 1x.

1x TTBS: 20mM Tris, 500mM NaCl, 0.05% Tween-20 (pH 7.5), (polyoxyethylene sorbitan monolaurate)(BioRad). For every 500ml of 1x TBS, 250µl of Tween-20 were added.

Blocking solution: Gelatin EIA grade (BioRad) 3% (w/v) in TTBS. 3g of gelatin was added to 100ml of TTBS. The solution was heated up in a microwave to below boiling point and cooled at room temperature.

Primary antibodies: Antibody to detect FMO3 specifically (provided by JR Cashman) was diluted in 1x PBS to give a working concentration of 15µg/ml. The antibody to detect FMO1, 2, 3 and FMO5 (provided by RM Philpot) was diluted in 1x TTBS to give a working concentration of (method 3.8).

Secondary antibodies: For detection using the Philpot primary antibody: Anti-goat IgG conjugated to alkaline phosphatase (AP). Antibody raised in rabbit (Sigma): 3.33µl of Anti-goat IgG was diluted into 100µl of 1x TBS.

For detection of FMO3 using the Cashman primary antibody: Goat-anti-rabbit IgG conjugated to alkaline phosphatase, (BioRad): 33µl of Goat-anti-rabbit IgG was diluted into 100µl of 1x TBS.

Colour developing solution: Alkaline phosphatase conjugate substrate kit (BioRad) containing: reagent A (nitroblue tetrazolium in aqueous

dimethylformamide (DMF) containing MgCl), and reagent B (5-bromo-4-chloro-3-indolyl phosphatin in (DMF)).

25x (AP) development buffer (BioRad).

2ml of (AP) colour development buffer was added to 48ml of distilled water. To this solution 500ml of reagent A and 500ml of reagent B. was added. The solution was mixed by shaking and immediately poured over the blot.

Protocol

The nitrocellulose membrane was removed from the gel transfer system and washed in 1x TBS for 5 minutes. The membrane was incubated with blocking solution for between 30-60 minutes. The membrane was incubated with primary antibody for approximately one hour. The membrane was washed in 1x TTBS (twice) for 5 minutes each time before incubation with secondary antibody for approximately one hour. It was then washed in 1x TTBS (twice) for 5 minutes each time and then in 1x TBS for 5 minutes. Alkaline phosphatase (AP) colour developing solution was prepared (as above) and immediately poured over the membrane. Colour was developed and the reaction stopped as appropriate by immersing the membrane in fresh distilled water containing 0.5M EDTA.

Washes and incubations were performed using a shaking platform at room temperature **(207, 208)**.

3.10 Reverse Transcriptase Polymerase Chain Reaction (RT-PCR)

Sterile conditions were observed at all times during this procedure. Gloves were changed frequently and all pipetting was carried out using irradiated aerosol resistant tips (Art Tips), (Molecular. Bio. Prods). All pipetting was performed in a fume cupboard.

Primers:

All primer pairs have been designed such that the 3' primer lies within the 3' non-coding sequence. The 5' primer lies upstream of the last intron, based on

the known gene structures of *FMO1* and *FMO3*. Each primer has a G or a C at its 3' and 5' ends. Each primer within the pair is of the same length, and in so far as possible has the same GC content. The primers have been checked for sequence similarity to all five FMOs. Primers were synthesised by Pharmacia.

FMO1 5' primer 18 nucleotides, 9 G/C 137.45 [pmoles/µl]; 3' primer 18 nucleotides, 10 G/C 172.11 [pmoles/µl]. PCR product of size 615 bp expected.
FMO2 5' primer 19 nucleotides, 9 G/C 139.89 [pmoles/µl]; 3' primer 19 nucleotides, 9 G/C 143.48 [pmoles/µl]. PCR product of size 464 bp expected.
FMO3 5' primer 19 nucleotides, 8 G/C 150.62 [pmoles/µl]; 3' primer 20 nucleotides, 9 G/C 167.94 [pmoles/µl]. PCR product of size 447 bp expected.
FMO4 5' primer 20 nucleotides, 10 G/C 146.57 [pmole/µl]; 3' primer 20 nucleotides, 10 G/C 220.58 [pmoles/µl]. PCR product of size 449 bp expected.
FMO5 5' primer 19 nucleotides, 10 G/C 182.34 [pmoles/µl]; 3' primer 18 nucleotides, 10 G/C 163.38 [pmoles/µl]. PCR product of size 544 bp expected.

Primer sequences (see table 8):

FMO1 **5'** GCT CAG AGT GCT GTC AAG - **3'**
3' GCT ACT GCA AGG CTT TAC - **5'**
FMO2 **5'** GTG AAG ATG GCA TTT CTG G - **3'**
3' CCC TCC CTT GAA GAT TCA C - **5'**
FMO3 **5'** GAG TAC TGC AAA AGA TGC - **3'**
3' GAC CAT ACA GAC AGA TTA C - **5'**
FMO4 **5'** GGG ATG CAC AAG ATA CTT GG - **3'**
3' GCC TAC ATG GAT GAT ATC GC - **5'**
FMO5 **5'** CAG GGC AGT GAC AAT AGG - **3'**
3' CTG GAA AGG CCA ACT CTT G - **5'**

Solutions

MuLV RT enzyme: (Moloney Murine Leukemia Virus Reverse Transcriptase), 5000 units /100ml (Perkin Elmer), 10x MuLV RT buffer (Perkin Elmer).

10mM dNTP Blend (Gene Amp®, Perkin Elmer), Total RNA, DTT at a final concentration of 10mM, RNA guard, BSA, sterile irradiated distilled water.

Reverse primers [10 pmole/µl], (Pharmacia): solutions of [10 pmole/µl] per primer were prepared by calculating the following:

10 pmole ÷ primer concentration x 100. This was then diluted into 100µl of sterile irradiated distilled water.

Protocol (209)

To a sterile Eppendorf tube sterile irradiated distilled water was added along with RNA and reverse primer. The tubes were covered with approximately 50µl of irradiated filter-sterile paraffin. The samples were incubated at 65^{0}C for 10 minutes in PCR machine (Hybaid Thermal cycler). The tubes were removed and the following components were added through the paraffin layer: dNTP's, 10x buffer, DTT, RNAguard, BSA and MuLV RT enzyme.

The samples were incubated at 37^{0}C for 90 minutes and at 65^{0}C for a further 10 minutes. Samples were removed from PCR machine and the bottom RT layer removed using ART tips. The RT samples were transferred to sterile irradiated Eppendorf tubes. Two volumes of irradiated ethanol were added to the RT samples before leaving them on dry-ice at -70^{0}C for 30 minutes. The Eppendorf tubes containing the samples were centrifuged in an Eppendorf bench centrifuge 5414 S for 10 minutes at room temperature. The resulting pellet was air dried and resuspended in 50µl of filter-sterile irradiated distilled water. The RT-samples were stored at -20^{0}C.

3.10.1 "Hot Start" Reverse Transcriptase Polymerase Chain Reaction (RT-PCR)

Solutions

Gene Amp® XL PCR kit (Perkin Elmer) containing:

*r*Tth DNA polymerase, XL. 3.3X XL buffer II, 25mM magnesium acetate $Mg(OAc)_2$ solution, Gene Amp® 10mM dNTP Blend.

Sterile irradiated distilled water. AmpliWax® PCR gems (Perkin Elmer). Primers (forward and reverse).

Protocol

For a 100µl reaction.

Into a sterile irradiated Eppendorf the following components were added to form two layers.

lower reagent mix:

3.3X XL buffer II (12µl), 10mM dNTP blend (8µl), Primer 1.(4µl), Primer 2. (4µl), $Mg(OAc)_2$ (6µl), sterile irradiated distilled water (6µl). Samples were vortexed and 1 AmpliWax® bead was added per Eppendorf tube. The samples were heated in a PCR machine to 80^0C for 10 minutes then cooled to room temperature ~ 5 minutes.

The Upper reagent mix

The following components was added to the Eppendorf tubes:

3.3X XL buffer II (18µl), *r*Tth DNA polymerase (1µl), sterile distilled water (1µl). The reverse transcribed (RT) sample was pre-diluted in sterile distilled irradiated water to a volume of 40µl. Approximately 10µl of RT sample was added to 30µl of water. The tubes were gently tapped to mix contents before placing in a PCR machine.

The PCR cycle for amplification consisted of the following programme:

DNA denaturation step at 94^0C for 1 minute. This was followed by incubation at an annealing temperature specific to the five different FMO primers.

Extension at 72^0C for 1 minute 15 seconds. Plus 1 second added per cycle for 30 cycles.

Annealing temperature

For each primer the appropriate annealing temperature was calculated using the formula below:

$$Tm^0C = 69.3 + (0.41 \times (G+C)\ \%) - 650 \div \text{length}$$

Where the Tm represents the melting temperature for the base pair duplex, and length represents the total number of bases in the oligonucleotide.

Electrophoresis of RT-PCR products was performed using a 1% agarose gel in 1x TBE (method 3.2.3).

3.10.2 First strand synthesis of cDNA from RNA

Solutions

RNasin (20 Units/µl), Random hexamer primers (Gibco), 10x MuLV RT buffer (Perkin Elmer). RNA.

Protocol

This protocol is based on a method adapted from RA Gibbs *et al* **(210, 211)**.

The following components were added to a sterile Eppendorf tube:

1-5µg RNA (3µl), 0.75µl Rnasin (14 Units),1µl of stock solution N6 random primers (10µg), 10x MuLV RT Buffer 1.5µl, Water up to 15.5µl

The reaction mix was heated for 1 minute at 95^0C, then chilled on ice at room temperature. To this mix the following reagents were added:

dNTP at 25mM	2µl
Rnasin (14 Units)	0.75µl
MuLV RT reverse transcription (12 units)	1µl

The mix was incubated for one hour at 37^0C after which time 30 µl of 0.7M NaOH / 40 mM EDTA mix was added. This was then incubated at 65^0C for 10 minutes, after which the following reagents were added:

2M ammonium acetate pH 4.5	(5µl)
100% Ethanol	(130µl)

The mix was chilled for a few minutes then centrifuged at 4^0C in an Eppendorf 5414S bench centrifuge for 10 minutes. The resulting pellet was washed in 200µl of 100% ethanol and re-centrifuged at 4^0C before drying at room temperature. The pellet was then resuspended in 50 µl sterile water.

3.11 Southern blotting of PCR products

Solutions

1M NaCl, 0.5M NaOH, 0.5 Tris (pH7.4), 1.5M NaCl, 20x SSPE, Supported Nitrocellulose membrane (BDH), Whatman 3MM blotting paper, distilled water

Denaturation solution: 1M NaCl, 0.5M NaOH,

Neutralisation solution: 0.5 Tris (pH7.4), 1.5M NaCl.

Transfer buffer: 10x SSPE solution,

Protocol

Samples of PCR-products from Human and Orang-utan brain (method 3.10.2), were electrophoresed at ~100 volts on a 1% agarose gel in 1xTBE (method 3.2.3). Electrophoresis was continued until the loading dye was approximately 1-2 cm from the end. The agarose gel was removed from the electrophoresis buffer and denatured by placing in a Tupperware box containing 1M NaCl and 0.5M NaOH, at room temperature **(212)**. The box containing the gel was placed on a slow rotating orbital shaker for 20 minutes. The solution was carefully poured off and the step repeated. The gel was rinsed in distilled water before placing it in a Tupperware box containing neutralisation solution at room temperature for 20 minutes. This step was repeated once. The nitrocellulose membrane was prepared by wetting with distilled water before soaking in transfer buffer. Hybridisation was carried out by means of capillary transfer. A large Tupperware container was used as a basin reservoir for the system. Into the Tupperware container a small box was placed at 2 cm above the buffer line. A glass plate was placed on top of the box and 3 pieces of filter paper 10cm longer than the glass plate previously soaked was placed on top. The gel was inverted and placed on top of the filter paper, and the membrane placed on top of the gel. Five pieces of thick dry filter paper cut to the size of the gel were placed on top of the apparatus before compressing with a heavy weight. The apparatus was covered with cling film and left at room temperature overnight.

Following blotting, the gel and membrane were inverted on a dry piece of Whatman paper and the wells marked with a soft pencil. The membrane was placed between 2 sheets of filter paper and baked in the oven at 80°C for 2 hours. The blot was hybridised as described in section (3.6.1).

3.12 Sequencing of PCR products (FMO3)

Sequencing of FMO3 PCR-products was carried out in the Department of Biology & Genetics at UCL using an automated sequencer.

Chapter Four

Results and Discussion

4.1 Northern blot analysis of brain mRNAs

The preliminary analysis of the expression of FMO mRNAs in human brain was carried out using Northern blotting. This is a technique which enables us to determine whether or not a mRNA of interest is present within a particular tissue. Northern multiple tissue blots (MTB) of various human brain regions were purchased from Clontech. These consisted of RNA from 7 different regions of the human brain: *amygdala, caudate nucleus, corpus callosum, hippocampus, substantia nigra, subthalamic nucleus, thalamus* and *whole brain.* Each RNA sample was from a pool of individuals. The blots were used in northern hybridisation studies with cDNA probes specific for human FMO1, FMO2, FMO3, FMO4 and FMO5 mRNA (method 3.6.2). The blots were prepared by electrophoresing 2μg of polyA$^+$ RNA for each brain region and from whole brain, on a 1.2% denaturing formaldehyde/agarose gel. This was then blotted on to a positively charged nylon membrane.

FMO 1

Hybridisation of a northern (MTB) blot with [^{32}P] radiolabelled cDNA, encoding FMO1 mRNA, demonstrated the absence of FMO1 mRNA in the human brain regions analysed. (figure 4.1a). The negative control RNA was from adult human liver. The FMO1 isoform has so far only been detected in foetal tissues **(129)** and adult kidney and skin **(130)** in humans. However, experimental work on rodent brain has confirmed FMO1 expression in this tissue **(159,164,167)**. A positive RNA control for FMO1 expression was unavailable. However, absence of hybridisation of FMO1 radiolabelled cDNA probe to the (MTN) blot and control confirmed that FMO1 was not expressed at the RNA level in these brain regions.

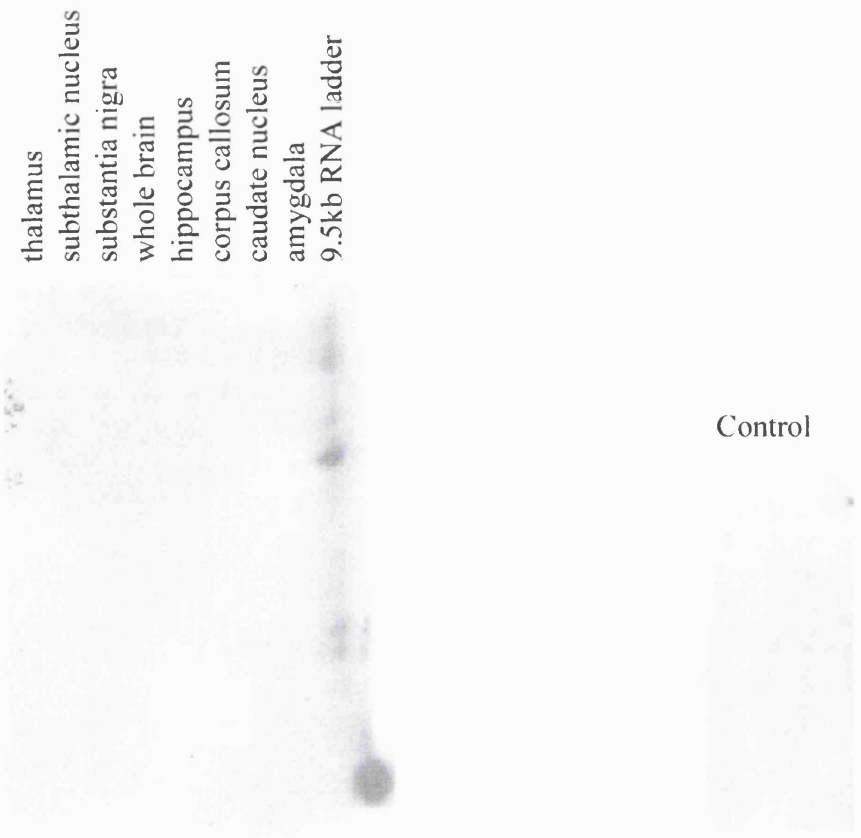

Figure 4.1a Northern blot (MTB) of 7 different regions of the human brain and whole brain. Each lane contains 2µg of poly A+ RNA. Hybridisation of cDNA probe encoding FMO1 isoform is not observed in any of the regions. The control blot contains 10µg human total liver RNA immobilised on to a nylon membrane. The negative control blot shows no hybridisation of FMO1 cDNA to probe RNA.

FMO 2

The (MTB) blot of human brain tissue was probed with [^{32}P] labelled cDNA specific for the FMO2 isoform. The resulting autoradiograph shows the absence of this isoform in the brain sections analysed (figure 4.1b). The positive control used was adult human lung RNA (figure 4.1b). FMO2 is the major isoform found in human lung although the protein for this isoform is not expressed **(99).** The positive result in the control dot blot demonstrates that the hybridisation conditions were correct and confirms the negative result obtained for the RNA isolated from human brain. However, Bhagwat *et al* in their research have suggested that human brain microsomes contain FMO2 **(166,167)**. This is a result which has not been confirmed by other groups working in the field and it remains a contentious analysis since FMO2 is not expressed in man.

FMO 3

A [^{32}P] labelled cDNA probe encoding the FMO3 isoform was used to reprobe the (MTB) blot of the various brain regions. The resulting autoradiograph from the (MTB) blot revealed the presence of three positive signals (figure 4.1c). The hybridising RNAs were from the *thalamus, subthalamic nucleus* and the *substantia nigra*. The hybridising band was estimated to be approximately 1.75 kb in length. This was determined from a standard curve using the Clontech 9.5kb RNA ladder as standards. The size of the FMO3 mRNA detected was very similar to that of FMO3 mRNA in liver (1.8kb). The band in lanes 1 and 2 (thalamus and subthalamic nucleus, respectively) are of a similar intensity, both leaving a darker trace than the band in lane 3 (substantia nigra). However, this difference may be inconsequential bearing in mind the fact that RNA used in the production of the (MTN) blot is from a pooled source of individuals varying widely in age and sex. The differences in band intensities may well be of no significance. The resulting autoradiographs for FMO3 mRNA also indicate the

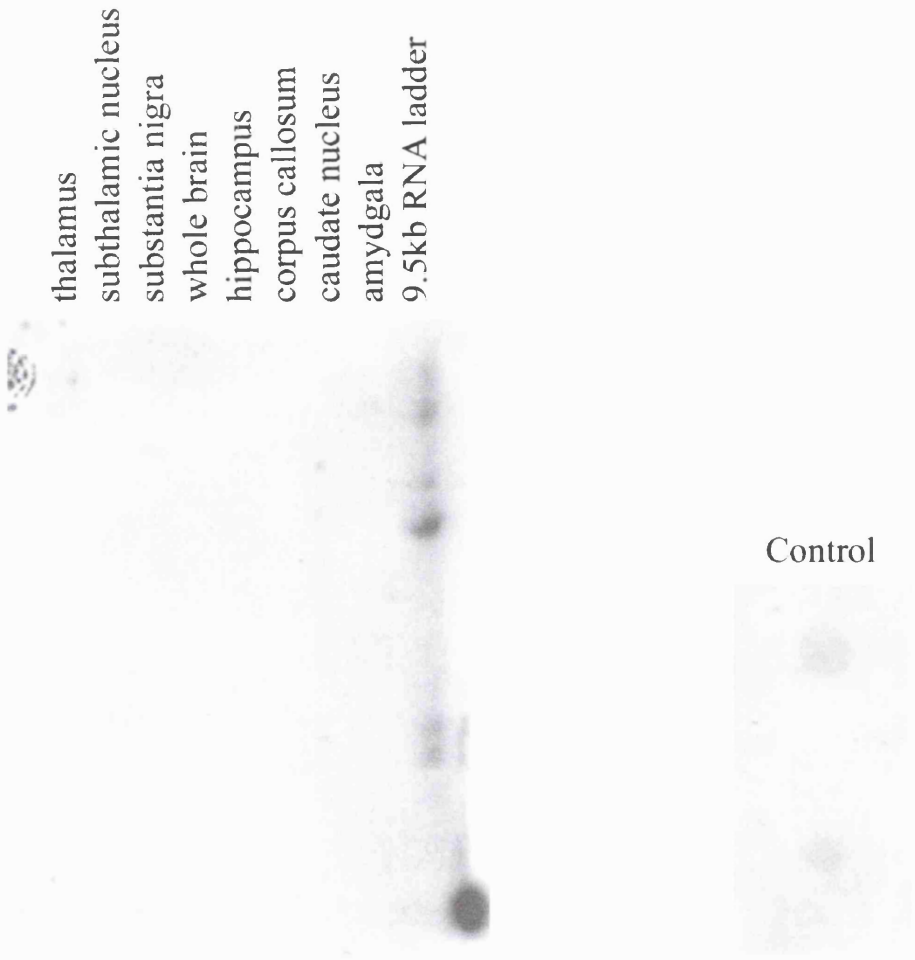

Figure 4.1b Northern blot (MTB) of 7 different regions of the human brain and of whole brain. Lanes 1 -8 contain 2µg polyA+ RNA. Hybridisation of cDNA probe encoding FMO2 isoform is not observed. The positive control blot contains 10µg adult marmoset lung total RNA immobilised on to a nylon membrane. The control blot shows binding of the cDNA probe encoding FMO2 isoform to lung RNA.

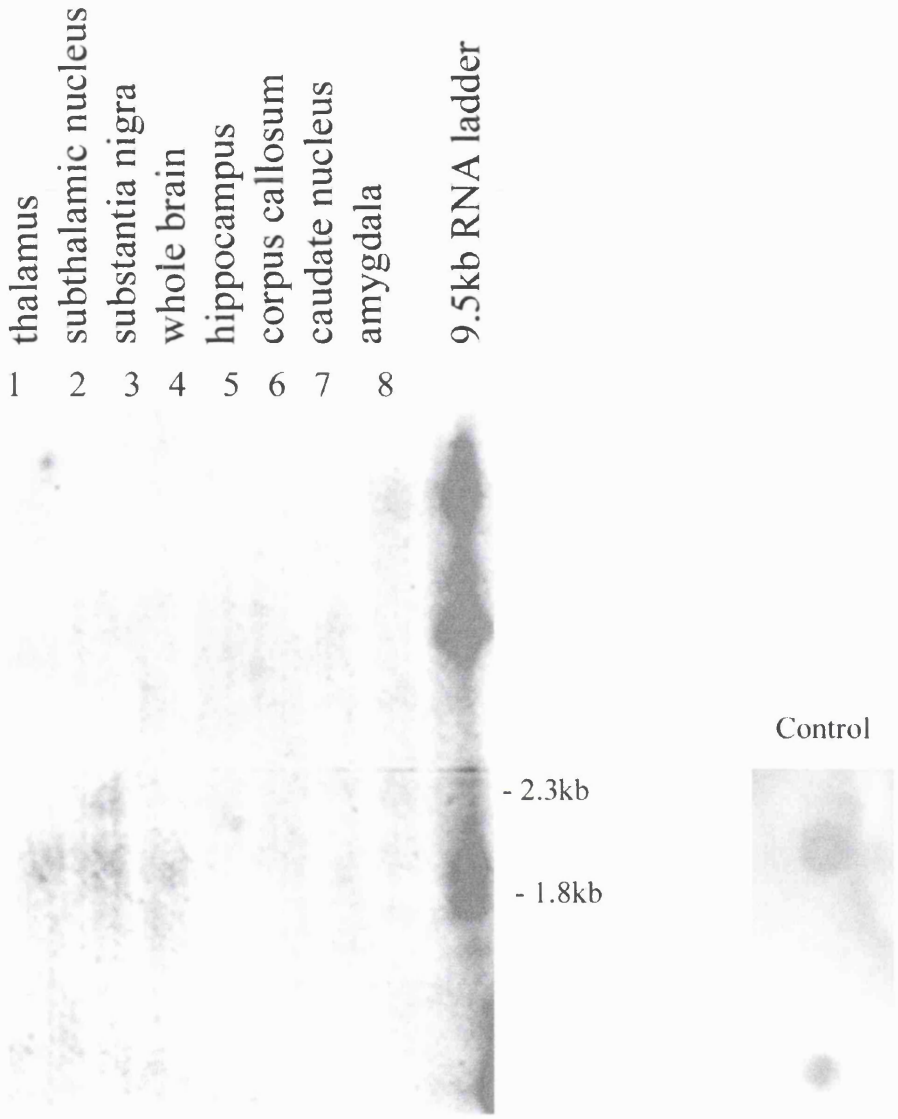

Figure 4.1c Northern blot (MTB) of 7 different regions of the human brain and whole brain. Lanes 1-8 contain 2µg polyA+ RNA. Hybridisation is observed for cDNA probe encoding FMO3 isoform (lanes 6,7,8), see text. The control blot contains 10µg adult human liver total RNA immobilised on to a nylon membrane. The positive control shows hybridisation of cDNA probe encoding FMO3 isoform to liver RNA.

presence of a second band corresponding to a size of approximately 2.3 kb. This band occurs only in lane 2 to which RNA from the subthalamic nucleus has been immobilised. The band occurred in multiple probings of the (MTB) blots regardless of changes made in the stringency of washes after hybridisation. The precise nature and significance of this band is unknown, but the possibility of an alternatively spliced product cannot be ruled out since multiple bands in the liver have been identified for FMO3 isoform by others **(49,53)**. However, the possibility remains that it may be an artefact of the northern hybridisation process in this particular case.

The positive control used for FMO3 was RNA from adult human liver. FMO3 is thought to be the major isoform expressed in human liver **(44,54,106)**, and so is expected to give a positive signal upon hybridisation with the [^{32}P]radiolabelled cDNA encoding FMO3. The resulting autoradiograph demonstrates that the cDNA probe is specific for FMO3 and that the hybridisation conditions were correct. It confirms the positive result obtained for RNA isolated from human brain.

FMO 4

Hybridisation of the (MTB) northern blot with [^{32}P] radiolabelled cDNA encoding FMO4 indicated the presence of FMO4 mRNA in the human brain. The autoradiograph shows a band in four different lanes (fig 4.1d). The bands occur at a position that correspond to size 2.3 kb against the Clontech 9.5kb RNA ladder. The size of the full length FMO4 in human liver is 2.2 kb and the position of the band signal on the autoradiograph corresponds closely to this. The bands indicate hybridisation of probe to the thalamus, subthalamic nucleus, substantia nigra and the corpus callosum RNAs. FMO4 isoform is constitutively expressed in all human tissues **(44)**, but at very low levels. The very low level of expression indicated by the presence of only faint positive signals suggests that, like in other tissues, the expression of FMO4 isoform in

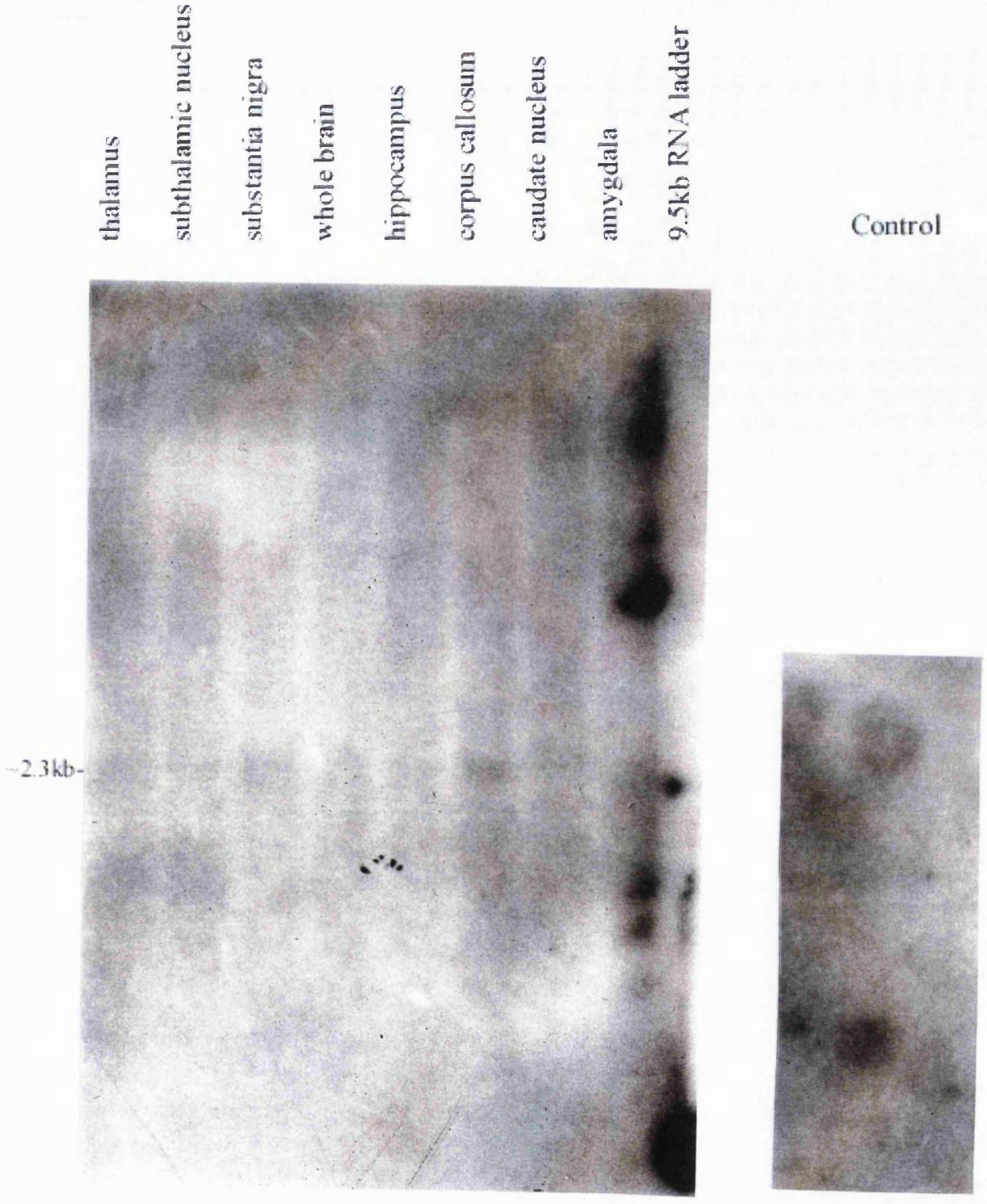

Figure 4.1d Northern blot (MTB) of 8 different regions of the human brain and of whole brain. Lanes 1-8 contain 2µg poly A+RNA. Hybridisation of cDNA probe encoding FMO4 isoform can be observed in four regions (lanes 8,7,6,3). The positive control blot contained 10µg of adult human liver RNA immobilised on to a nylon membrane. The control blot shows hybridisation of cDNA probe encoding FMO4 isoform.

brain is low. The positive control used consisted of an RNA dot blot of adult human liver. The control demonstrated the specificity of the FMO4 cDNA probe, and the low level expression of this isoform in human liver was as expected. Research by Philpot and Blake **(168)** has also confirmed the presence of FMO4 in brain. Blake *et al* used PCR techniques to determine FMO4 expression in the rabbit brain concluding that rabbit FMO4 isoform was expressed at the mRNA level.

FMO 5

Detailed information regarding the FMO5 isoform is still in its infancy, however, it is known that FMO5 is found predominately in adult human liver **(106)** but to a lesser degree than isoform FMO3. The [^{32}P]radiolabelled cDNA probe encoding FMO5 was hybridised to the (MTB) blot alongside a control blot consisting of human liver RNA. The resulting autoradiograph revealed the absence of a signal in all lanes of the human brain tissue blot (fig 4.1e). However, a signal corresponding to the binding of the cDNA probe specific for this isoform was present in the control blot. This result served to confirm the integrity of the cDNA radiolabelled probe in terms of activity and specificity, as well as to confirm the absence of FMO5 isoform from human brain tissue in the regions analysed at the RNA level.

In conclusion the overall results of the northern blots indicate expression of FMO3 and FMO4 in human brain tissue at the RNA level. However, FMO1, FMO2 and FMO5 seem not to be expressed in these specific regions at the RNA level (see table 5). With reference to FMO3 and FMO4 there are a number of points that are worth comment. Firstly, both isoforms gave positive results in the thalamus, subthalamic nucleus and substantia nigra. The expression pattern of FMO4 differed only in its expression in an additional

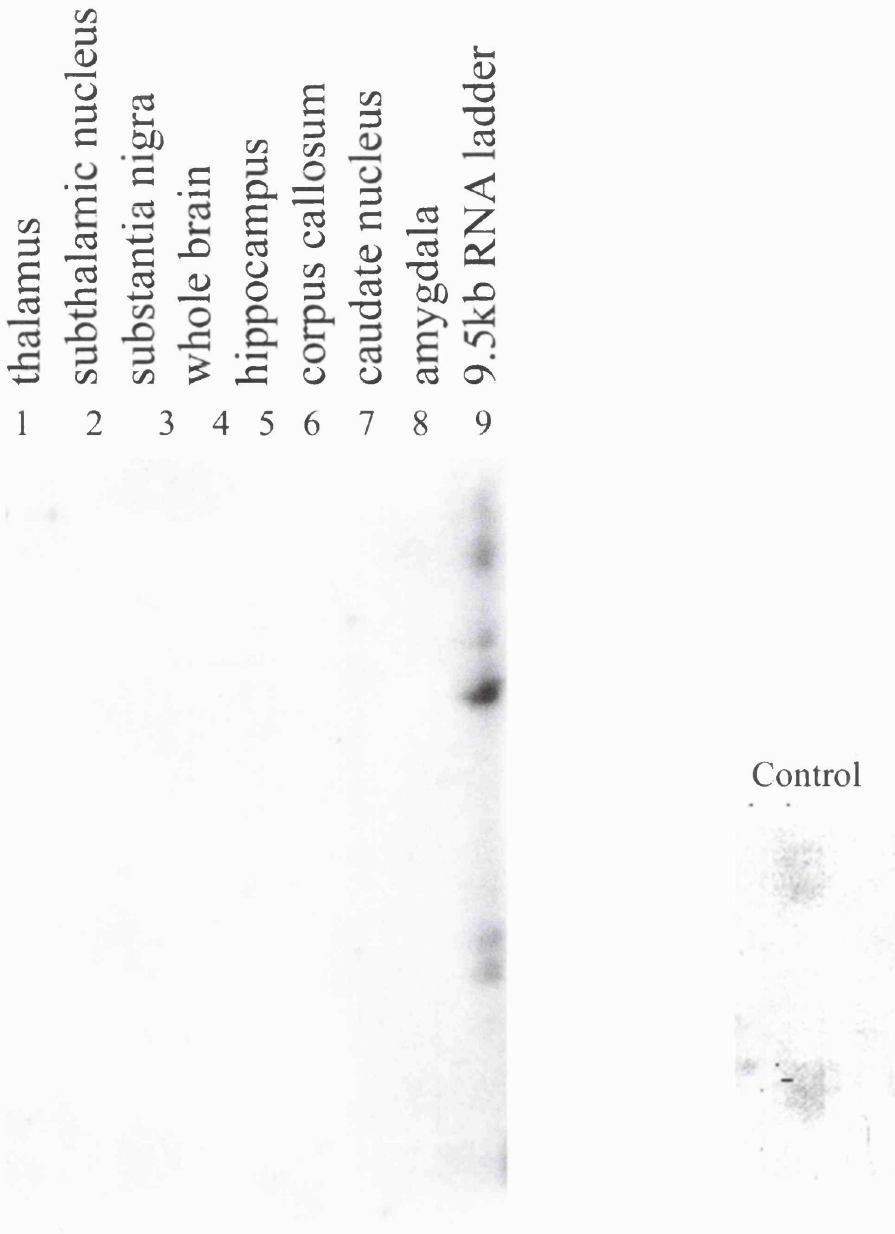

Figure 4.1e Northern blot (MTB) of 7 different regions of the human brain and whole brain. Lanes 1-8 contain 2µg poly A+ RNA. Hybridisation of cDNA probe encoding FMO5 isoform is not observed in any of the regions. The control blot contains 10µg human liver total RNA immobilised on to a nylon membrane. The control blot shows binding of cDNA probe encoding FMO5 isoform to liver RNA.

region, the corpus callosum. Secondly, FMO4 expression indicated a transcript at a position corresponding to a size of approximately 2.3 kb, whereas the FMO3 transcript was approximately 1.75 kb. However, there is an exception to this in lane 2 (subthalamic nucleus region) (fig 4.1c), where the FMO3 probe hybridises to two transcripts of approximately 1.7 kb *and* 2.3 kb. This second result begs the question are the two transcripts for both isoforms at position 2.3 kb coincidental, or could this be an isoform with similarities to both FMO3 and FMO4, since these isoforms are the only ones to give positive results in these experiments ? Under the hybridisation and washing conditions used, it is unlikely that the 2.3 kb transcript in lane 2 (figure 4.1c) is due to cross hybridisation of the FMO3 cDNA probe to FMO4 mRNA.

Northern blotting using cDNA probes specific for FMO isoforms allowed a preliminary analysis of their expression in human brain tissue. Limitations associated with northern blotting is largely the degree of sensitivity that can be achieved. The technique is sensitive enough to allow confirmation of the presence of a particular gene product expressing the RNA of interest, as well as an estimation of mRNA length. However, a cautionary remark on the specificity of the control dot blots for northern analysis has to be noted at this point. Due to lack of human mRNA control blots consisted of dot blots of RNA. In northern blotting the mRNA population is separated according to size by gel electrophoresis and any cross hybridizing species is therefore separated from the mRNA of interest. However, with a dot blot, because electrophoresis has not occurred an assumption is made that the hybridisation signal is all due to the mRNA of interest.

A second method, *in-situ* hybridisation, which will allow visualisation of the specific cell type(s) responsible for mRNA expression within tissues forms the basis of a more specific series of investigations.

FMO	Amygdala	Caudate nucleus	Corpus callosum	Hippocampus	Whole brain	Substantia nigra	Subthalamic nucleus	Thalamus.
FMO1								
FMO2								
FMO3						++	+++	+++
FMO4			++			+	+	+
FMO5								

Table 5. Northern blot analysis of adult brain tissue (human) Probed using [^{32}P]α dCTP labelled cDNA for FMOs 1-5. Specific activity in each case was ~ 7x10^{8}cpm/μg, (+) indicates relative abundance.

4.2 Cell-specific expression of FMO3 and FMO4 using *In situ* hybridisation

A major advantage of using *in situ* hybridisation as a means of analysis is its ability to dramatically visualise and outline the distribution of a given mRNA and to identify the precise area of expression of an RNA within a given tissue. Patterns of dispersion of that RNA within a specific tissue as well as determination of the cell type in which its expression occurs is detected by this technique. For this reason this method was employed as a means of identifying those cell types expressing FMO3 and FMO4 mRNAs in human brain. Only these two FMO mRNAs were analysed in this way. This is because cDNAs for these two FMOs gave a positive hybridisation signal when northern blotting was carried out (section 4.1), and human brain material was very scarce.
It was first necessary to prepare DNA constructs that could be used to synthesize antisense and sense riboprobes for FMO3 and FMO4 mRNAs.

Sense and antisense RNA probes were transcribed *in vitro* using pBluescript KS II plasmid into which an insert of the sequence of interest had been sub-cloned (method 3.7.1). The strategy for producing an FMO3 antisense probe is shown in (figure 4.2a). cRNA sense and antisense probes were generated for FMO isoforms 3 and 4 using either RNA polymerase T3 or T7 (method 3.7.3). Non-specific binding was kept to a minimum by ensuring that the transcripts were free of contaminating vector sequence. This was achieved by digesting the template using the appropriate restriction enzymes downstream of the insert and by treating the RNA probes with DNase I.
Coronal sections of the *basal ganglia* and cross sections of the *midbrain* including the substantia nigra were used in tissue specific *in situ* hybridisation analysis (method 3.7.5). The basal ganglia comprise of the substantia nigra, subthalamic nucleus, caudate nucleus and lentiform nucleus. The lentiform nucleus forms rows of connecting fibres crossing the internal capsule, and are

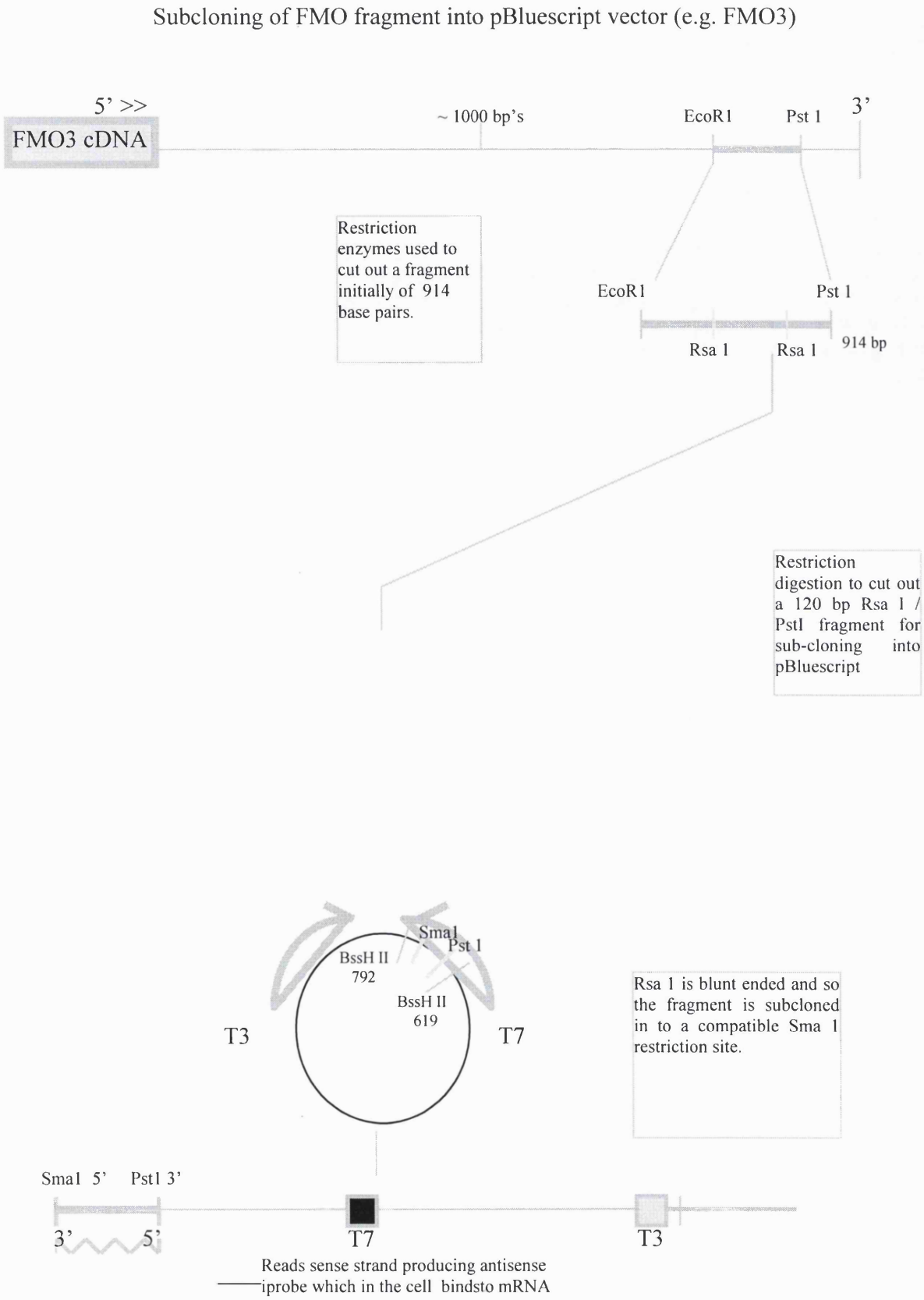

Figure 4.2a Subcloning of an FMO3 fragment in to pBluescript KS II to produce a cRNA riboprobe for use in *in situ* hybridisation.

collectively known as the corpus striatum. The corpus striatum connects also with the substantia nigra and thalamus (see figure 2.1).

The brain sections analysed were prepared by Louise Bray of the Parkinson's Disease Brain Bank, London. The individuals analysed consisted of a group made up of both Parkinson's and non-Parkinson's patients, and their conditions can be seen in table 6.

The results of the *in situ* hybridisation studies using sense and antisense [^{35}S]radiolabelled cRNA probes specific for FMO3 and FMO4 can be seen in figures (4.2 b-z) for FMO3 and figures (4.2.1 a-p) for FMO4 and in table 6.

FMO 3

Data gained from this set of experiments using slide sections hybridised to antisense probe, identified dopaminergic neurons in the substantia nigra of the midbrain sections, (figures 4.2 c) and neurones in the red nucleus (figure 4.2 e). heavily labelled with probe. Surrounding areas of the crus cerebri (figures 4.2 f,g) and superior colliculus (figures 4.2 h,i). did not hybridise to the antisense probe. Sections hybridised to the sense RNA probe revealed only low level background signal (figure 4.2 b,d). Slides were counterstained with either cresyl violet or toluidine blue. Initial interpretation of cell types was performed by Anne Kingsbury of the Parkinson's Disease Brain Bank, London.

In the coronal sections, inclusive of the basal ganglian network, silver grains were most marked in the antisense hybridised sections of the subthalamic nucleus (figure 4.2 j). Smaller neurons of the lower thalamus and the globus pallidus (figures 4.2 m,o,q) were also positive. However, hybridisation to cRNA FMO3 probe in the corresponding sense treated sections did not occur, (figures l,n,p). Granular cells of Ammon's horn located in the pes-hippocampus demonstrated intense binding of cRNA antisense probe (fig 4.2x). However, nearby cells of the dentate gyrus and choroid plexus showed no binding in sense or antisense treated sections (fig 4.2 y,z).

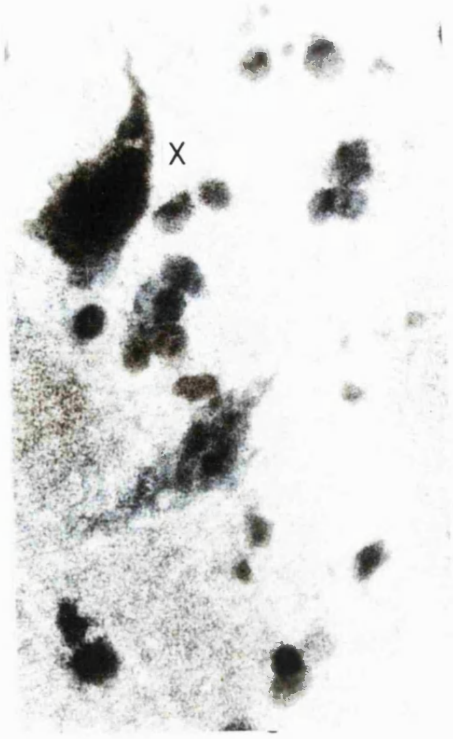

Figure 4.2 (b)

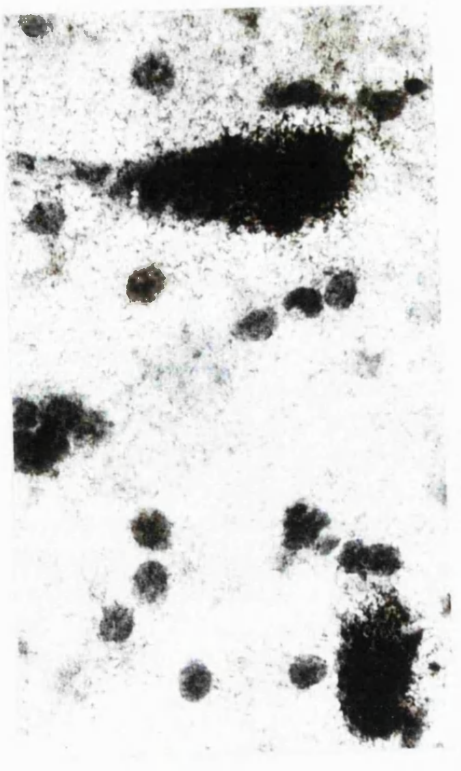

Figure 4.2 (c)

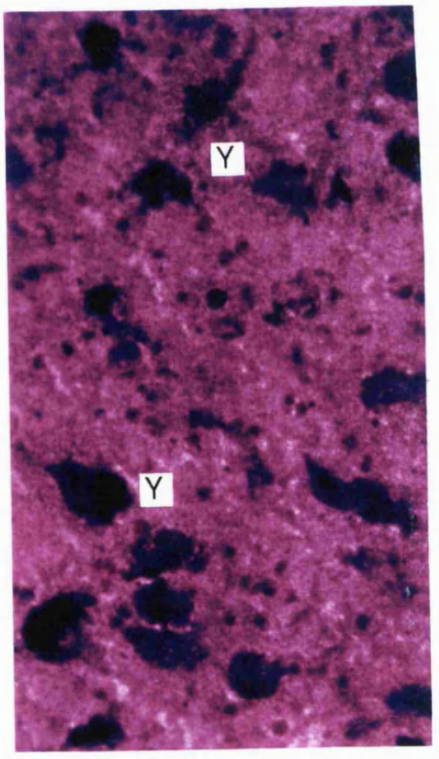

Figure 4.2 (d)

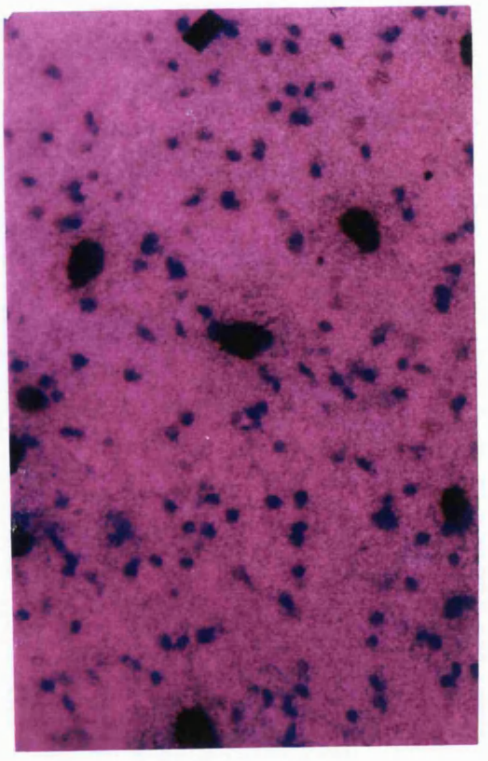

Figure 4.2 (e)

Figure 4.2 (b-e) In-*situ* hybridisation of specific regions within the human brain.
Figure(b) sense, figure(c) antisense (substantia nigra). Tissue from Control male. Magnification x600
Figure(d) sense, figure(e)antisense (midbrain). Tissue: Parkinsons disease male Magnification x200.
Figure **b** shows no hybridisation of FMO3 cRNAsense probe to neurons. Figure **c** shows hybridisation of FMO3 cRNA antisense probe to dopaminergic neurons. Figure **d** shows no hybridisation of cRNA sense probe to neurons in the red nucleus (midbrain) while Figure **e** shows binding of FMO3 antisense probe to cells in this region. The dark stained cells in figure 4.2d (y) and 4.2b (x) are Nissl substance found in the cells of the substantia nigra which stains dark and does not represent probe binding.

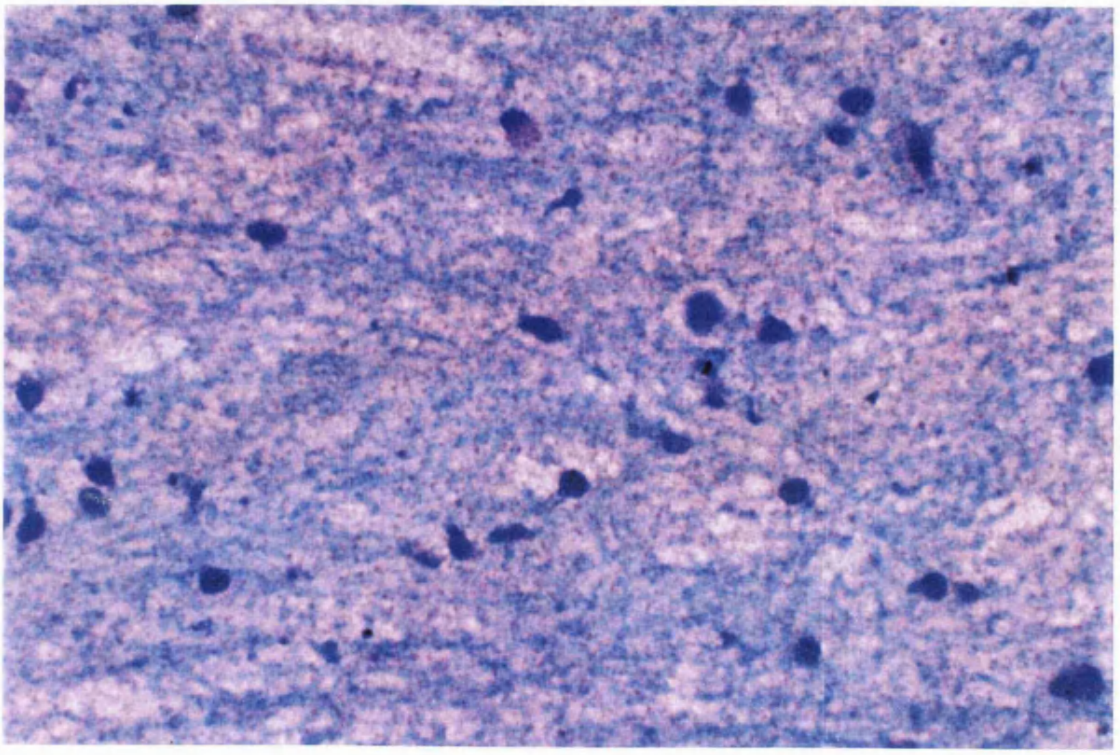

Figure 4.2 (f)

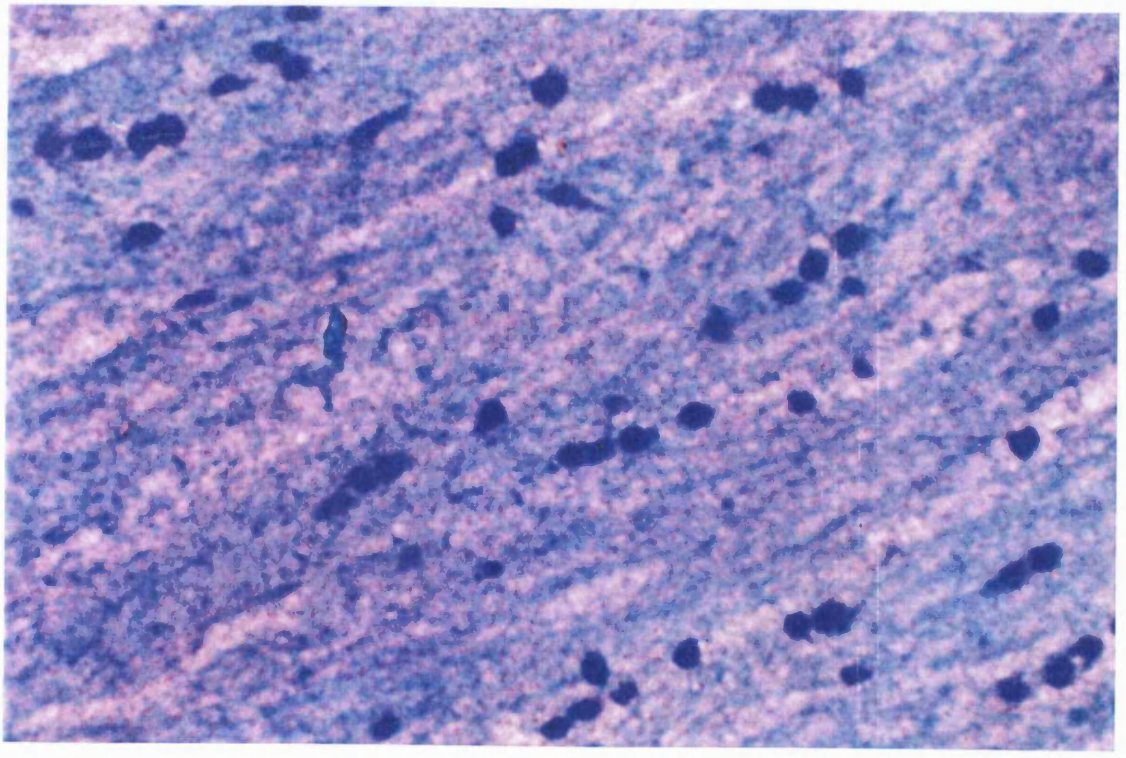

Figure 4.2 (g)

Figure 4.2 (f-g) In-*situ* hybridisation of specific regions within the human brain.
Figure(f) sense, figure(g) antisense (crus cerebri). Tissue from Control male. Magnification x400
Figures **f** and **g** show no hybridisation of either FMO3 cRNA sense probe (f) or FMO3 cRNA antisense probe (g) to neurons; thus demonstrating the absence of signal for FMO3 in this sub-regio of the midbrain.

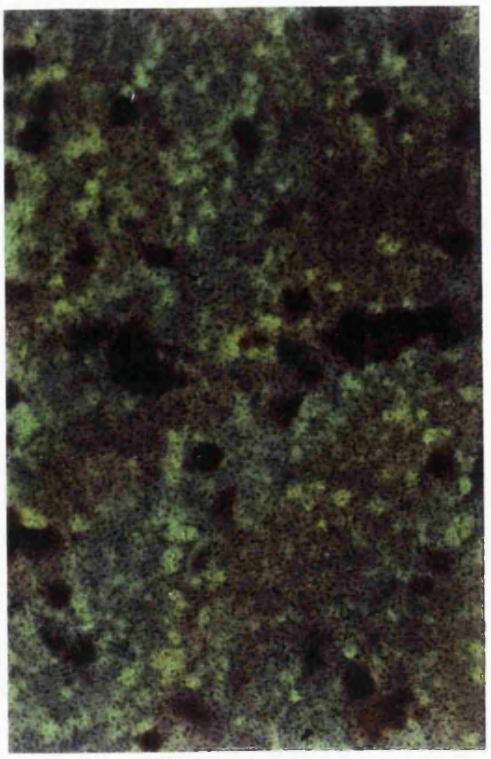

Figure 4.2 (h)

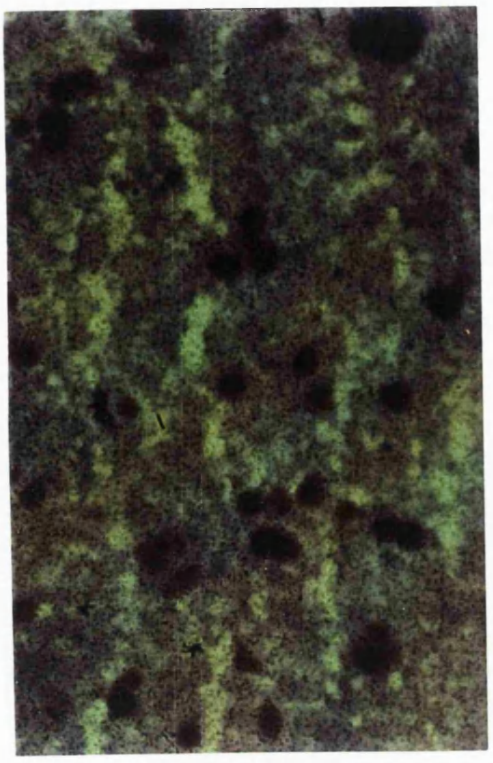

Figure 4.2 (i)

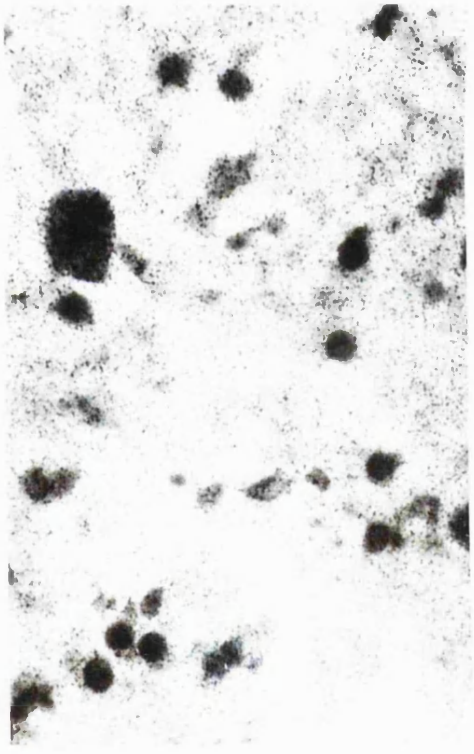

Figure 4.2 (j)

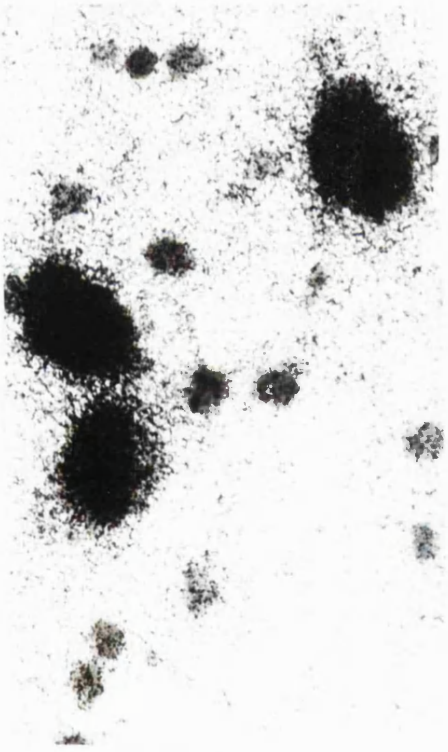

Figure 4.2 (k)

Figure 4.2 (h-k) In-*situ* hybridisation of specific regions within the human brain.
Figure(h)sense, figure(i)antisense (superior colliculus). Parkinson's disease male Magnification x400. Figure(j)sense, figure(k)antisense (subthalamic nucleus).Parkinson's disease female Magnification x600. Figures **h** and **i** show no binding of cRNA FMO3 sense or antisense probe to cells in this region Indicating the specific nature of the binding pattern of FMO3 in the sub-regions of the basal ganglia. Figure **j** sense, shows no hybridisation of cRNA sense probe to these neurons, while Figure **k** shows intense binding of FMO3 antisense cRNA probe to neurons of the subthalamic nucleus.

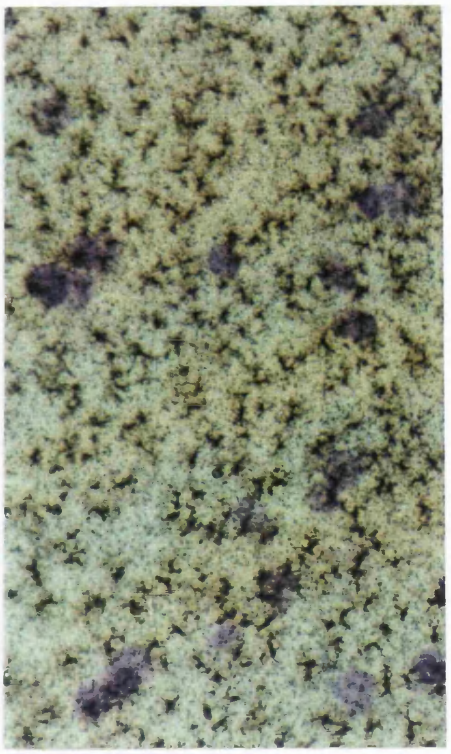

Figure 4.2 (l)

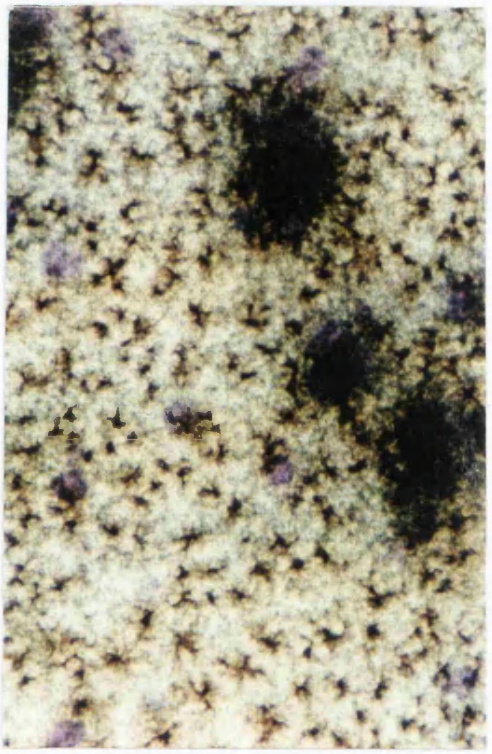

Figure 4.2 (m)

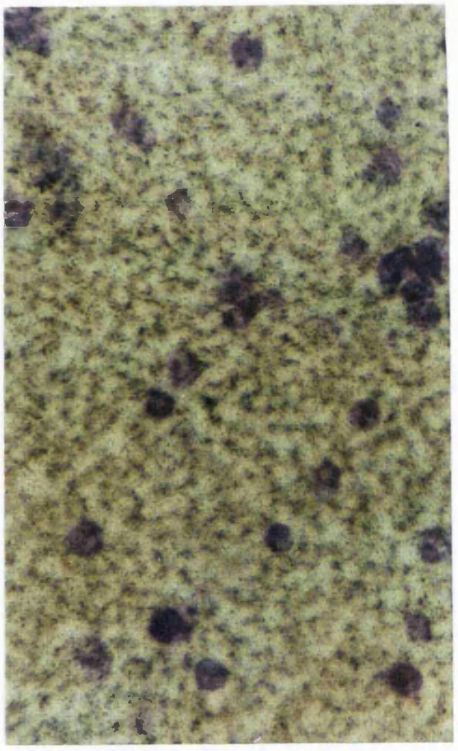

Figure 4.2 (n)

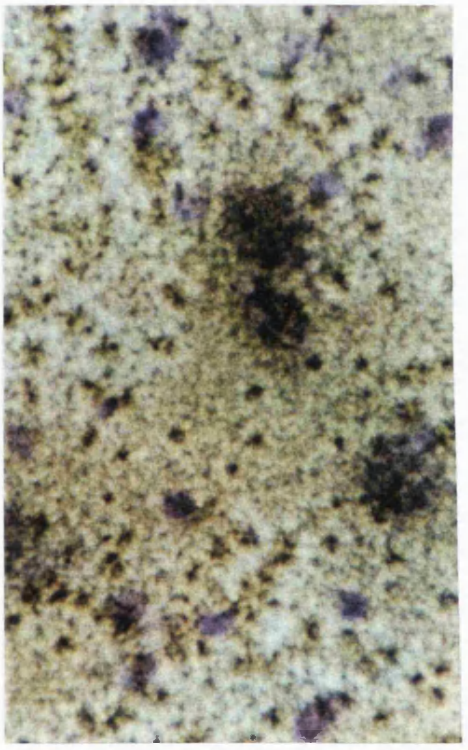

Figure 4.2 (o)

Figure 4.2 (l-o) In-*situ* hybridisation of specific regions within the human brain.
Figure(l) sense, figure(m) antisense (thalamus). Tissue: Parkinson's disease male Magnification x600.
Figure(n) sense, figure(o) antisense (thalamus).Tissue: Parkinson's disease female Magnification x600
Figure **l** shows no hybridisation of FMO3 cRNA sense probe to the medium neurons of the thalamus. Figure **m** shows hybridisation of FMO3 cRNA antisense probe to these neurons. Figure **n** shows no hybridisation of cRNA sense probe to the medium neurons of the thalamus, while Figure **o** shows binding of FMO3 antisense probe to medium neuronal cells in this region.

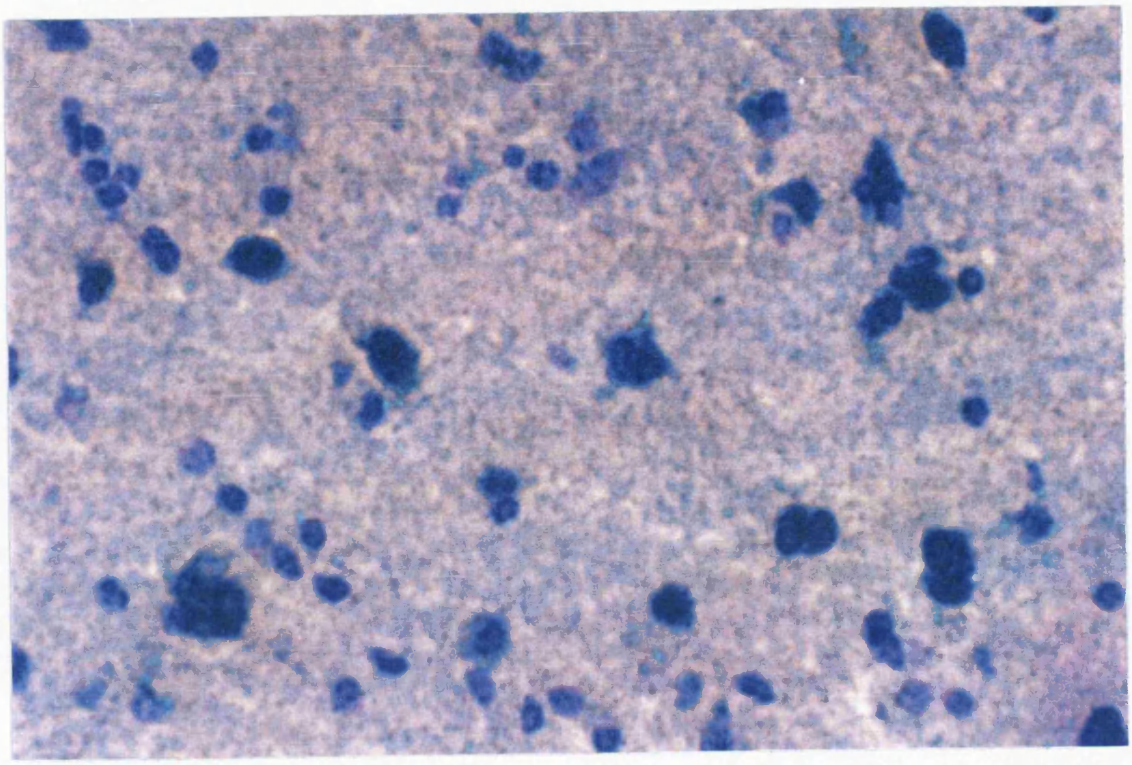

Figure 4.2 (p)

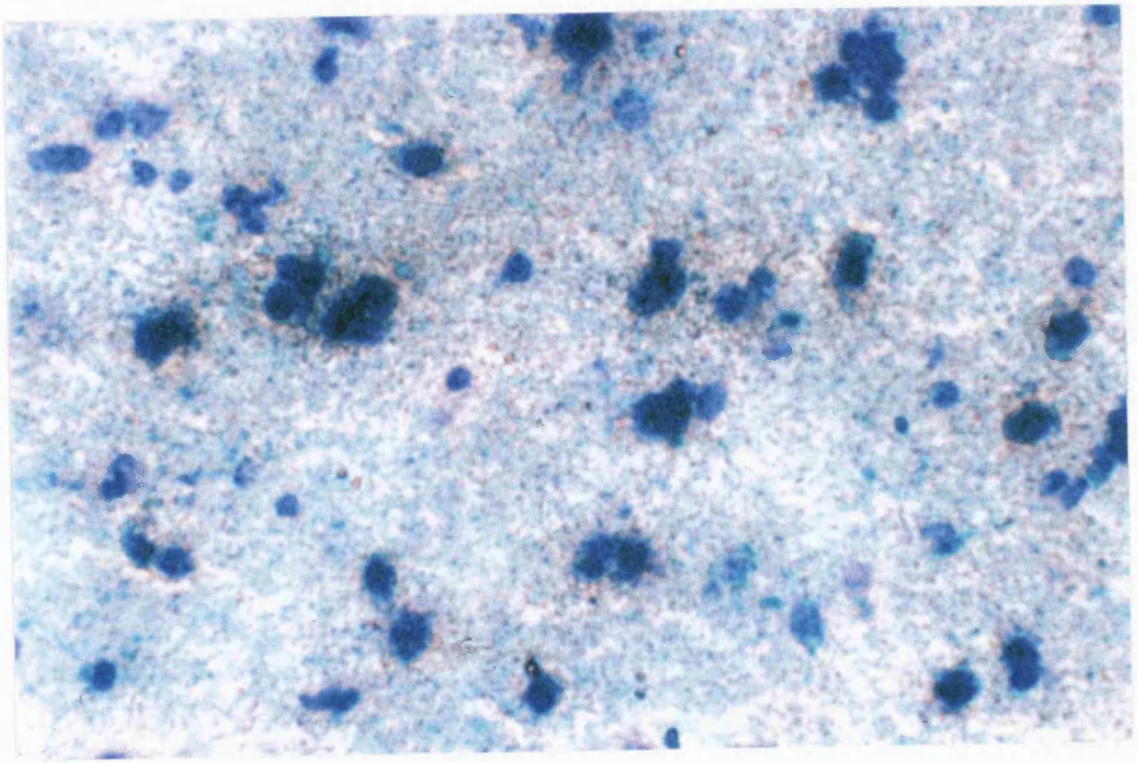

Figure 4.2 (q)

Figure 4.2 (p-q) In-*situ* hybridisation of specific regions within the human brain.
Figure(p)sense, figure(q) antisense (globus pallidus). Tissue from Control male. Magnification x400
Figure **p** shows no hybridisation of FMO3 cRNA sense probe to neurons in this region. Figure **q** demonstrates binding of cRNA antisense probe to neurons within the specific region of the globus pallidus.

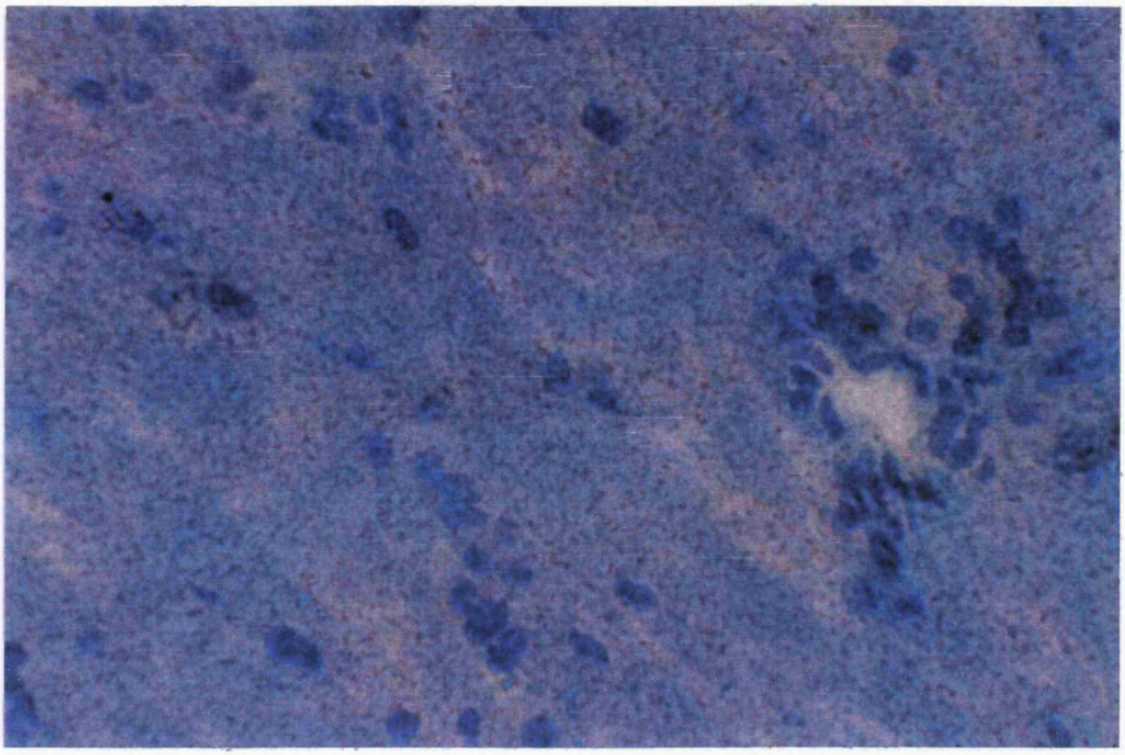

Figure 4.2 (r)

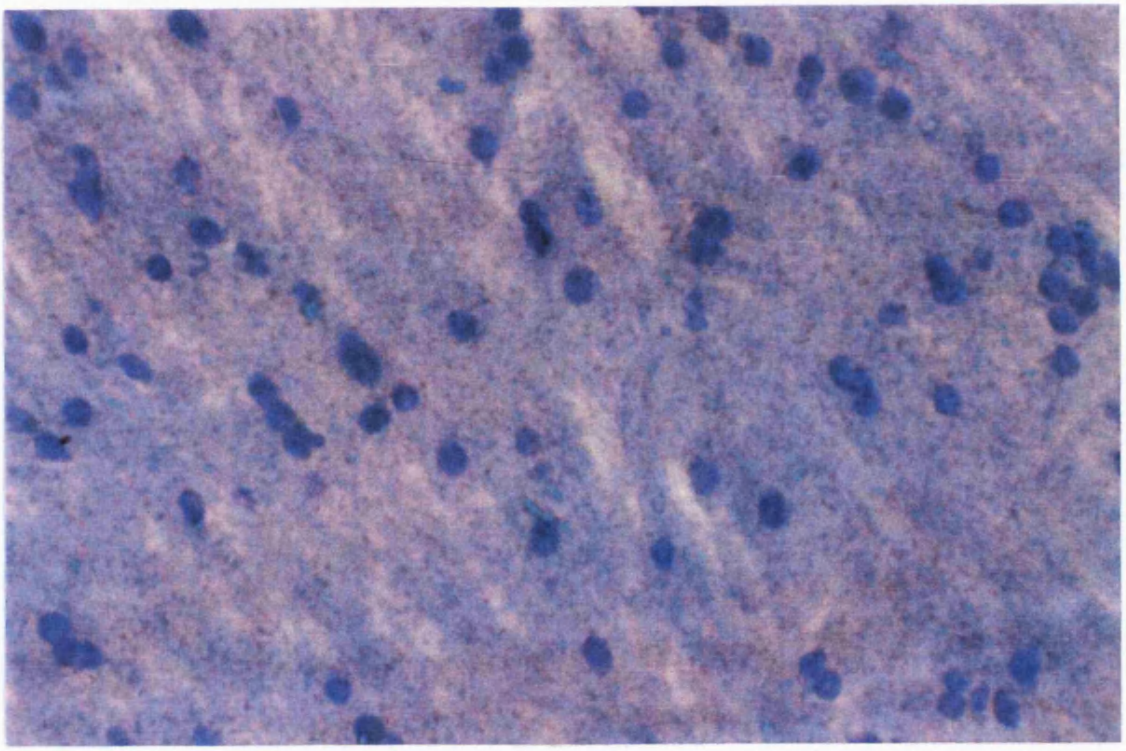

Figure 4.2 (s)

Figure 4.2 (r-s) In-*situ* hybridisation of specific regions within the human brain.
Figure(r) sense, figure(s) antisense (internal capsule). Tissue: Control female. Magnification x400
Figure **r** shows no hybridisation of FMO3 cRNA sense probe to the cells of the internal capsule. Similarly, Figure **s** shows no hybridisation of FMO3 cRNA antisense probe to cells in this region. Thus indicating the specific nature of FMO3 cRNA probe binding in this region.

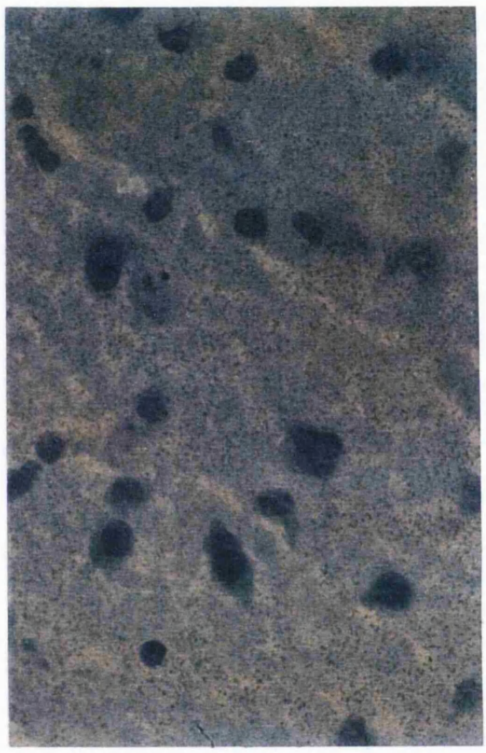

Figure 4.2 (t)

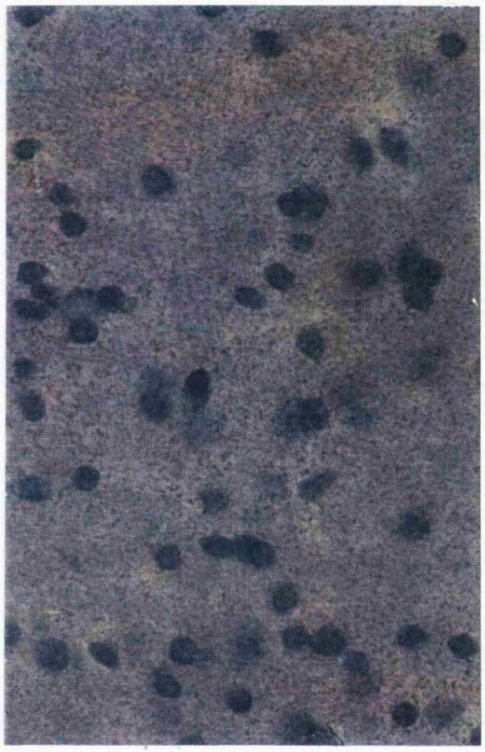

Figure 4.2 (u)

Figure 4.2 (t-u) In-*situ* hybridisation of specific regions within the human brain.
Figure(t)sense, figure(u) antisense (putamen). Parkinsons disease female. Magnification x450.
Figure **t** shows no hybridisation of cRNA sense probe to neurons, similarly, Figure **u** shows no binding of FMO3 antisense cRNA probe, thus demonstrating a region specific binding pattern of FMO3 in the basal ganglia.

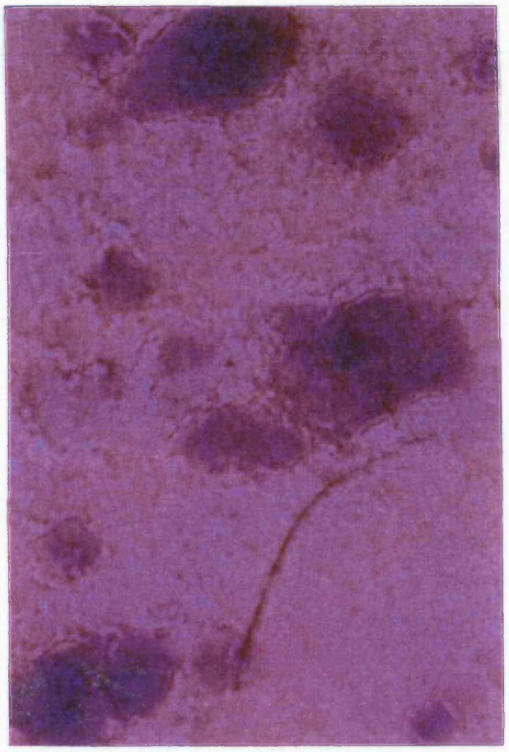

Figure 4.2 (v1)

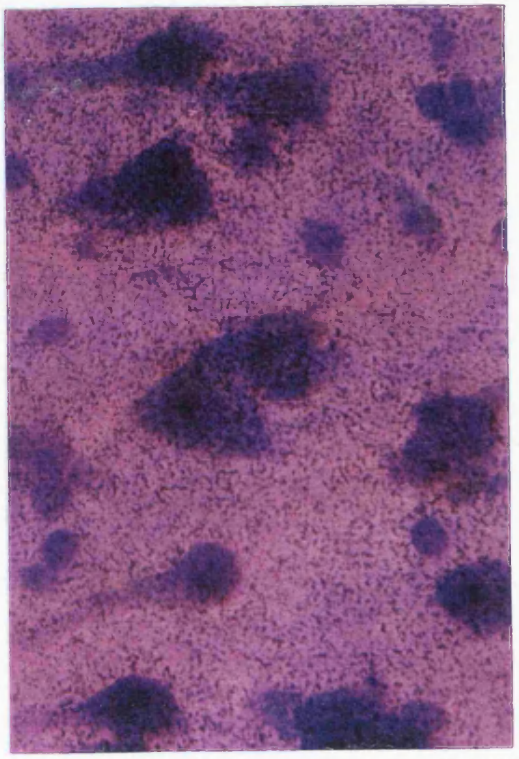

Figure 4.2 (v2)

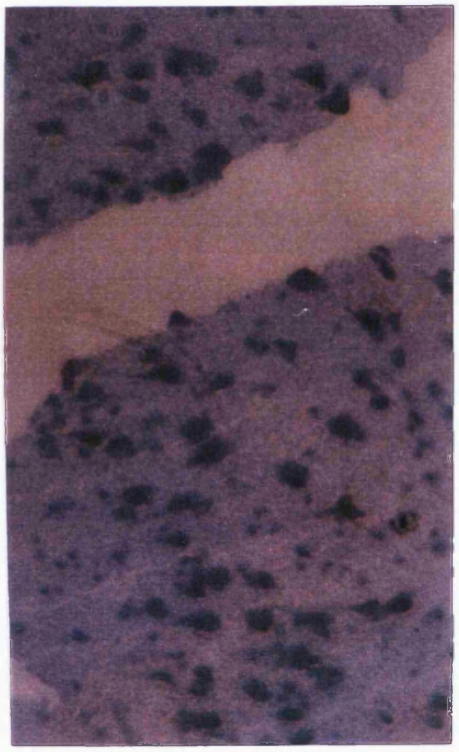

Figure 4.2 (v3)

Figure 4.2 (v1- 3) In-*situ* hybridisation of specific regions within the human brain.
Figure(v1) sense, figure (v2) antisense (hippocampus). Tissue: Control female. Magnification x450.
Figure(v3) antisense (hippocampus). Tissue control male. Magnification x150.
Figure **v1** shows no hybridisation of FMO3 cRNA sense probe to the pyramidal cells of the hippocampus. Figure **v2** shows intense hybridisation of FMO3 cRNA antisense probe to these cells. Figure **v3** shows a large section of the hippocampus region at low magnification to indicate a swathe of positively stained pyramidal cells.

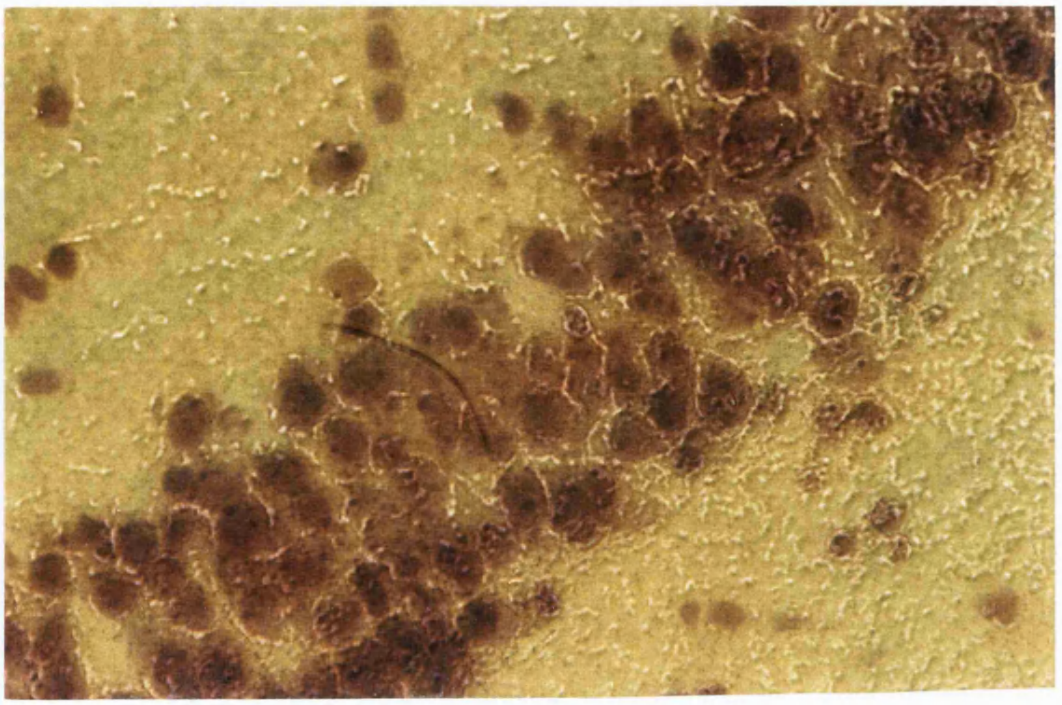

Figure 4.2 (w)

Figure 4.2 (x)

Figure 4.2 (w-x) In-*situ* hybridisation of specific regions within the human brain.
Figure(w) sense, figure(x) antisense (Ammon's horn). Tissue from Control male. Magnification x 600
Figure **w** shows no hybridisation of FMO3 cRNA sense probe to the granular cells of Ammon's horn.
Figure **x** shows hybridisation of FMO3 cRNA antisense probe to these cells.

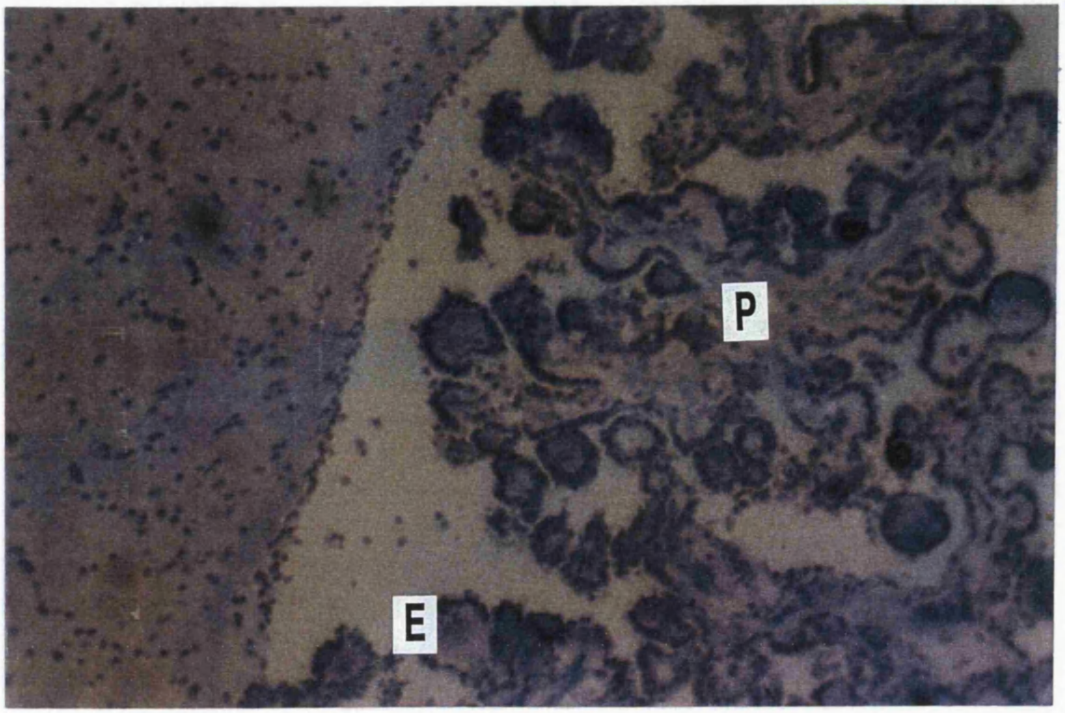

Figure 4.2 (y)

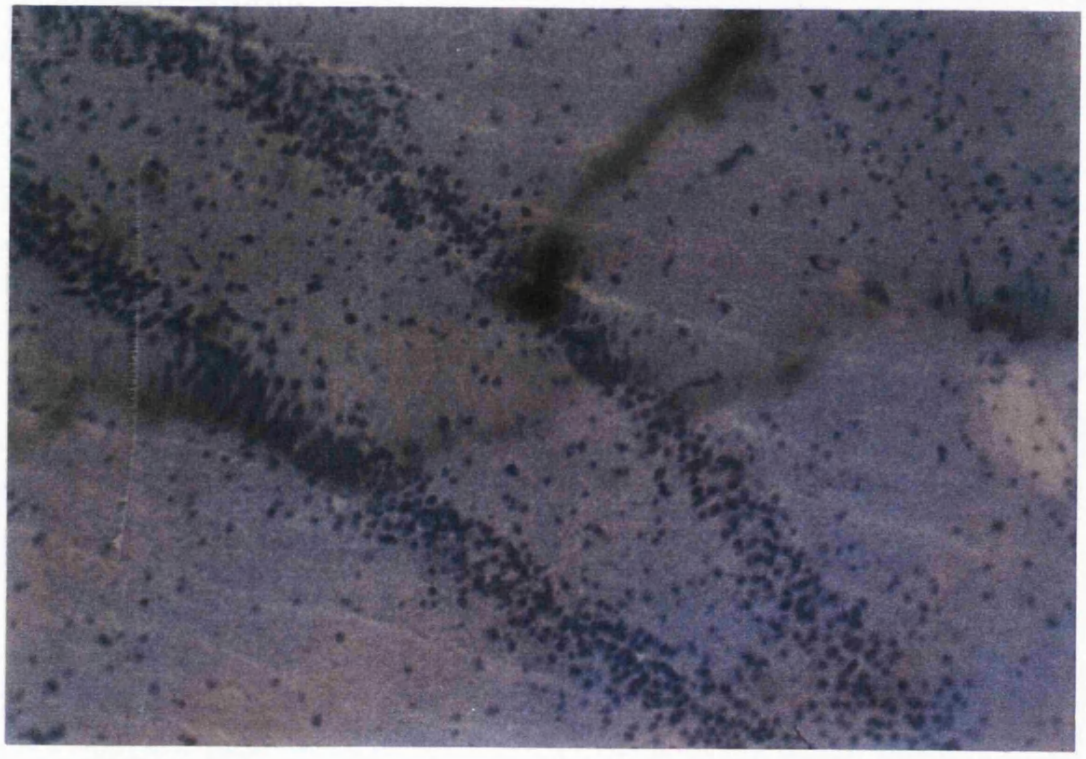

Figure 4.2 (z)

Figure 4.2 (y-z) In-*situ* hybridisation of specific regions within the human brain.
Figure(y) choroid plexus figure(z) dentate gyrus (Hippocampus region). Tissue from Control male. Magnification x150. Figure **y** shows no hybridisation of FMO3 cRNA antisense probe to the ependyma cells (*E*) or pia mater (*P*) of the choroid plexus in the hippocampus region. Figure **z** shows no hybridisation of FMO3 cRNA antisense probe to the granular cells of the dentate gyrus in the hippocampus region. Magnification x150.

Name	Sex	Age	Condition	Drugs prescribed
Me1c	Male	77	CONTROL	
Fi1p	Male	74	PARKINSON'S	Madopar/Selegiline
Ha2p	Female	81	PARKINSON'S	Melleril
Sn3p	Male	88	PARKINSON'S	Madopar/ Selegiline
Ba2c	Female	77	CONTROL	
Al3c	Male	65	CONTROL	
Pe4c	Female	73	CONTROL	
Pa4p	Female	82	PARKINSON'S	Madopar

Table 6. Makeup and medical condition of individuals providing brain tissue (slides).

Binding of probe also occurred in pyramidal cells of the pes hippocampus (figure 4.2 v2,v3), and cells of Ammon's horn, (figure 4.2 x).

Surrounding tissues of the internal capsule (figure 4.2 r,s), putamen (figure 4.2 t,u), choroid plexus of the lateral ventricle (figure 4.2 y) and dentate gyrus (figure 4.2 z) did not hybridise to the antisense FMO3 probe. Such differential binding of probe within the same organ and between adjacent regions gives further weight to the specificity and integrity of the cRNA probes used. The binding pattern exhibited by FMO3 led to the identification of specific neurons expressing this isoform in specific regions. In the midbrain, neurons binding FMO3 were identified as dopaminergic neurons, which are actively involved in motor coordination and movement. The pyramidal neurons are involved in output pathways, projecting their axons into the thalamus or cerebral cortex, caudate nucleus and putamen. In the lower thalamus (figures 4.2 m,o) and striatum (figure 4.2 q), the small dense neurons were labelled to the greatest extent with silver grains, while the large neurons bound antisense probe in the subthalamic nucleus (figures 4.2 k). Control samples show no binding of sense probe or very low level background. These figures are located next to their respective positives in each section to aid comparison.

There was little difference in the results obtained from normal and Parkinson's disease brain sections. Though the latter samples had fewer neurons.

There does seem to be a difference between sections from some of the males and some females. The results suggest that silver grain binding in antisense treated sections is more intense in tissue derived from males than those from females, see figures 4.2 c,e,k,o,v2,v3 for males, compared with figures 4.2 i,m, for females . This possible difference in expression may be on an individual basis or on the basis of gender since variation in expression within and between different gender groups has been suggested for FMO in a number of species **(67,69,70,74,75)**. However, it could equally be as a result of age differences amongst the group and / or tissue integrity after postmortem. These results expand the more general results gained by others in the field suggesting FMO expression in the brain of rodents, **(157,158,159)**, rabbit **(168)** and in man **(165,166,167)**.

FMO 4

Brain sections from the individuals noted in table 6 were also hybridised to FMO4 antisense and sense probes.

The binding of the antisense probe specific for FMO4 confirmed its presence in the human brain in a number of regions of the basal ganglia, figures (4.2.1 a-p).

In the sections of the mid brain region analysed the intensity of probe binding was higher in the dopaminergic neurons of the substantia nigra, than it was in the sections of the basal ganglia (figure 4.2.1 b,d). Like FMO3, surrounding areas of the crus cerebre and medial genticulate body did not hybridise to the FMO4 antisense probe (figures 4.2.1 e). Again, as was observed for FMO3, there was little difference between Parkinson's diseased brain tissue samples and normal brain tissue samples. However, the slight difference between the males and females observed for FMO3 was not observed in the brain regions probed with the FMO4 antisense riboprobe.

Slides of coronal sections demonstrated evidence of probe binding in the neurons of the thalamus (figure 4.2.1 i), and subthalamic nucleus (figure 4.2.1 g). Surrounding regions such as internal capsule which spans an area separating the globus pallidus from the thalamus did not hybridise to the antisense probe (figure 4.2.1 l). As was found for FMO3, the pyramidal cells of Ammon's horn, in the region of the pes hippocampus gave positive results for the binding of FMO4 probe (figure 4.2.1 n). While surrounding areas of the dentate gyrus (figure 4.2.1 o) and choroid plexus of the lateral ventricle (figure 4.2.1 p) did not hybridise to the FMO4 antisense probe.

Figure 4.2.1 (a)

Figure 4.2.1 (b)

Figure 4.2.1 (c)

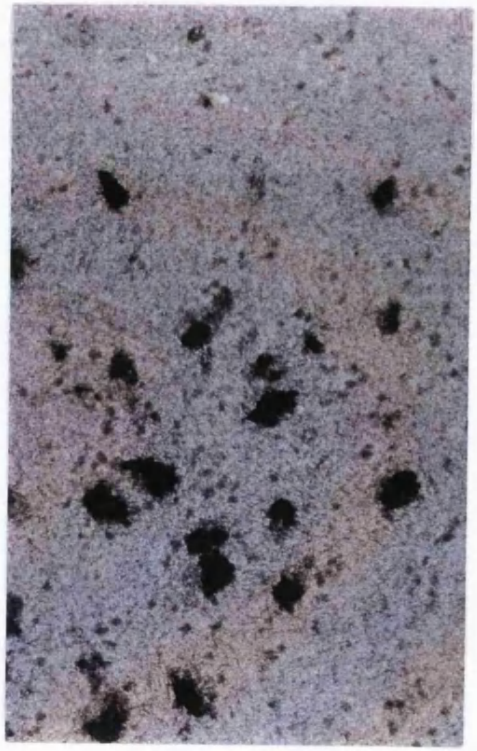

Figure 4.2.1 (d)

Figure 4.2.1 (a-d) In-*situ* hybridisation of specific regions within the human brain.
Figure(a) sense, figure (b) antisense (midbrain). Tissue: Control female. Magnification x350.
Figure(c) sense, figure (d) antisense (midbrain). Tissue: Control male. Magnification x250. Figure **a** shows no hybridisation of FMO4 cRNAsense probe to neurons. Figure **b** shows hybridisation of FMO4 cRNA antisense probe to dopaminergic neurons. Figure **c** shows no hybridisation of cRNA sense probe to neurons in this region, while Figure **d** shows intense binding of FMO4 antisense probe to neurons.

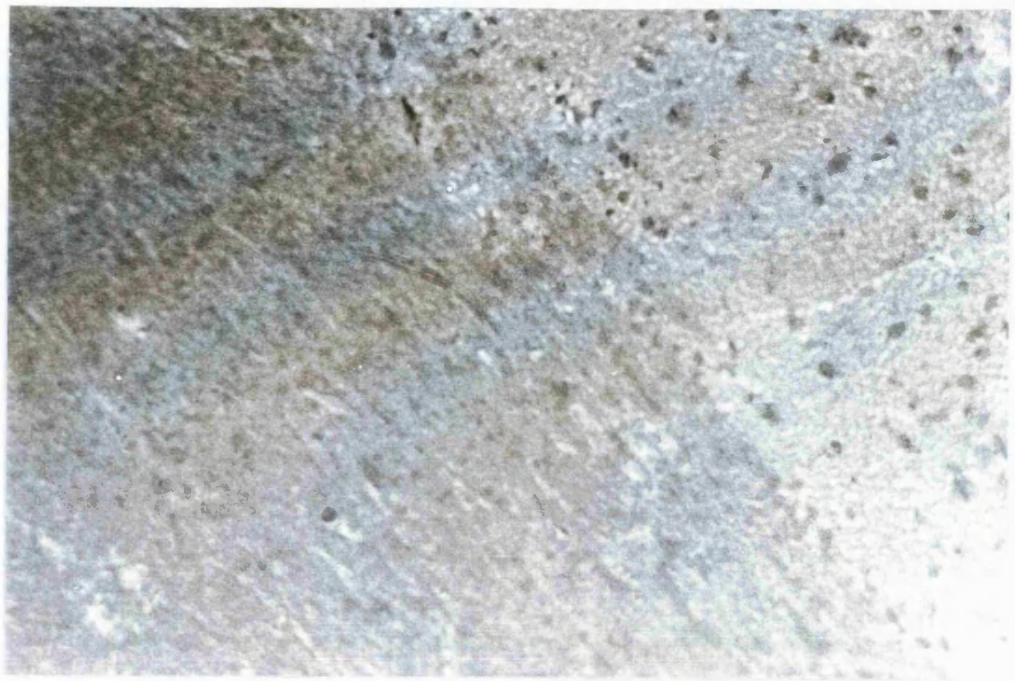

Figure 4.2.1 (e)

Figure 4.2.1 (f)

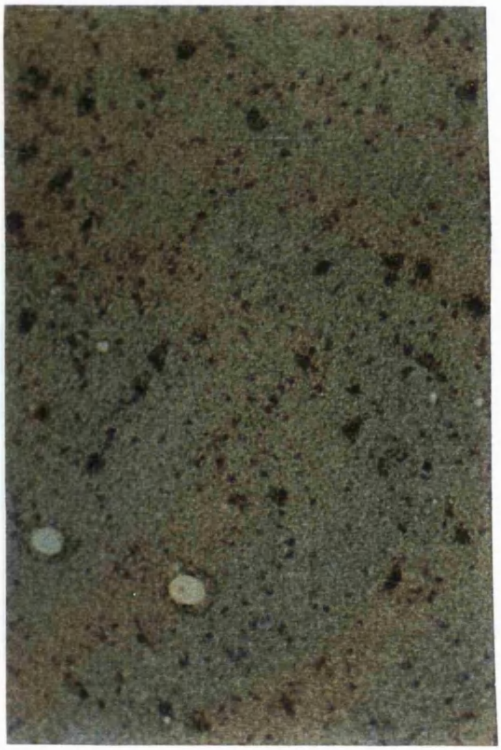

Figure 4.2.1 (g)

Figure 4.2.1 (e-g) In-*situ* hybridisation of specific regions within the human brain.
Figure(e) (midbrain). Tissue: Parkinson's diseased female. Magnification x250. This section shows no hybridisation of FMO4 antisense cRNA to cells in the area encompassing the crus cerebre and part of the medial genticulate body. Figure(f) sense, figure (g) antisense (midbrain).Tissue:Parkinson's diseased female. Magnification x250. Figure **f** shows no hybridisation of FMO4 cRNAsense probe to neurons. Figure **g** shows a positive hybridisation of FMO4 cRNA antisense probe to neurons.

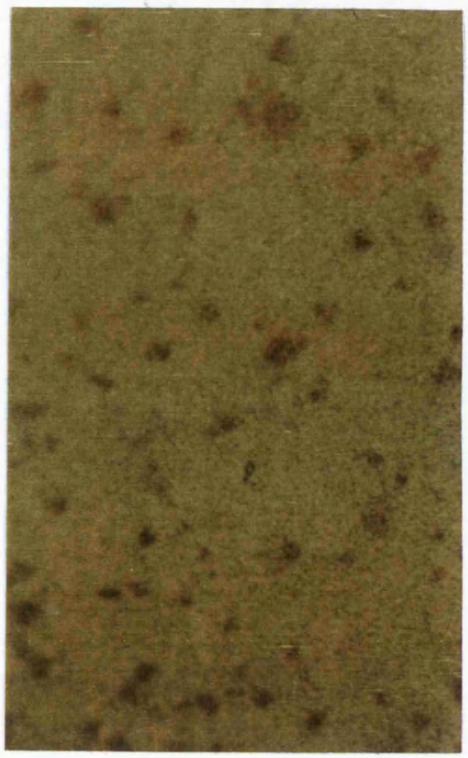

Figure 4.2.1 (h)

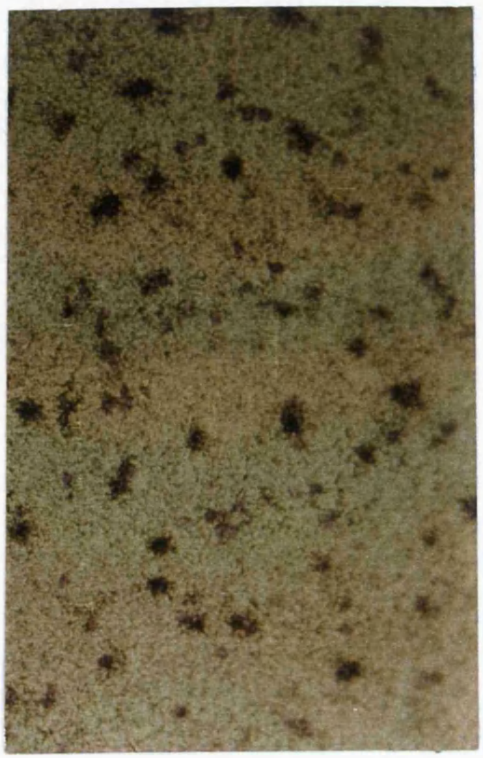

Figure 4.2.1 (i)

Figure 4.2.1 (j)

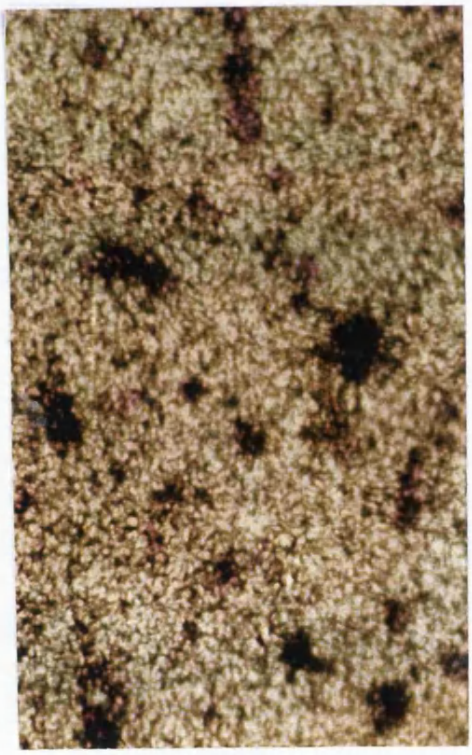

Figure 4.2.1 (k)

Figure 4.2.1 (h-k) In-*situ* hybridisation of specific regions within the human brain.
Figure(h) sense, figure (i) antisense (Thalamus). Tissue: Control female. Magnification x350.
Figure(j) sense ,figure (k)antisense (Lentiform nucleus). Tissue:Control male. Magnification x450.
Figure **h** shows no hybridisation of FMO4 cRNAsense probe to neurons. Figure **i** shows hybridisation of FMO4 cRNA antisense probe to neurons. Figure **j** shows no hybridisation of FMO4 cRNA sense probe to neurons in this region, while Figure **k** shows intense binding of FMO4 antisense probe to neurons.

Figure 4.2.1 (l)

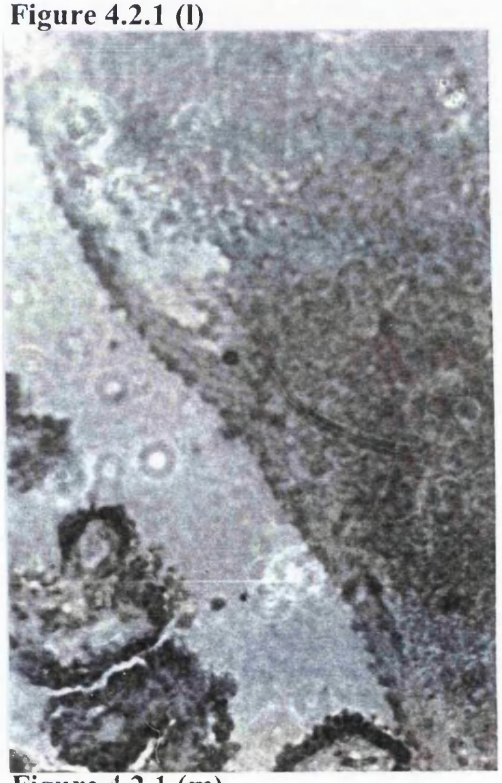

Figure 4.2.1 (m)

Figure 4.2.1 (n)

Figure 4.2.1 (l-n) In-*situ* hybridisation of specific regions within the human brain.
Figure(l) (internal capsule). Tissue: Control male. Magnification x150. Cells in this region show no binding of FMO4 antisense cRNA probe.
Figure(m) sense, figure (n) antisense (Hippocampus region). Tissue: Control male. Magnification x250. Figure **m** shows no hybridisation of FMO4 cRNAsense probe to cells in the hippocampus region. Figure **n** shows hybridisation of FMO4 cRNA antisense probe to pyramidal cells in the same region.

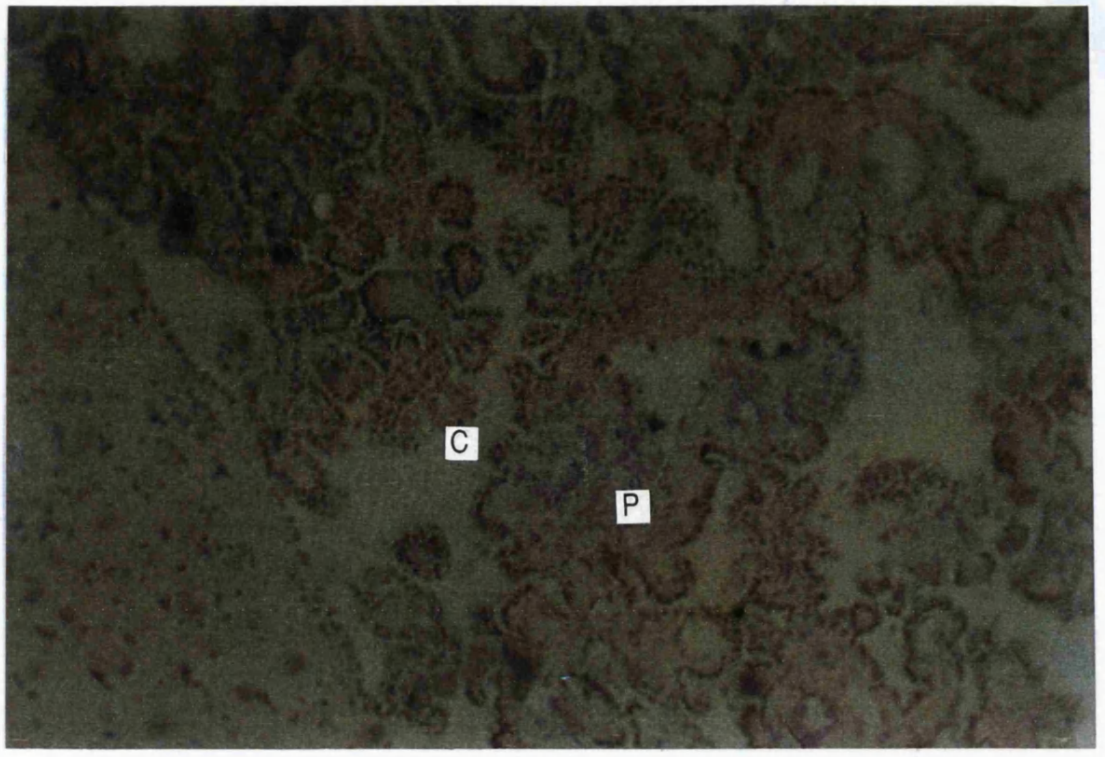

Figure 4.2.1 (o)

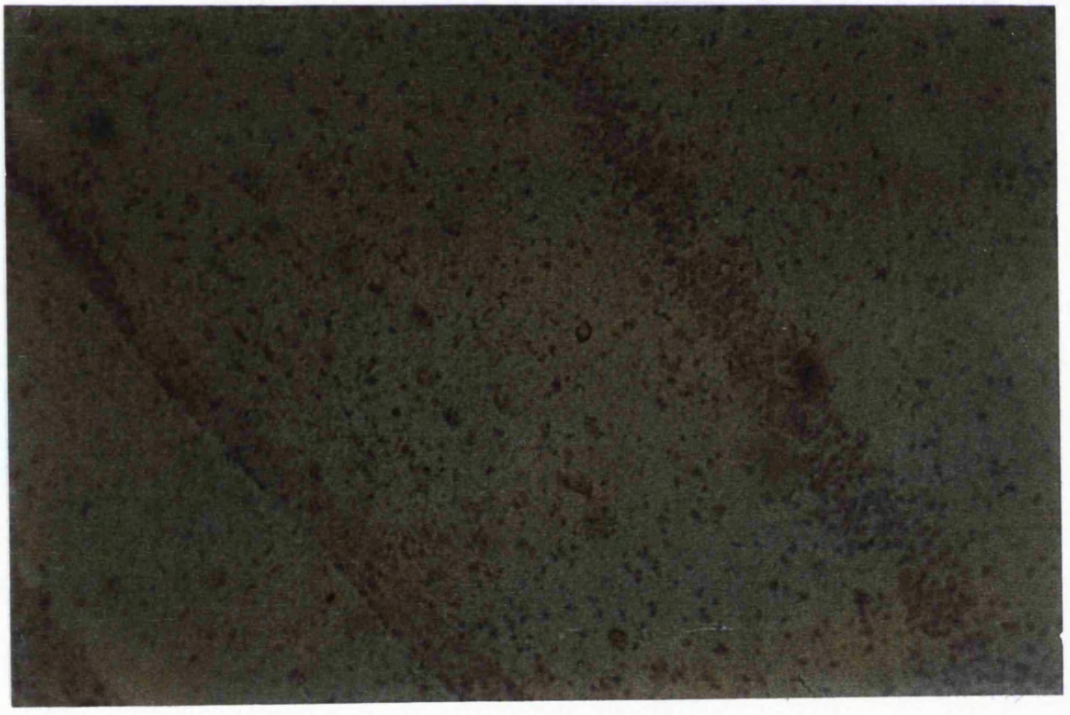

Figure 4.2.1 (p)

Figure 4.2.1 (o-p) In-*situ* hybridisation of specific regions within the human brain.
Figure(o) (Choroid plexus of the lateral ventricle). Tissue: Control male. Magnification x250.
Figure(p) (Hippocampus). Tissue: Control male. Magnification x250.
Figure **o** shows no hybridisation of FMO4 cRNA antisense probe to the ependyma cells of the choroid plexus (*C*), or the pia matter (*P*) in the hippocampus. Figure **p** shows no hybridisation of FMO4 cRNA antisense probe to granular cells of the dentate gyrus in this region.

The controls for FMO3 and FMO4 consisted of brain sections hybridised to sense to FMO3 or FMO4 cRNA probes, and although there was some background binding in control sections of FMO3 (figures 4.2 j,l,n), and FMO4 (figures 4.2.1 f,h,n), the levels were very low in comparison to the antisense signal. The binding of sense probe observed is due to high background in terms of signal to-noise-ratio. The problems of background could be due to a range of factors including type of fixative used in the pre-treatment of the brain tissue. Background problems could also be due to: too high a probe concentration in the hybridisation mix, such that target RNA strands are over saturated; hybridisation mixture being too viscous; or too long a hybridisation period.

However, resulting background in this case is likely to be a combination of viscosity of the hybridisation mix and/or too long a hybridisation period, since concentration of probe was carefully calculated, and the fixative used was optimised for these tissues. In terms of brain tissue from Parkinson's disease and normal individuals there seems to be little difference in the background observed.

The results from this series of experiments identify flavin-containing monooxygenases expressed at the RNA level in the human brain. This series of experiments concurs with research from others in the field Blake *et al* **(168)** who have identified FMO4 in rabbit brain. The levels of expression are different for isoforms 3 and 4 and seem to fall within the general parameters of known expression patterns for these two mRNAs, in that FMO3, when expressed, is present in higher amounts **(42,44,49,54,116)**, than is FMO4 **(58,107,111)**. Although FMO3 and FMO4 RNAs are synthesised in various brain regions, *in situ* hybridisation is unable to indicate whether or not the message is being translated into its protein. In order to ascertain whether or not expression of FMO at the RNA level represents redundancy, or if the protein is expressed, a series of experiments for protein detection and expression were employed.

4.3 Immunocytochemistry

In immunocytochemical studies the properties of the antigen and the condition of the tissue, whether it is frozen or paraffin embedded can dictate the choice of fixative used. Some antigens are very stable, while others are less resilient to fixatives and may require use of detergents such as Triton X-100 to detect intracellular antigens. The fact that FMO in the human brain represented an unknown quantity, in terms of its expression and behaviour, a first set of experiments was undertaken without detergent. The results of these were inconclusive. Detection of antigen was relatively unsuccessful. A following set of investigations were carried out using Triton X-100 to facilitate antibody diffusion. The result of these experiments was more successful.

Human brain sections were incubated with a primary antibody specific for FMO3, consisting of IgG-Rabbit-anti-Human (kindly provided by JR Cashman). Initially, antibody was used at a concentration of 10mg/ml. However, the results of this series of experiments demonstrated only very low level binding of antibody, therefore the concentration was increased to 15mg/ml. This became the working concentration throughout all subsequent procedures, as at this concentration antibody was shown to bind selective areas in the sections of brain tissue.
The sections used in this series of experiments were slides of a cross section of the mid brain region, and slides of coronal sections of the basal ganglia and were from the individuals described in table 6.

Immunocytochemical analysis of the frozen human brain sections using antisera to FMO3 indicated the presence of immunoreactive protein. In the sections probed, the immunoreactivity was located in the neuronal cell bodies. In particular, in the basal ganglia, staining was observed in the small neurones of the striatum, the neurons of the thalamus and the larger motor neurons of the subthalamic nucleus, figure (4.3 e,b,c).

Figure 4.3 (1)

Figure 4.3 (2)

Figure 4.3 (3)

Figure 4.3 Immunocytochemistry of regions within the human brain. Brain tissue was incubated with human IgG FMO3 antibody at a concentration of 15µg/µl. Figure **1**(thalamus) and figure **2**(subthalamic nucleus) each gave a positive result, indicating the presence of immunoreactive protein. Figure **3**(subthalamic nucleus), shows the control for human FMO3. This figure shows a negative result. In the control section (figure 3) only secondary antibody is present. Neurons in the subthalamic nucleus control do not stain in the absence of antibody for human FMO3. Chromogen DAB. Magnification x350 for figures 1, 2 and 3.

In sections from the midbrain FMO3 expression was detected in the large dopaminergic neurons located in the substantia nigra, figure (4.3 d). Control sections for both the basal ganglia and mid brain regions did not demonstrate binding of FMO3 antibody figures (4.3 c and f) respectively.

FMO expression in human brain protein microsomes has been detected using immunocytochemical techniques **(160,167)**. However, in these and other studies, although FMO has been detected in a range of areas including the spinal cord **(159,167)**, this has been achieved by using a rabbit FMO2 antibody probe. The results of these previous investigations are surprising. This is because FMO2 is not expressed in humans **(99)**, and as such, experimental data by Bhamre *et al* is anomalous in comparison with our research and others in the field **(168)**. These investigators also show that human brain microsomes metabolise imipramine, a substrate for FMO1. However, FMO1, although abundant in rodent brain has not been detected in rabbit or human brain, Blake (168) and this study.

Figure 4.3 (4)

Figure 4.3 (5)

Figure 4.3 (6)

Figure 4.3 Immunocytochemistry of regions within the human brain. Brain tissue was incubated with human IgG FMO3 primary antibody at a concentration of 15µg/µl . Figure **4** (midbrain) and Figure **5** (striatum) each gave a positive result, indicating the presence of immunoreactive protein. Figure **6** (thalamus), shows the second control for human FMO3. This figure shows a negative result. In the control section (figure 6) both primary and secondary antibody are absent. Neurons in the thalamus control do not stain in the absence of primary antibody for human FMO3 and secondary antibody. Chromogen DAB. Magnification x350 for figures 4, 5 and 6.

4.4 Western blotting

Whole tissue homogenates were prepared from selected brain regions of eight different individuals. Of the eight individuals from which brain tissue was obtained, four were clinically diagnosed as having Parkinson's disease and four had no known neurological disorders. The interval between death, autopsy and flash-freezing ranged between 4 and 28 hours. Of the Parkinson's diagnosed group, 2 were female and 2 were male, whereas in the group of 4 patients exhibiting normal brain function, 3 were female. Ages of the patients ranged from 73 years to 94 years with an average age of 82.7 years (see table 7). The homogenates were prepared from the substantia nigra, subthalamic nucleus and thalamus as described in method (3.9). Brain tissue homogenates were also prepared for protein blotting from selective areas of the brain from a healthy male adult Orang-utan and a 6 hour old baby male Gorilla. The areas which were dissected from the Orang-utan were the midbrain, substantia nigra, thalamus and surrounding area encompassing part of the corpus callosum. From the gorilla brain only two areas were accessible for dissection, the thalamus and substantia nigra with some surrounding tissue.

A series of western blotting experiments were carried out initially using 40μg of protein, but the results were inconclusive. Therefore, the protein concentration of the brain samples was increased to 80μg per sample in a total volume of 20μl. These results can be seen in figures 4.4 a,b and c.

Blot (4.4a) consisted of human brain samples of four individuals as stated above. Blot (4.4b) consisted of the two other primate samples. Blot (c) was identical to blot (b), however, this was incubated with a different primary FMO3 antibody than blots (a) and (b). Blots (a) and (b) were incubated with a primary antibody specific for human FMO3, IgG-Rabbit-anti-Human [15mg/ml] (JR Cashman). While blot (c) was incubated with primary antibody supplied by RM Philpot. This primary antibody which was raised to human FMO3 in rabbit.

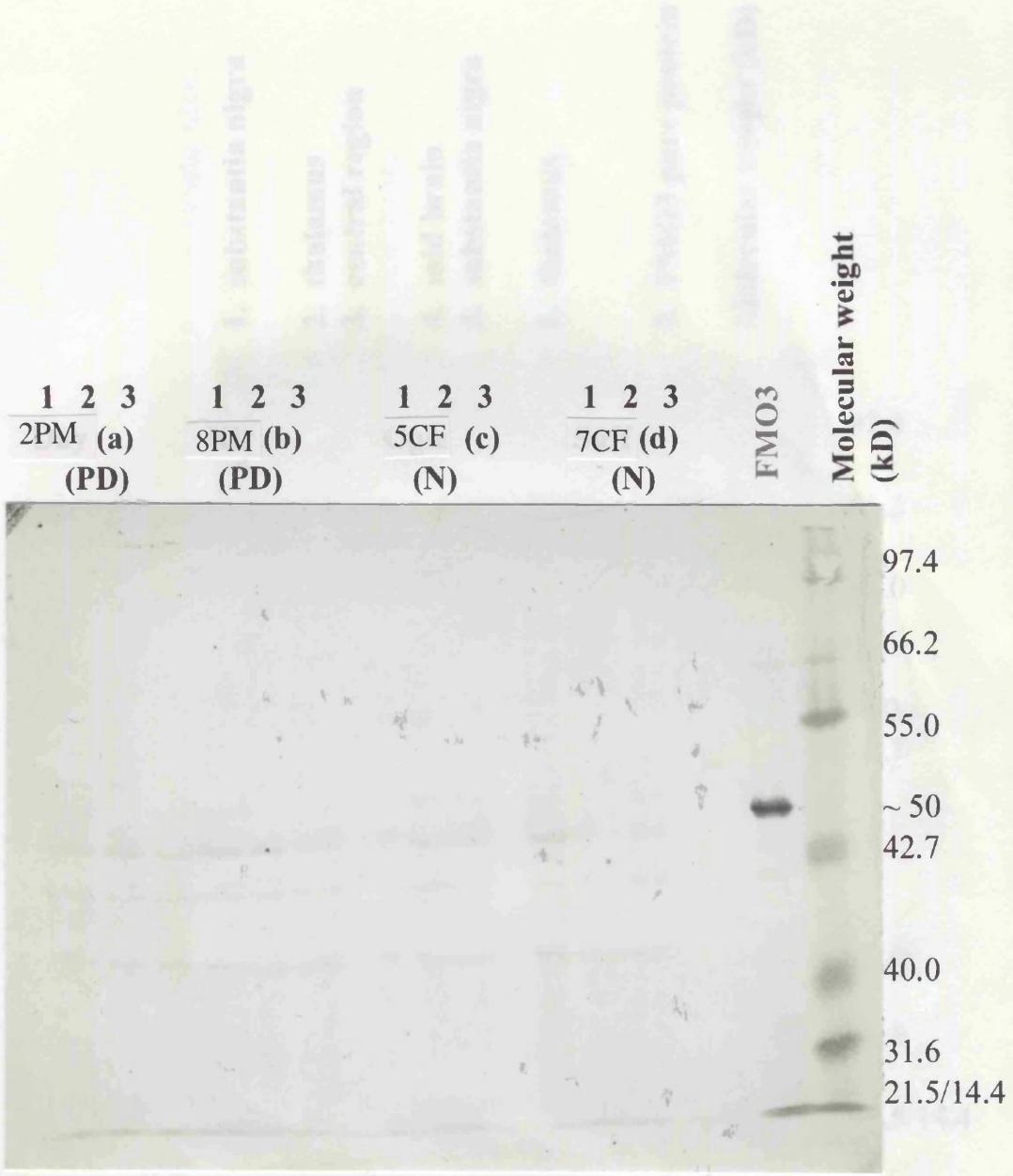

Figure 4.4a Western blot of human brain samples from four individuals comprising 2 Parkinson's subjects (a,d) and 2 non-Parkinson's subjects (b,c). Each lane consisted of 80µg of protein homogenate.The control lane was ~20µg of an extract from E.coli in which human FMO3 cDNA had been expressed. (FMO3) . Lanes 1-3 consisted of: thalamus, subthalamic nucleus and substantia nigra. The blot was probed with Primary antibody specific for human FMO3 (from JR Cashman).

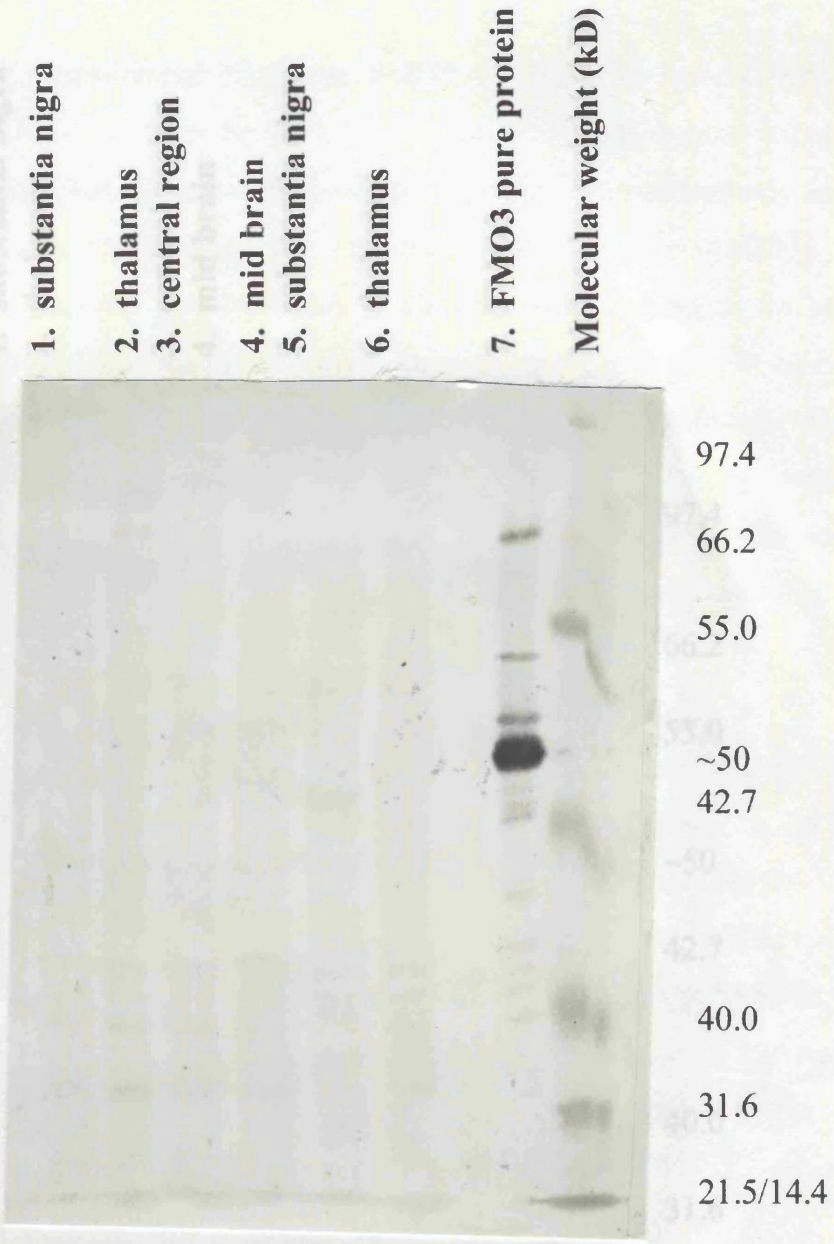

Figure 4.4b Western blot of baby Gorilla and adult Orang-utan brain samples probed with anti-human FMO3 serum. Lanes 1-2 contained gorilla samples. Lanes 3-6 contained Oran-gutan samples. Lane 7 contained a control of FMO3 heterologously expressed in E.coli. The blot shows no binding of "Cashman" FMO3 antibody in the gorilla samples, however a faint band in the substantia nigra lane of Orang-utan is visible but at a lower molecular weight than the control of human FMO3 protein.

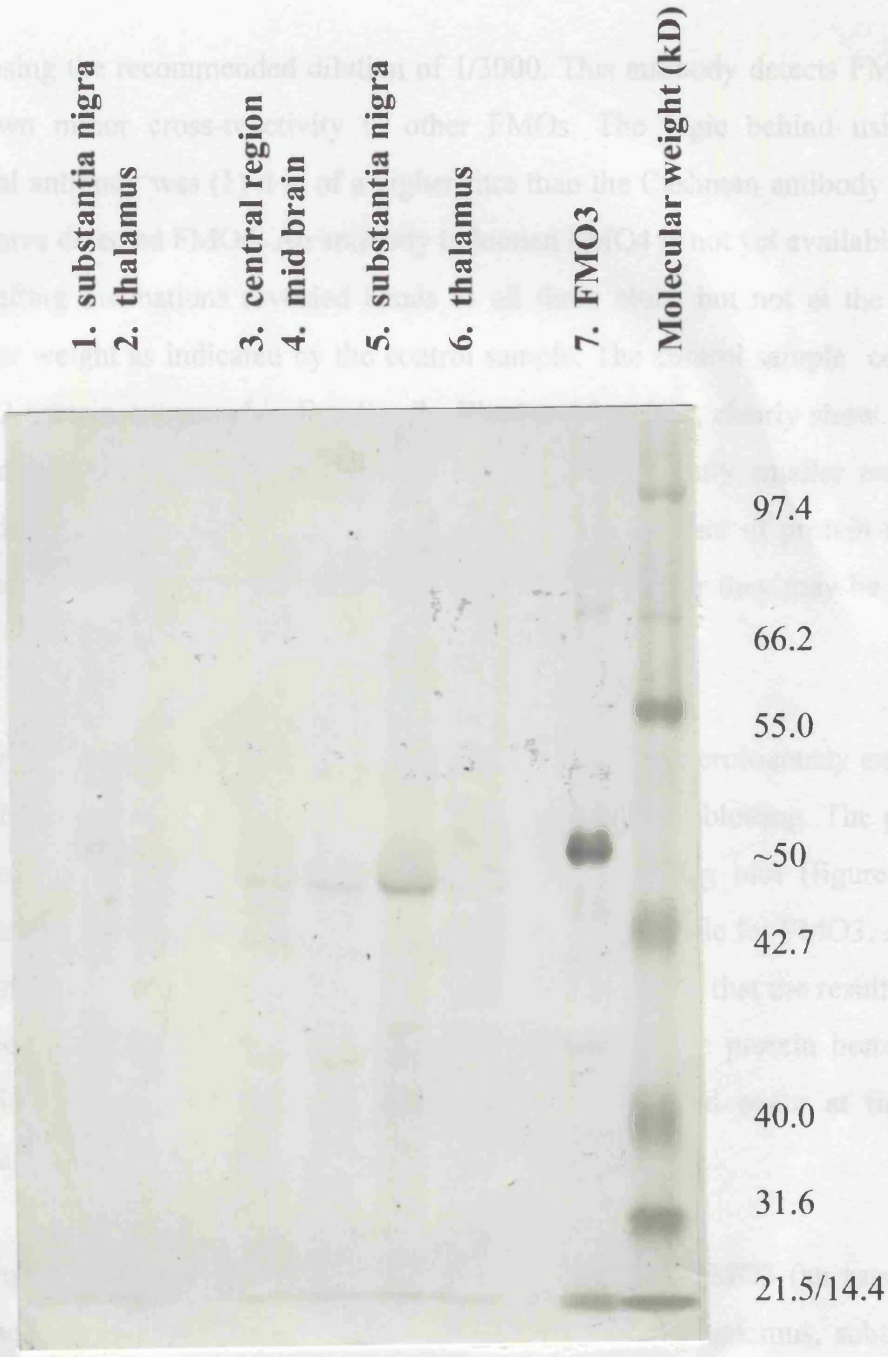

Figure 4.4c Western blot of baby Gorilla and adult Orang-utan brain samples. Lanes 1-2 contained gorilla samples. Lanes 3-6 contained Orang-utan samples. Lane 7 contained a control of FMO3 heterologously expressed. The blot shows faint binding of "Philpot" FMO3 antibody in both the gorilla samples (lanes1 and 2). Binding of antibody is also detected in the Orang-utan brain samples (lanes 3-6) in all lanes, however, lane 5 which corresponds to the substantia nigra shows more intense binding.

FMO3 using the recommended dilution of 1/3000. This antibody detects FMO3 but has shown minor cross-reactivity to other FMOs. The logic behind using this additional antibody was (1) it is of a higher titre than the Cashman antibody and (2) it may have detected FMO4. An antibody to human FMO4 is not yet available.
The resulting incubations revealed bands in all three blots, but not at the correct molecular weight as indicated by the control sample. The control sample consisted of FMO3 protein expressed in E.*coli* cells. Figures 4.4 a, b, c, clearly show that the protein detected in brain protein homogenates shows a slightly smaller molecular weight than the control. This could be due to the high amount of protein samples loaded on the gel, or the positive bands may not be FMO3, or they may be another FMO.

To ensure the specificity of the Cashman FMO3 antibody heterologously expressed FMO1, FMO2, FMO3 and FMO5 were prepared for immunoblotting. The proteins were electrophoresed as for blots a, b and c. The resulting blot (figure 4.4 d) demonstrated conclusively that Cashman's antibody was specific for FMO3. Another benefit of using heterologously expressed FMOs as controls, is that the resulting blot would be able to tell us if FMO3 was being detected in the protein homogenate preparations. If so the band in the pure protein blot would occur at the same molecular weight position as for blots a, b and c.

Assuming the band detected in the human brain samples is FMO3 (an assumption not without problems), then expression was detected in the thalamus, subthalamic nucleus and substantia nigra for all four individuals. However, the samples from $\overline{6PF}$ showed greatest expression in the thalamus. Although the differences are small, the Parkinson's patients $\overline{2PM}$ and $\overline{8PM}$ show higher amounts of FMO3 in the three regions analysed than does $\overline{5CF}$ and $\overline{7CF}$ (non-Parkinson's patients). Whether or not the clinical condition of the individuals has any effect on the expression observed is unknown. Both $\overline{8PM}$ and $\overline{2PM}$, prior to death, were undergoing drug therapy for their condition using deprenyl, a known substrate of FMO. Therefore, could this mean

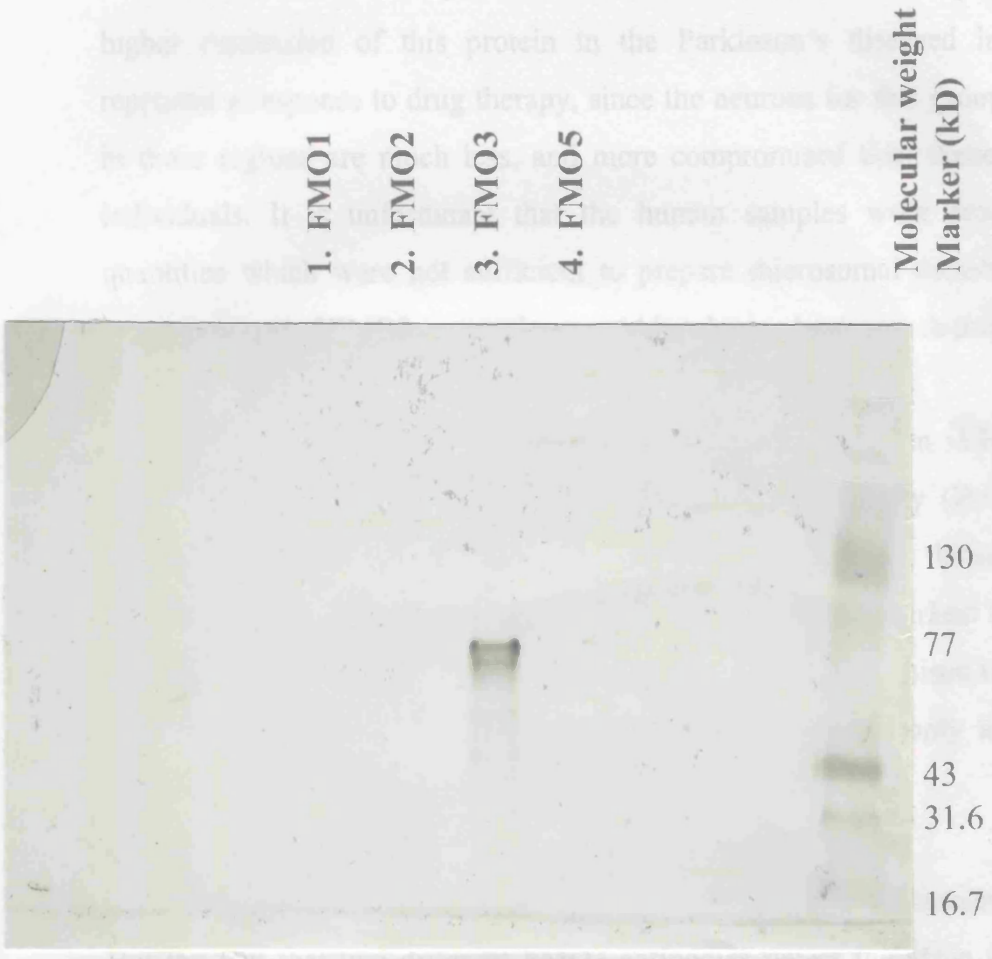

Figure 4.4d Western blot of heterologously expressed human FMOs 1,2,3 and 5 to test the specificity of human FMO3 antibody (JR Cashman). The lanes 1-4 contain FMO1 protein (0.1pmole), FMO2 (0.04pmole), FMO3 (0.5pmole),FMO5 (0.5pmole). Only FMO3 protein is detected by JR Cashman antibody. The amounts of FMO in each sample were calculated by the Philpot laboratory who supplied the heterologously expressed FMOs.

that FMO in these people was at artificially higher levels ? Given that detection and expression of FMO3 so far is centred within the basal ganglian region in specific areas such as the thalamus, subthalamic nucleus and substantia nigra; the seemingly higher expression of this protein in the Parkinson's diseased individuals may represent a response to drug therapy, since the neurons for this group of individuals in these regions are much less, and more compromised than those of the control individuals. It is unfortunate that the human samples were provided in small quantities which were not sufficient to prepare microsomal membranes. A much clearer picture of FMO3 expression would be obtained using such membranes.

The results from the other primate samples showed expression in both Orang-utan and Gorilla. For the Orang-utan the human FMO3 antibody (Philpot), indicated expression of protein in the midbrain region, substantia nigra, thalamus and central region. However, the midbrain and substantia nigra gave the darkest bands, while the thalamus and central region were very faint. Using antibody raised to human FMO3 (Cashman) figure 4.4b, expression of protein was detected only in the substantia nigra sample lane.

The bands detected are of a lower molecular weight than the human FMO3 control. But the fact that two different FMO3 antibodies detect the same size band in the Orang-utan brain raises confidence that it is FMO3 being detected.
In the baby Gorilla samples, a very faint band is present in the substantia nigra and thalamus. These bands are between the human FMO3 control and the bands detected in the Orang-utan (figure 4.4c).

If more human samples had been available it would have been interesting to probe these with the Philpot FMO3 antibody. This antibody is clearly superior to that of the Cashman antibody for the purpose of western blotting.
The possibility remains that FMO3 expression was poorly detected in the gorilla brain since expression of FMO in early post-natal subjects has shown to be highly dependent upon hormonal and developmental regulation **(67,70)** and the gorilla was neo-natal prior to death. Given that we are finding FMO expression in brain of other

primates, then the poor expression in gorilla may well have been a function of its age.

Name	Sex	Age	Condition	Drugs prescribed
1CF	Female	73	CONTROL	
2PM	Male	73	PARKINSON'S	Melleril
3CM	Male	73	CONTROL	
4PF	Female	87	PARKINSON'S	Madopar
5CF	Female	94	CONTROL	
6PF	Female	88	PARKINSON'S	Madopar
7CF	Female	88	CONTROL	
8PM	Male	86	PARKINSON'S	Sinemwt and Selegiline

Table 7. Makeup and medical condition of individuals providing brain tissue.

4.5 Polymerase chain reaction (PCR) of FMO sequence in human brain and Southern blotting

The results presented in section 4.2 show that FMO3 and FMO4 mRNAs are expressed, in discrete neurons, in regions of the midbrain and basal ganglia. To confirm that the FMO RNA detected by *in situ* hybridization is FMO3 and FMO4 these sequences were amplified by RT-PCR. The aim being to isolate the amplified band and determine its DNA sequence. RT-PCR was also carried out using primers for FMO1, FMO2 and FMO5 as these mRNAs were not analysed by *in situ* hybridization because of the negative northern blot results (section 4.1). However, the possibility existed that each of these mRNAs are expressed in a few discrete neurons and if this is the case these sequences should be amplified by the PCR.

For each of the FMOs, two primers were designed, one forward and one reverse primer. Each primer pair was designed to amplify across an intronic sequence, exons 8-9 for FMOs 1,2,3 and 5. For FMO4, amplification was to be across exons 1-2. This would ensure that any amplification products from contaminating genomic DNA would be clearly visible on an agarose gel. Each amplified product would also contain a diagnostic restriction enzyme site (see table 8).

Initially, RNA template was isolated from the thalamus of eight individuals, three were male and five were female. Four of these had been diagnosed as having Parkinson's disease. The sex, age and status of these individuals is shown in Table 7. The thalamus was selected because both FMO3 and FMO4 mRNAs were detected in neurons in this area of the brain. Unfortunately, tissue samples from the subthalamic nucleus and substantia nigra were not available. The integrity of the RNA samples is shown in Figure 4.5a.

FMO	PCR primers 3'	PCR primers 5'	expected size of PCR fragment	Restriction enzyme and fragment sizes
FMO1	+GCTCAGAGTGCTGTCAAG -	+GCTACTGCAAGGCTTTAC-	615 bp	Hinf 1 249 & 366
FMO2	+GTGAAGATGGCATTTCTGG -	+CCCTCCCTTGAAGATTCAC -	464 bp	Mbo 1 360 & 104
FMO3	+GAGTACTGCAAAAGATGC -	+GACCATACAGACAGATTAC -	447 bp	Mbo1 88 & 359
FMO4	+CCCACAGAGGATACAGTTTGG -	+GGTACCTGGGTTCTTGGGCG -	449 bp	Hinf 1 217 & 242
FMO5	+CAGGGCAGTGACAATAGG -	+CTGGAAAGGCCAACTCTTG -	544 bp	Mbo 1 396 & 148

Table 8. FMO PCR Primers.

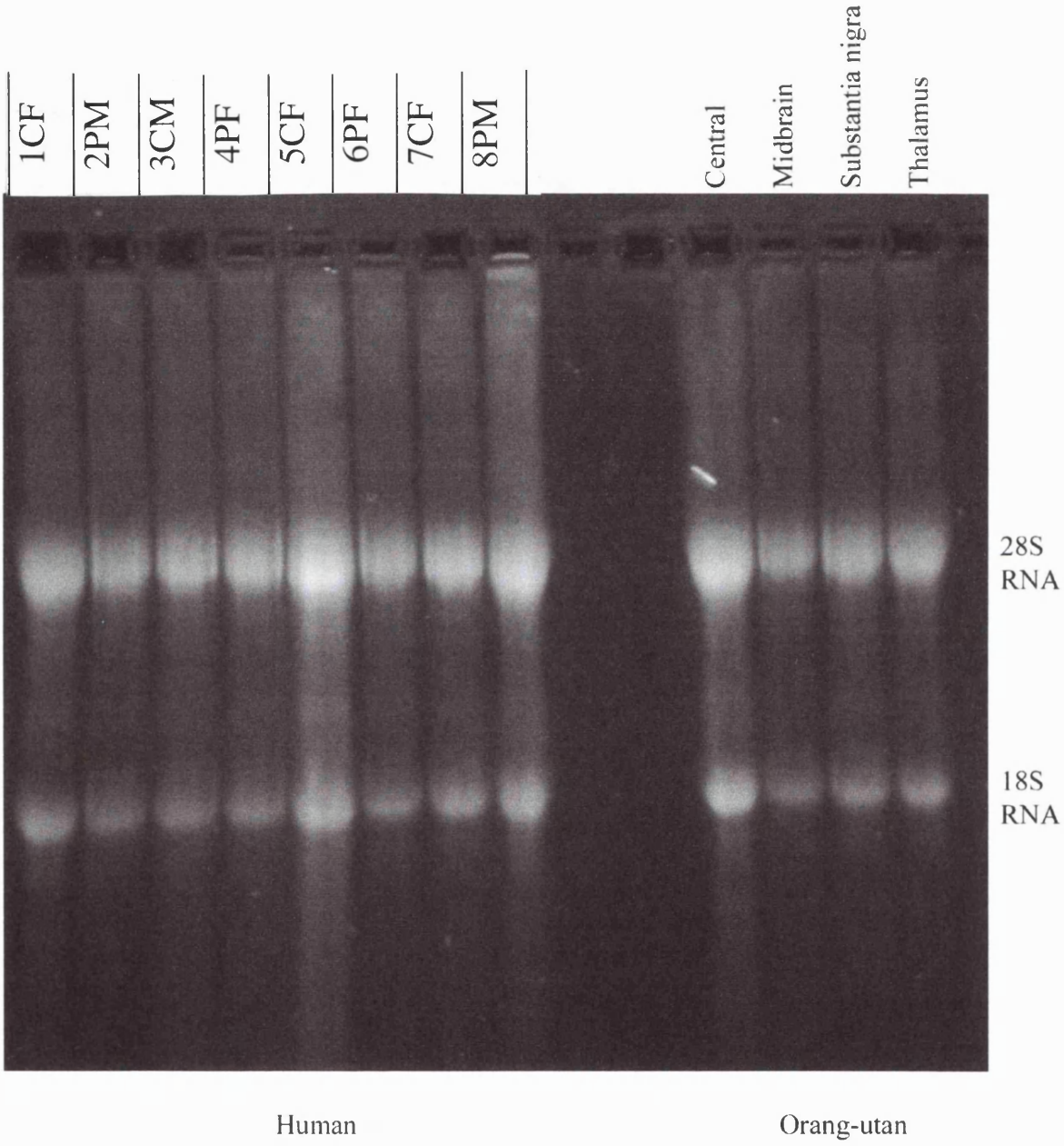

Figure 4.5a RNA extracted from human and Oran-gutan brain regions was electrophoresed on a RNA gel to check its integrity. Both the 18s and 28s RNA bands are clearly visible.

Initially the PCR had a number of problems associated with it, these were eventually overcome by systematically eliminating one aspect of the procedure at a time. A series of magnesium acetate $Mg(OAc)_2$ titrations were performed to ascertain the optimum salt concentration to drive the reaction. A series of dilutions were set up ranging in concentration from: 0.8mM, 1.2mM, 1.5mM and 2.0mM with concentrations of the dNTP mix of 400mM or 800 mM. The results from this set of experiments suggested a concentration of 1.5mM $Mg(OAc)_2$ would be the most appropriate to use with an optimum dNTP concentration of 800mM (figure 4.5b). The same optimum conditions was found for each FMO primer pair.

Each RNA template was copied using the appropriate FMO 3' primer and MuLV reverse transcriptase. This was then used as the template in the PCR reaction. A band was observed in all cases including the negative control (data not shown). A number of attempts were made to get rid of the contaminating band. These included increasing the annealing temperature in small increments while holding other conditions stable. This failed to work and multiple bands were still occurring in sample lanes. Another procedure involved reducing the length of cycles by between 2 and 5, and raising the denaturation temperature. None of these approaches were successful. Therefore it was decided to amplify all RNAs, not with an FMO 3' primer, but using a random hexamer primer method. This method has been found to give a cleaner RT product and has been used successfully **(210)**.
This approach proved more successful in producing a better set of results in terms of clarity and reproducibility. The results for three of the five FMOs are shown in Figures 4.5 (d,e, and f). Results for FMO1 and FMO2 and human samples are not shown. See table 9 for an overall view.

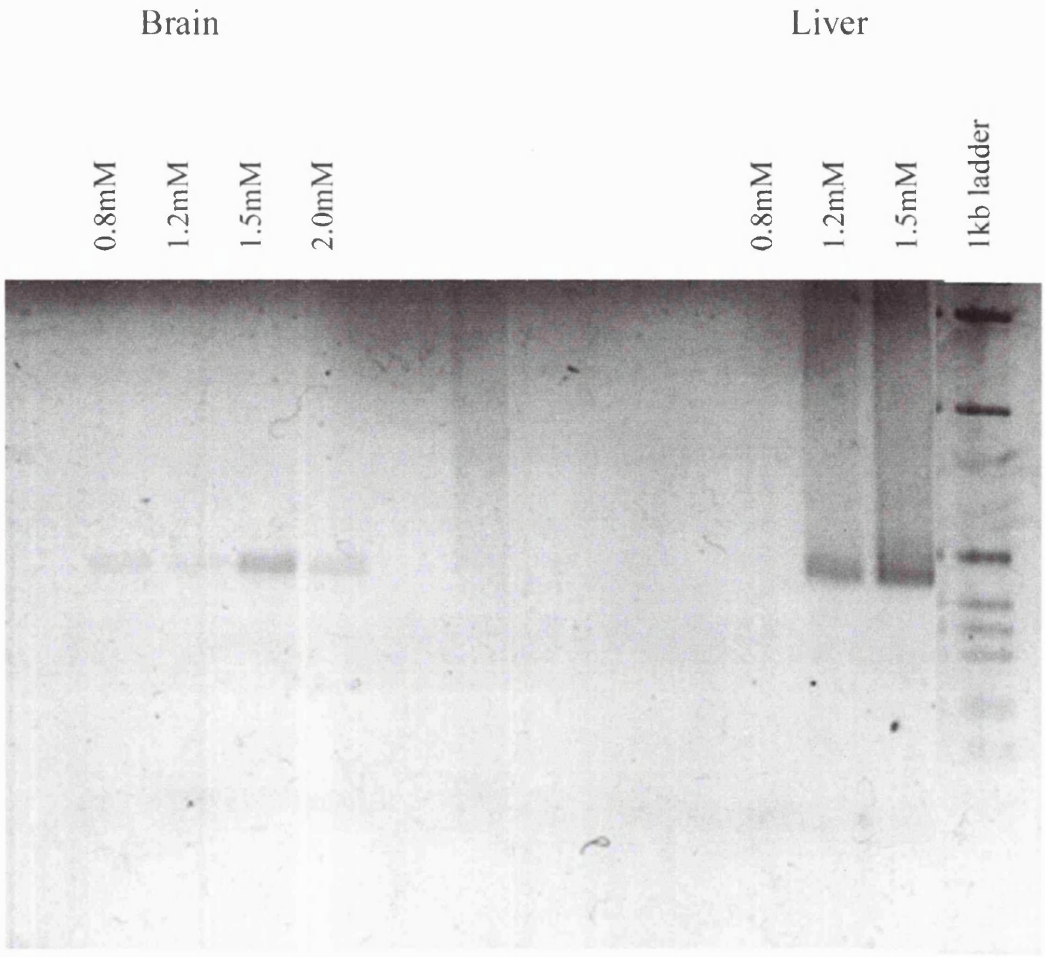

Figure 4.5b Optimisation for PCR conditions. The blot shows a series of magnesium acetate Mg(OAc)2 titrations to establish the most reliable concentration required to give consistent results. RNA was transcribed first from the thalamus or liver prior to the PCR reaction. This figure shows the amplification of FMO3 sequences. The molecular weight markers are the 1 kb ladder from GibcoBRL.

At this stage an Orang-utan brain became available and it was decided to analyse the RNA from the individuals shown in Table 7 together with RNA isolated from regions of the Orang-utan brain using the second RT-PCR method. The thalamus, subthalamic nucleus, substantia nigra, and the central region between the thalamus and the corpus callosum were dissected from the Orang-utan brain. RNA was prepared from each of these samples. The integrity of these samples is shown in Figure 4.5 a.

Figure 4.5 c shows no amplification product observed for FMO1 or FMO2 in the Orang-utan brain samples. None of the 8 human thalamus RNA samples amplified with primers for FMO1 and FMO2. Both FMO1 and FMO2 sequences were amplified from the positive control, human genomic DNA. The sizes were as expected, that of 615 bp for FMO1 and 464 bp for FMO2, (data not shown).
FMO3 sequences were amplified from six of the eight individuals analysed. The two samples that failed to amplify were from 3CM and 7CF. FMO3 sequences were amplified from the central area, mid brain and substantia nigra, but not from the thalamus of the Orang-utan. The reasons for the failure of certain samples to amplify is not known. The amplified product was of the expected size, 447 bp.

FMO5 RNA was not detected by northern blot hybridisation (section 4.1). However, RT-PCR shows this mRNA to be present in the single human subthalamic nucleus RNA sample analysed which comprised of pooled RNA from a number of different individuals. The amplified product was of the expected size of 544 bp. FMO5 mRNA was not present in the eight thalamus RNA samples analysed.

FMO5 sequences were not amplified from the central region, substantia nigra, thalamus and mid brain regions of the Orang-utan brain.

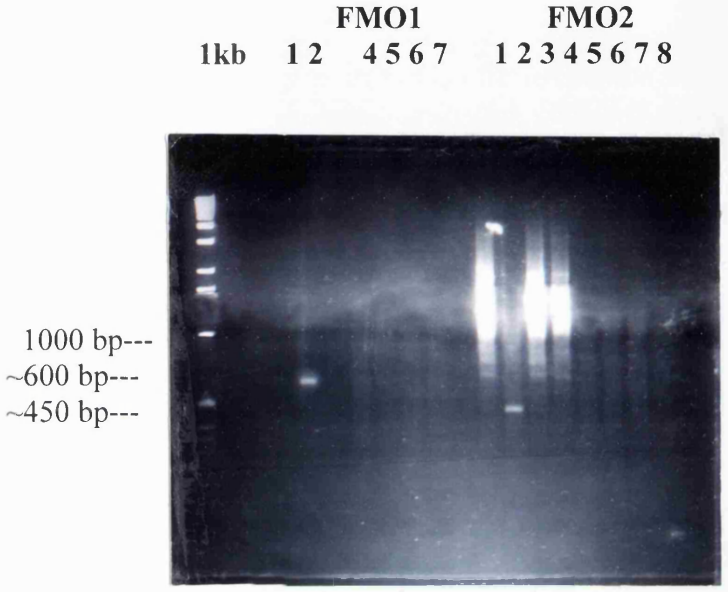

Figure 4.5c RT-PCR products for FMO1 and FMO2 using RNA extracted from Orang-utan brain tissue. FMO1: Lane 1 contains negative control, lane 2 contains the positive control at ~ 600 bp, lane 3 shows PCR control. Lanes 4-7 show no amplification products. FMO2: lane 1 and 3 show negative control, lane 2 shows the positive control at ~460 bp. Lanes 4-7 show no amplification products. Lane 8 is shows PCR control. Lane 4 is central region; Lane 5 is the mid brain; Lane 6 is substantia nigra and lane 7 is thalamus.
The molecular weight markers are the 1 kb ladder from GibcoBRL.

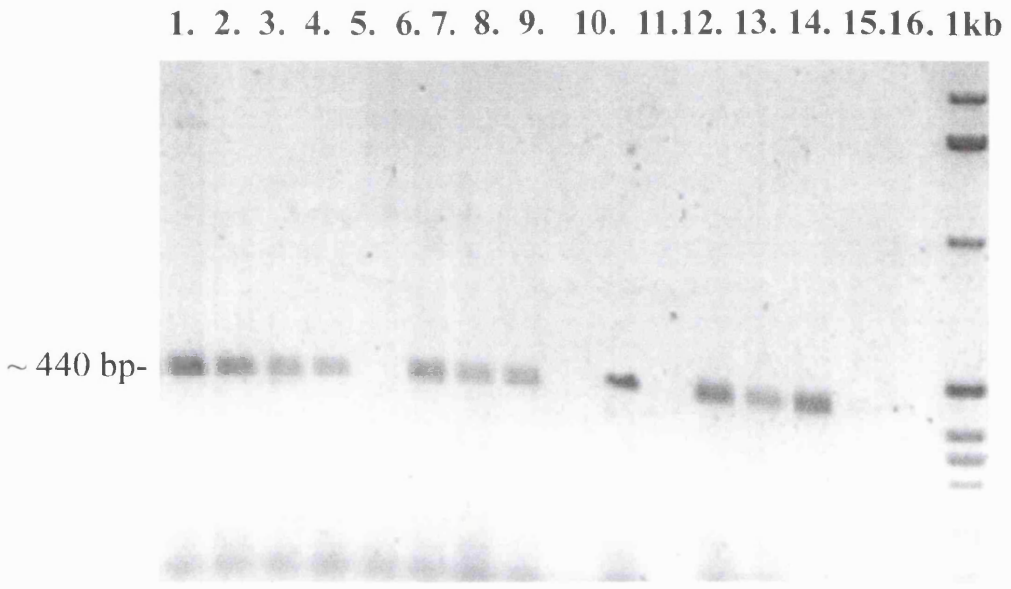

Figure 4.5d Agarose gel electrophoresis of PCR amplified FMO3 products from human brain thalamus region and Orang-utan brain regions. Lanes 1-2 show the positive control of human liver. Lane 11 shows negative control (sample without *r*Tth enzyme). Lane 16 shows PCR control (water in replace of enzyme). Lanes 3-10 show human products, Lanes12-15 show Orang-utan products for central area (12), mid brain (13), substantia nigra (14) and the thalamus (15). Human brain samples in lanes 5 and 9 failed to amplify as did Orang-utan sample in lane 15 (thalamus) . The molecular weight markers are the 1 kb ladder from GibcoBRL.

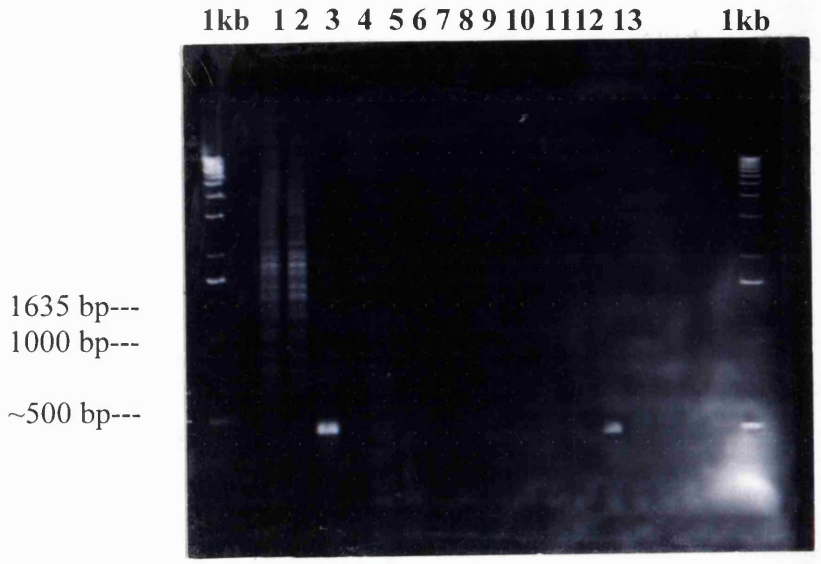

Figure 4.5E Amplification of PCR products for FMO5 using RNA extracted from human brain tissue. Lanes 1-2 contain the negative controls, lane 3 contains the positive control at ~ 550 bp, lane 4 shows PCR control. Lanes 5-12 show no amplification products for the 8 individuals analysed. Lane 13 however, shows an amplification product. Lane 13 contains an amplification product derived from human subthalamic nucleus RNA, unlike lanes 5-12 which are amplification products from RNA derived from the thalamus.
The molecular weight markers are the 1 kb ladder from GibcoBRL.

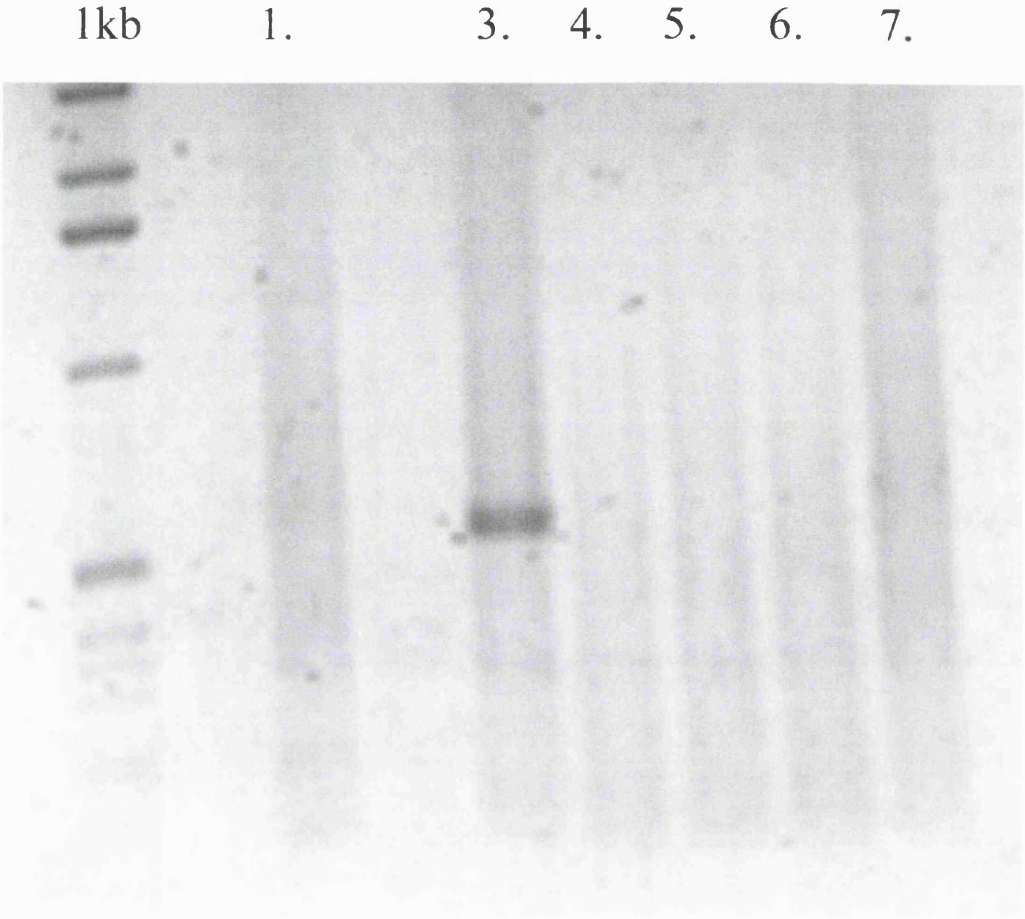

Figure 4.5f Agarose gel showing amplified PCR products for FMO5 and Orang-utan samples. Lane 1 shows negative control, lane 3 shows positive control at ~550 base pairs (expected size 544 bp). Lanes 4 (central area), 5 (mid brain), 6 (substantia nigra) and lane 7 (thalamus) contain primate brain samples which have undergone PCR but have failed to amplify. The molecular weight markers are the 1 kb ladder from GibcoBRL.

The amplification of FMO4 sequences proved very difficult. Each reaction met with increased contamination. DNAse treatment of liver RNA was performed and a series of elimination steps were used to try to improve the results, however, a signal in the negative control continued to appear. Therefore, a set of negative and positive controls for both the RT and PCR steps were put through the amplification process to establish whether or not the difficulties could be due to the sequence selected to be amplified. The results of this series can be seen in (figure 4.5g).

Only the positive control (i.e.) RT-PCR amplification of FMO4 liver RNA should produce a band, however, the RNA sample alone also gave a positive result as did the PCR control. A new set of primers was designed that crossed two introns between exons 2-4 in the region spanning 866 to 1101 base pairs of the cDNA sequence. This would produce a 235 base pair product upon amplification via PCR. The resulting set of experiments can be seen in (figure 4.5h).
The new primers were more promising, in that the PCR and RT controls no longer produced an amplification product. The positive control, liver RNA, resulted in an amplification product of the expected size 235 bp (figure 4.5 h, lane 2).

FMO4 sequences were not amplified from four Orang-utan brain regions, the central area, mid brain, substantia nigra and thalamus. Instead a smear was observed. Similarly, FMO4 sequences were not amplified from eight human thalamus RNA samples. Results not shown.
FMO4 mRNA is expressed in the thalamus (see sections 4.1 and 4.2). Therefore failure to amplify this sequence was not understood. A series of experiments was set up to optimise FMO4 amplification. The annealing temperature was varied, 49°C, 50°C and 54°C were tried. The number of cycles was increased from 30 to 35. However, no amplification of FMO4 sequences was possible. Closer observation of the FMO4 mRNA sequence revealed a high degree of secondary structure **(58,111,127)**. The problem may therefore lie in the inability to transcribe the RNA through a hairpin loop structure. Subsequently, newer reverse transcriptases have become available that permit hairpin loops to be transcribed.

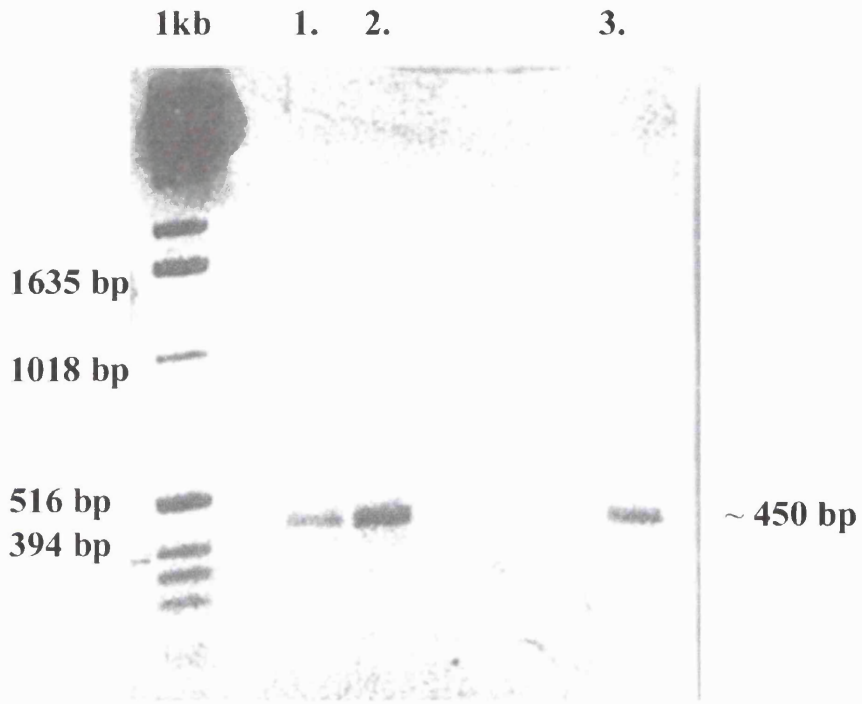

Figure 4.5g Agarose gel electrophoresis of PCR amplified products of human brain RNA for FMO4. Lane 1 (-ve)control, lane 2: (+ve)control, lane 3 human liver RNA . The gel shows RT- RNA in lane 3 which suggests that there may be secondary structure interference in this region of FMO4. The molecular weight markers are the 1 kb ladder from GibcoBRL.

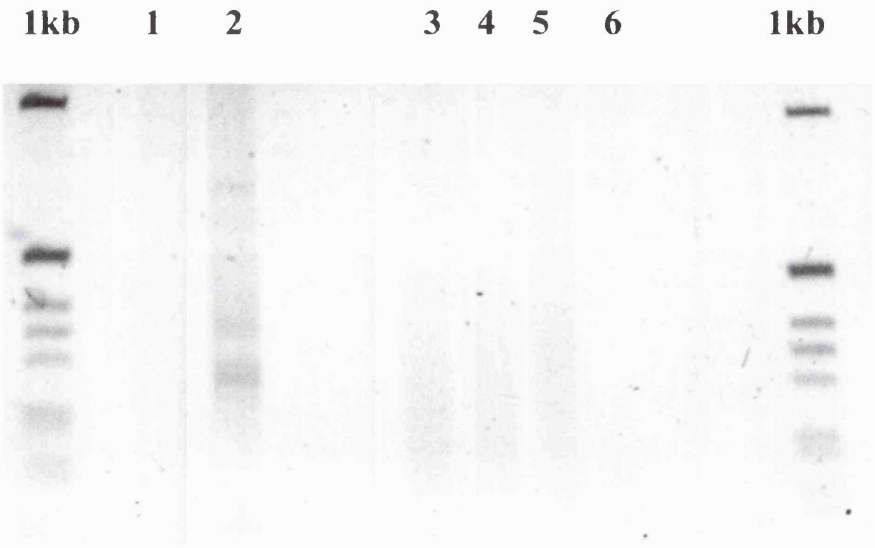

Figure 4.4h Agarose gel of PCR amplified fragments using FMO4 specific primers. Lane 1 shows the negative control, lane 2 shows the positive control of human liver total RNA. Lanes 3, 4, 5, and 6 failed to show Orang-utan amplifications. The molecular weight markers are the 1 kb ladder from Gibco-BRL.

Because of the controversial literature published on the identity of the FMO isoform present in human brain **(163,165,166)**, a series of experiments was carried out to conclusively prove that FMO3 is expressed in human brain.

Confirmation that the amplification product obtained with FMO3 primers was obtained by restriction digest of a selection of human and Orang-utan PCR products (figure 4.5i). Here, the expected FMO3 fragments of 359 bp and 88 bp were observed via agarose gel electrophoresis when digested with the appropriate enzyme MboI. Although the Orang-utan PCR product was cleaved to produce a 359 bp fragment, the band at 447 bp remained, which suggests that only partial digestion occurred, or that the Orang-utan is heterozygous for the MboI site. The Orang-utan FMO3 DNA sequence has not been elucidated.

Although there hasn't been any published work regarding FMO and Orang-utan specifically, research with FMO and other primates has found FMO2 expression at both the RNA and protein levels **(99,100)**, but not FMOs 3 or 4. FMO4, however, has been detected in brain tissues of the rabbit using PCR method by Blake *et al* **(168)**.

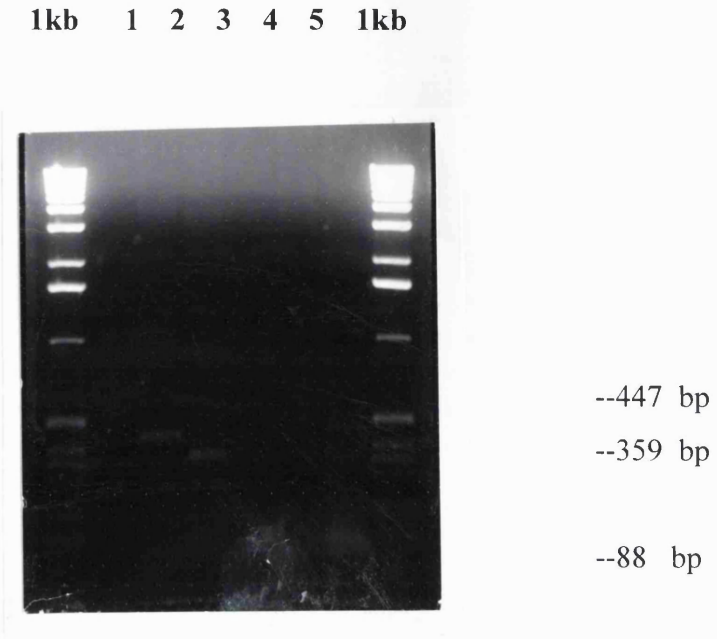

Figure 4.5 i Agarose gel electrophoresis of PCR amplified products for FMO3. Amplification products were digested with Mbo1 to produce fragments at 359 bp and 88 bp. Lane 1. contains a control of uncut PCR product. Lanes 2, 3 and 4 contain human thalamus amplified product cut with restriction enzyme Mbo1 from individuals coy, day and scott respectively. Lane 5 contains digested amplified fragment from Orang-utan substantia nigra sample. Lane 5 shows only partial digestion, giving bands of 359 bp, 88 bp as well as the uncut 447 bp product. Molecular weight standards are the 1 kb ladder from GibcoBRL

.

FMO	Positive control (RNA)	negative control (*r*Tth Enzyme absent)	Human (Thalamus)	Orang-utan *(Cen. Mb. SNi. Th.)
FMO1	Marmoset liver	Marmoset liver	Negative	Negative
FMO2	Human lung	Human lung	Negative	Negative
FMO3	Human liver	Human liver	Positive	+ve +ve +ve -ve
FMO4	Human liver	Human liver	Negative	Negative
FMO5	Human liver	Human liver	Negative	Negative

Table 9. PCR results for FMOs 1 -5.(Cen. Mb. SNi. Th) refer to brain regions: central, midbrain, substantia nigra and thalamus, respectively

4.5i Southern Blotting of PCR-products of FMO3

PCR products generated by primer sequences specific for FMO3 from human and Orang-utan brain regions were electrophoresed on a 1% agarose gel and transferred on to a nitro-cellulose membrane overnight then baked at 80^0C to immobilise the DNA (method 3.11). A [^{32}P] labelled cDNA probe encoding the FMO3 isoform was used to probe the blot of PCR amplified fragments. The resulting autoradiograph from the blot revealed the presence of 7 strongly positive signals in 7 of the 8 human thalamus samples, and one very weak sample from 3CM. All four of the Orang-utan samples were observed in the Southern blot .

The hybridising bands were estimated to be approximately 450 bp in length which was the expected size for the FMO3 amplified products. This was determined from a standard curve using the 1 kb ladder (GibcoBRL) as standards. The Orangutan samples exhibited a second more weakly hybridising band of about 800 bp.

The result of the Southern blotting confirms the presence of FMO3 mRNA in the brain of humans and probably also in the brain of Orang-utans.

The Southern blot also confirmed the presence of FMO3 in the thalamus of Orang-utan. Observations of an ethidium bromide stained gel had been negative for Orang-utan thalamus, (see figure 4.5d). Also all eight human PCR products hybridised to the FMO3 probe. Previously two individuals, 3CM and 7CF failed to show a product on an ethidium bromide stained gel (figure 4.5e).

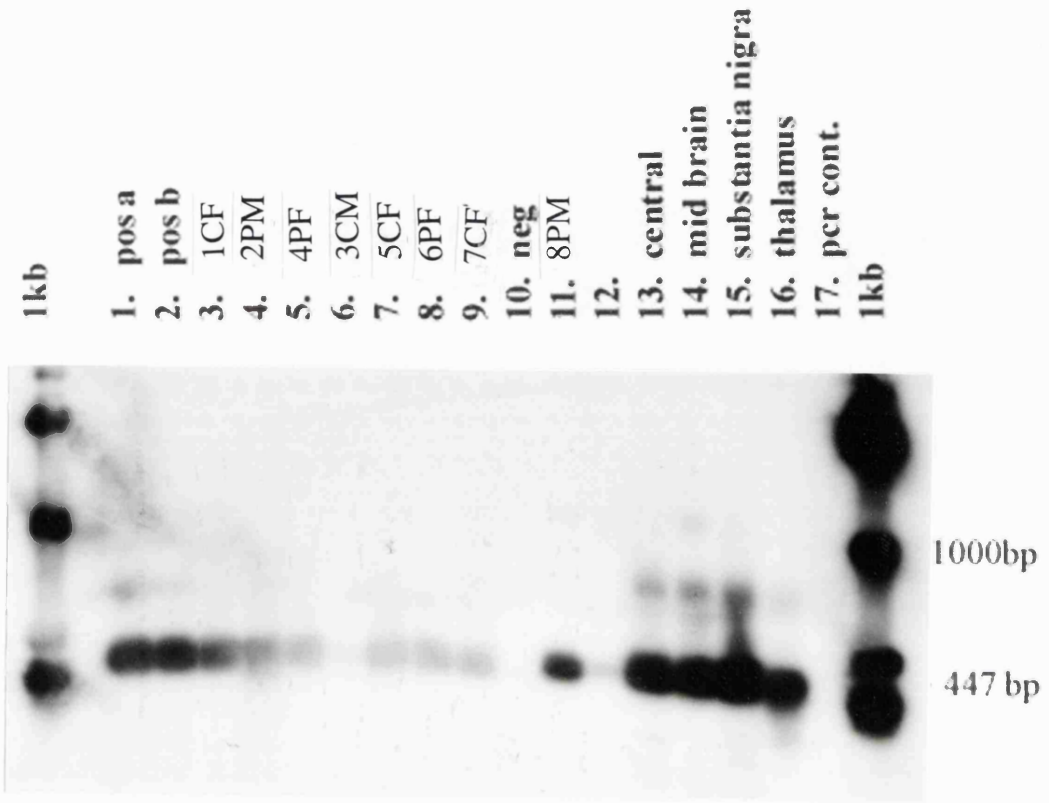

Figure 4.5i a. Southern blotting of PCR amplification products for FMO3. lane 1 (positive control from RT-PCR), lane 2 (positive control from first strand PCR). Lanes 3-9 FMO3 brain amplification products. Lane 10 negative control. Lanes 13-16 Orang-utan FMO3 amplification products. The sample for Pym (lane 6) hybridises very weakly, a PCR product for this individual was not seen on the ethidium bromide stained gel.

4.6 DNA Sequencing of purified PCR products

Two PCR derived products generated from primers specific for FMO3 as outlined in section 4.5, were chosen to use in sequencing reactions. An aliquot from the individual 4PF and the amplification product from the substantia nigra region of the Orang-utan were electrophoresed on a 1% low melting point agarose gel. After electrophoresis the bands were excised. The gel slices were then purified (method 3.2.5.) and used as a template for DNA sequencing using an automated sequencer and the forward primer.

The results were as follows:
The sequence obtained from the human sample was aligned with FMO3 cDNA sequence from the Dolphin *et al* **(107)** using the MacVector® software programme. The resulting alignment is shown in figure 4.6a.

There is excellent agreement between the two sequences, except at the 5' end. The sequence obtained from the Orang-utan amplified sample was aligned with FMO3 cDNA sequence in the same way as the human sequence, however, there was a match of less than 60%. The Orang-utan PCR product had not sequenced well, and there were several ambiguities in the sequence.

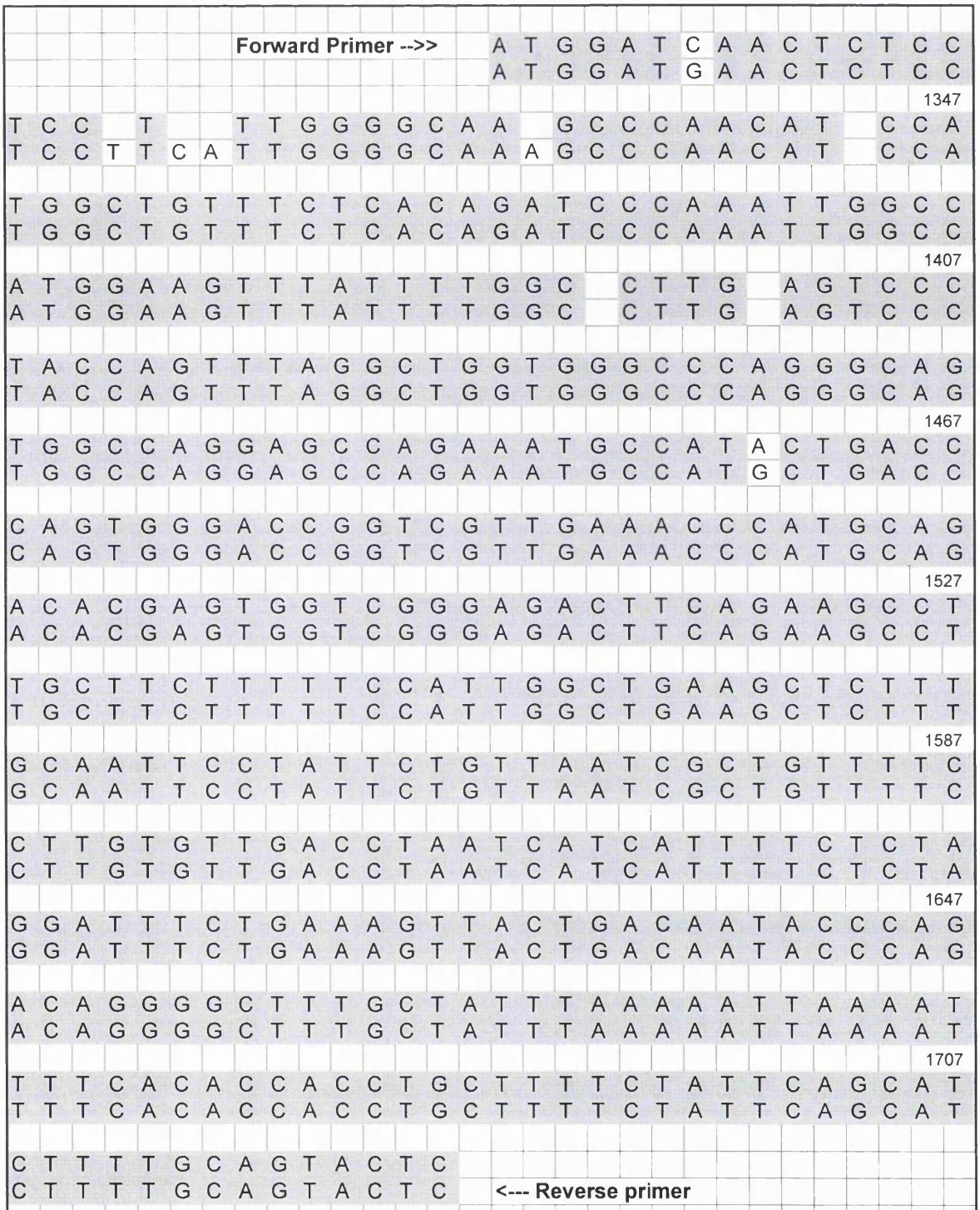

Figure 4.6 Alignment of the sequence of FMO3 PCR amplified fragment from human brain RNA (top line) and FMO cDNA sequence (bottom line).

In the light of the PCR results and the Southern blot of Orang-utan samples, reasons as to why the Orang-utan PCR product failed to sequence could be due to a number of factors. Possibly not enough template starting material, a PCR product contaminated with primer or insufficiently purified from agarose. Further studies need to be carried out to absolutely confirm that FMO3 is expressed in Orang-utan brain.

Concluding Discussion

During the course of this project the expression patterns of FMOs in the basal ganglia of the human brain were determined. In the liver and extra-hepatic tissues such as the lung, kidney and skin, FMOs play a primary role in xenobiotic metabolism. Many clinical drugs, which are substrates for FMOs are not fully metabolised in the liver and pass the blood-brain barrier to exert their effects on the human brain. These include neuroleptic drugs from the phenothiazine family and many tricyclic anti-depressants. These substances are used to manage depression and also to curb psychotic behaviour **(176,184-187)**. It is known for example, that the concentration of the neurotoxin MPTP rises in the brain of mice pre-treated with substrates of hepatic FMOs. Therefore the saturation of FMOs by their substrates, in tissues other than the brain, can increase the concentration of potentially harmful substances that cross the blood-brain barrier. An important role for FMOs might be to ensure that foreign chemicals present in the brain are oxygenated thus aiding their clearance from the cell and ultimately the body. The rapid removal of xenobiotics from neuronal cells would be paramount for the protection of this important cell type.

Interestingly, recent evidence indicates that FMOs have a role in metabolism of naturally occurring neurotoxin TIQ in the mammalian brain **(191-193, 195,196)**. TIQ is produced primarily in the caudate nucleus area of the human brain and if methylated leads to a reduction in Parkinson's symptoms **(192)**. A number of compounds such as TIQ derivatives have been identified in the brain as Parkinson's disease related. Furthermore, research has shown that the methylated form of TIQ leads to a reduction in Parkinson's symptoms **(192,195)**. Conversely, if TIQ methylated levels are reduced then Parkinson's symptoms persist. TIQ is known to be metabolised to either Parkinsonism inducing compound 1 Benzyl 1,2,3,4-tetrahydroisoquinoline (1 BnTIQ) or

Parkinson's preventing compound 1 methyl-tetrahydroisoquinoline (1 MeTIQ) depending on whether or not MAO-B is inhibited or not **(195,196)** see figure 2.4b. Although this study was carried out in a rodent brain, it may well be that one of the FMO isoforms expressed in human brain as identified in this thesis, is a candidate in the metabolism of TIQ.

When the work presented in this thesis began the presence of FMO was unconfirmed in the human brain, although a number of groups have now identified FMO expression in brain from rodents **(157,158,159,164, 167)** and rabbit **(168)**. However, it was not until recently that expression of FMO has been detected in human brain using human FMO probes. Evidence presented by one research group of FMO expression in tissue derived from adult human brain remains controversial **(163,165,166)**. This is because in their studies, they detected FMO expression using an antibody to rabbit FMO2. The human orthologue of this isoform is not expressed at the protein level in man because of a mutation that causes a premature stop codon **(99)**. The mutant FMO2 protein is inactive when expressed in a baculovirus / insect cell system **(99)**. The presence of FMO2 protein in the brains of humans or rodents has not been corroborated by other workers in this field.

Evidence presented in this thesis is a systematic analysis of FMO expression in the human brain. Some studies were carried out on an Orang-utan brain. The results confirm FMO3 expression in man at both the mRNA level and protein level. FMO4 was detected at the mRNA level. FMOs 1 and 2 mRNAs were not detected in the regions analysed. Evidence from PCR experiments suggest that FMO5 may be expressed in the subthalamic nucleus (figure 4.5e).
The sequence determination of PCR products confirmed the presence of FMO3 in the basal ganglia (figure 4.6 a). This isoform has not been detected in rodent and rabbit brains **(166-168)**. Our ability to detect FMO3 is probably due to the methods and brain regions used. Both FMO3 and FMO4 are localised to specific neurons within the basal ganglia and studies using total RNA isolated from whole brain would be unlikely to detect these isoforms. The localisation

of FMO5 to the basal ganglia suggests a specific role for this protein in this brain region.

We have also demonstrated that FMO3 is located in a number of different kinds of neuronal cells and in a number of different regions and sub-regions; pyramidal cells in the hippocampus region, the granular cells of Ammon's horn, neurons in the thalamus, substantia nigra and subthalamic nucleus. The regions in which the FMOs are located are interesting in that they form part of a loop-like system involved in coordination of movement and behaviour. This area which when damaged causes neurodegenerative disorders such as Parkinson's syndrome and Huntingtons disease. The fact that surrounding regions such as the lentiform nucleus, crus cerebre, choroid plexus and dentate gyrus show no FMO3 expression strongly suggests a localised role for the protein in this region.

An organising principle of brain tissue is that neurons are grouped as regular repeating units, which are functionally important. These repeated regular groupings of neurons occur in areas such as the cerebral cortex and striatum. Pyramidal cells represent a series of neurons which are essentially output pathways, where their axons project in to the thalamus or cerebral cortex or caudate and putamen. Substantial loss of these pyramidal neurons in the frontal and temporal regions correlates with the degree of dementia in Alzheimer's disease. Similarly, loss or damage to dopaminergic neurons of the mid brain and motor neurons of the basal ganglia are both involved in the aetiology of Parkinson's syndromes (see Chapter two). The neurons in the striatum are the medium spiny neurons which receive input from the cerebral cortex, thalamus and substantia nigra, as well as sending signals back. All these regions gave a positive signal in *in-situ* hybridisation experiments (see section 4.2, figures 4.2 c,e,q, 4.2.1 k). The presence in these regions of specific FMO isoforms, implies an important protective or key endogenous role for these proteins. It will be interesting to establish whether polymorphic variation in FMOs 3, 4 and 5 contribute to a pre-disposition to neurodegenerative disease and /or to

variations in an individual's response to a particular drug therapy in the case of mental illness.

Mutations in the *FMO3* gene cause primary trimethylaminuria (fish odour syndrome). Affected individuals do not seem to be more susceptible to Parkinson's disease or other neurodegenerative disorders than non-trimethylaminuria individuals. However, many sufferers of trimethylaminuria are prone to bouts of severe depression and anxiety. The depression often results from the social isolation experienced because of the unpleasant body odour associated with the disorder. However, true clinical depression does present in a number of individuals and may be the direct result of an inability to metabolise an FMO3 substrate(s). The use of anti-depressant drugs, which are substrates for FMOs exacerbates the symptoms of trimethylaminuria presumably due to the complete saturation of any residual FMO3 activity. In a few trimethylaminuria individuals an attack similar to an epileptic type fit is preceded by a strong fishy odour **(138,140)**. These symptoms have been diagnosed as a defect in the basal ganglia (personal communication with patients and families). Taken together these disorders suggest an important role for FMO3 in the human brain.

Theraputic drugs such as Selegiline (deprenyl) may have an adverse effect on the patient if s/he has a mutation or carries a polymorphic variant in an *FMO* gene. Selegiline is an MAO inhibitor which when metabolised leads to a number of end products, one of which is metamphetamine. Metamphetamine can be further metabolised by FMO3 to its *N*-oxide **(197)**. The build up of metamphetamine, which is itself an irreversible inhibitor of MAO, therefore leads to increased dopamine levels which can have a negative effect on the individual. The intriguing relationship between FMOs and MAOs has yet to be fully elucidated. Perhaps members of the two classes of proteins act to maintain the concentration balance of an as yet unidentified important endogenous metabolite and also of drugs given as therapy.

FMO mediated metabolism of drugs acting on the brain is likely to play an important role in the pharmokinetic modulation of neurotoxic and / or psychoactive drugs, but to what degree this occurs remains to be ascertained.

Future Work

A number of interesting avenues of research have been opened up by the work carried out in this project these include:

- Further analysis of the two FMO3 transcripts, of 2.3 and 1.8 Kb, observed in the subthalamic nucleus.
- Is FMO5 expressed only in the subthalamic nucleus? The study should be extended to include samples taken from a panel of individuals comprising those that suffered from neurodegenerative disorders such as motor neurone disease in which the subthalamic nucleus is affected.
- Studies of non-human primate samples should be extended and include an analysis of the sequence identities of the primate FMO PCR amplified products to those derived from the human brain samples.
- To use a cell culture, such as a neuroblastoma line, to determine the metabolic capacity of FMOs. If a useful cell line can be identified then these studies can be extended to knock-out specific FMO expression using anti-sense technology. The role of an FMO in the metabolism of compounds such as TIQ could be determined and the consequences for the cell of a null or compromised FMO phenotype investigated.
- Stable neuronal cell lines expressing individual FMOs or panels of FMOs could be created by transfection with plasmids encoding FMO cDNAs. These would prove invaluable for biotransformation and toxicity studies.

Bibliography

1. GG Gibson and P Skett Introduction to drug metabolism 2nd Edition, Blackie Academic and Professional (Chapman Hall) UK.1994

2. DM Ziegler (1991) Unique properties of the enzymes of detoxification. *Drug Metab. Disp.* **Vol. 19**: 847-52

3. E Hodgson and PE Levi (1992) The role of flavin containing monooxygenase in the metabolism and mode of action of agricultural chemicals. *Xenobiotica* **Vol. 22**: 1175-1183

4. Y Ohmiya and HM Mehendale (1984) Species differences in pulmonary *N*-oxidation of chlorpromazine and imipramine. *Pharmacology* **Vol. 28**: 289-295

5. J Caldwell (1982) Conjugation reactions in foreign compound metabolism: definition, consequences and species variation. *Drug Metab. Rev.* **Vol. 13**: 745-778

6. DM Ziegler (1980) Microsomal flavin-containing monooxygenase: oxygenation of nucleophilic Nitrogen and Sulfur compounds, in *Enzymic Basis of Detoxification* (WB Jakoby Ed.) **Vol. 1**: Academic Press, New York. pp201-227

7. FP Guengerich (1990) Enzymic oxidation of xenobiotic chemicals. Critical reviews in *Biochem and Molecular Biology* **Vol. 25**: 1990-2153

8. WB Jakoby and DM Ziegler (1990) The enzymes of detoxification. *J. Biochem.* **Vol. 265**: 20715-20718

9. RM Philpot, E Arinc and JR Fouts (1975) Reconstitution of the rabbit pulmonary microsomal mixed function oxidase system from solubilised components. *Drug Metab. Disp.* **Vol. 3**: 118-126

10. PJ Sabourin, BP Smyser and E Hodgson (1984) Purification of the flavin-containing monooxygenase from mouse and pig liver microsomes. *Int. J. Biochem.* **Vol. 16**: 713-720

11. S Coecke, A Segaert, A Vercruysse and V Rogiers (1993) Expression of flavin-containing monooxygenases activity in adult rat hepatocytes under various culture conditions. *Toxic. in Vitro* **Vol. 7**: 487-491

12. FF Kadlubar, EM Mckee and DM Ziegler (1973) Reduced pyridine nucleotide dependent *N*-hydroxy amine oxidase and reduction activities of hepatic microsomes. *Arch. Biochem. Biophys.* **Vol. 156**: 46-57

13. V Massey and CH Williams Ed. (1982) Flavins and flavoproteins. Developments in Biochemistry **Vol. 21**. Flavoprotein monooxygenases D P Ballou pp 301-309. Elsevier Biomedical.

14. DM Ziegler (1984) Metabolic oxygenation of organic nitrogen and sulfur compounds. *Drug Metabolism and Drug Toxicity* pp33-53. (JR Mitchell & MG Hornings eds.) Raven Press. New York

15. DM Ziegler (1988) Flavin-containing Monooxygenases: Catalytic mechanisms and substrate specificity. *Drug Metabolism Rev.* **Vol. 19**:1-32

16. DM Ziegler, CH Mitchell (1972) Microsomal oxidase IV. Properties of a mixed function amine oxidase isolated from pig liver microsomes. *Arch. Biochem. Biophys.* **Vol. 150:** 116-125

17. LL Poulsen (1981) Organic sulfur substrates for the microsomal flavin-containing monooxygenase. *Rev. Biochem. Toxicol.* **Vol. 3**: 33-49

18. NP Hajjar and E Hodgson (1980) Flavin adeninedinucleotide-dependent monooxygenase: its role in the sulfoxidation of pesticides in mammals. *Science* **Vol. 209**: 1134-1136

19. A Lemoine, M Johann and TG Cresteil (1990) Evidence for the presence of distinct flavin containing monooxygenases in human tissue. *Arch. Biochem. Biophys.* **Vol. 276**: 336-342

20. PF Coccia and WW Westerfield (1967) The metabolism of chlorpromazine by the liver microsomal enzyme systems. *J. Pharmacol. Exp. Ther.* **Vol. 157**: 446-458

21. RE Tynes, PJ Sabourin and E Hodgson (1985) Identification of distinct hepatic and pulmonary forms of flavin-containing monooxygenases in mouse and rabbit. *Biochem. Biophys. Res. Commun.* **Vol. 126**: 1069-1075

22. Y Ohmiya and H Mehendele (1983) *N-oxidation* of *N,N*-dimethylaline in the rabbit and rat lung. *Biochem. Pharmacol.* **Vol. 32**: 1281-1285

23. RE Tynes and E Hodgson (1985) Catalytic activity and substrate specificity of the flavin-containing monooxygenase in microsomal systems: characterisation of the hepatic, pulmonary and renal enzymes of the mouse, rabbit and rat. *Arch. Biochem. Biophys.* **Vol. 240**: 77-93

24. N B Beaty & D P Ballou (1981) The reductive half-reaction of liver microsomal FAD-containing monooxygenase. *The Journal of Biological Chemistry* **Vol.** 4611-4618

25. N B Beaty & D P Ballou (1981) The oxidative half-reaction of liver microsomal FAD-containing monooxygenase. *The Journal of Biological Chemistry* **Vol. 256** 4619-4625

26. KC Jones and DP Ballou (1986) Reaction of the 4a-Hydroperoxide of the liver microsomal flavin-containing monooxygenase with nucleophilic and electrophilic substrates. *J. Biol. Chem.* **Vol. 261**: 2553-2559

27. DM Ziegler (1991) Mechanism, multiple forms and specificity of the flavin-containing monooxygenases in, *N-Oxidation of Drugs: Biochemistry, Pharmacology, Toxicology* (ed.)P Hlavic, LA Damani, pp 59-68. London: Chapmand and Hall.

28. S Ball & T C Bruice (1980) Oxidation of amines by a 4α-Hydroperoxyflavin. *J. Am. Chem. Soc.* **Vol. 102**: 6498-6503

29. LL Poulsen (1991) The multisubstrate FAD-containing monooxygenase, in: F Miller (ed) Chemistry and Biochemistry of Flavoenzymes. CRC Press, Boca Raton, FL, 2, pp 87-100

30. DM Ziegler (1993) Recent studies on the structure and function of multi-substrate flavin-containing monooxygenases. *Annu. Rev. Pharmacol. Toxicol.***Vol. 33**: 179-199

31. KL Taylor and DM Ziegler (1987) Studies on substrate specificity of the hog liver flavin-containing monooxygenase. Anionic organic sulfur compounds. *Biochem. Pharmacol* **Vol. 36**: 141-146

32. JR Cashman (1995) Structural and catalytic properties of the mammalian flavin-containing monooxygenase. *Chem. Res. Toxicol.* **Vol. 8**: 166-181

33. LL Poulson & D M Ziegler (1979) The liver microsomal FAD-containing monooxygenase: spectral characteristics and kinetic studies. *J. Biol. Chem* **Vol. 254** 6449-6455

34. DM Ziegler (1990) Flavin-containing monooxygenases: enzymes adapted for multisubstrate specificity. *TIPS* **Vol. 11**: 321-324

35. LL Poulsen, K Taylor, DE Williams, BSS Masters and DM Ziegler (1986) Substrate specificity of the rabbit lung flavin-containing monooxygenase for amines: oxidation products of primary alkylamines. *Mol. Pharmacol.* **Vol. 30**: 680-685

36. FJ Gonzalez (1990) Molecular genetics of the P450 superfamily. *Pharmac. Ther.* **Vol. 45**: 1-38

37. FP Guengerich (1991) Reactions and significance of cytochrome P450 enzymes. *J. Biol. Chem.* **Vol. 266**: 10019-10022

38. CJ Decker and DR Doerge (1991) Rat hepatic microsomal metabolism of ethylenethiourea. Contributions of the flavin-containing monooxygenase and cytochrome P450 isozymes. *Chem. Res. Toxicol.* **Vol. 4**: 482-489

39. N Lomri, J Thomas and JR Cashman (1993) Expression in *Escherichia coli* of the cloned flavin-containing monooxygenase from pig liver. *J. Biol. Chem.* **Vol. 268**: 5048-5059

40. LL Poulsen and DM Ziegler (1995) Multisubstrate flavin-containing monooxygenases: applications of mechanism to specificity. *Chemico. Biological Interactions* **Vol. 96**: 57-73

41. T Nagata, DE Williams and DM Ziegler (1990) Substrate specificities of rabbit lung and porcine liver flavin-containing monooxygenases: Differences due to substrate specificity. *Chem. Res. Toxicol.* **Vol. 3**: 372-376

42. JR Cashman, Z Yang, L Yang and SA Wrighton (1993) Sterio- and regio-selective *N* and *S* oxidation of tertiary amines and sulfides in the presence of adult human liver microsomes. *Drug Metab. Dispos.* **Vol. 21**: 492-501

43. MP Lawton, R Gasser, RE Tynes, E Hodgson and RM Philpot (1990) The flavin-containing monooxygenase enzymes expressed in rabbit liver and lung are products of related but distinctly different genes. *J Biol. Chem.* **Vol. 265**: 5855-5861

44. IR Phillips, CT Dolphin, P Clair, MR Hadley, AJ Hutt, RR M^{c}Combie, RL Smith and EA Shephard (1995) The molecular biology of the flavin-containing monooxygenases of man. *Chemico. Biol. Inter.* **Vol. 96**: 17- 32

45. J Ozols (1994) Isolation and structure of a 3rd form of liver microsomal monooxygenase. *Biochemistry* **Vol. 33**: 3751-3757

46. R Gasser, RE Tynes, MP Lawton, KK Karsmeyer, DM Ziegler and RM Philpot (1990) The flavin-containing monooxygenase expressed in pig liver; primary sequence, distribution and evidence for a single gene. *Biochemistry.* **Vol. 29**: 119-124

47. N Lomri, Q Gu and JR Cashman (1992) Molecular cloning of human liver. *Proc. Natl. Acad. Sci. U.S.A.* **Vol. 89**: 1685-1689

48. ME McManus, I Stupans, W Burgess, JA Koenig, P Hall, M Dela and DJ Birkett (1987) Flavin-containing monooxygenase activity in human liver microsomes. *Drug Metab. Dispos.* **Vol. 15**: 256-261

49. J Ozols (1991) Multiple forms of liver microsomal flavin-containing monooxygenases: Complete covalent structure of form 2. *Arch. Biochem. Biophys.* **Vol. 290**: 103-115

50. NJ Cherrington, JG Falls, RL Rose, KM Clements, RM Philpot, PE Levi and E Hodgson (1998) Molecular cloning, sequence, and expression of mouse flavin-containing monooxygenases 1 and 5 (FMO1 and FMO5). *J Biochem Mol Toxico.* **Vol.12** :205-12

51. MS Gold and DM Zeigler (1973) Dimethylaniline *N*-oxidation and aminopyrene *N*-dimethylone activities of human liver tissue. *Xenobiotica.* **Vol 3**: 179-189

52. WXA Guo and DM Ziegler (1991) Estimation of flavin-containing monooxygenase activities in crude tissue preparation by thiourea-dependent oxidation of thiocholine. *Anal. Biochem.* **Vol. 198**: 143-148

53. LL Poulsen, RM Hyslop and DM Ziegler (1979) *S*-oxygenation of *N*-substituted thioureas catalysed by the pig liver microsomal FAD containing monooxygenase. *Arch. Biochem. Biophys* **Vol. 198**: 78-88

54. N Lomri, Z Yang and JR Cashman (1993) Expression in Eschericha coli of the flavin-containing monooxygenase D (form II) from adult human liver: Determination of a distinct tertiary amine substrate specificity. *Chem. Res. Toxicol.* **Vol. 6**: 425-429

55. RN Hines, JR Cashman, RM Philpot, DE Williams and DM Ziegler (1994) The mammalian flavin-containing monooxygenases: molecular characterisation and regulation of expression. *Toxicology and Appl. Pharmacol.* **Vol. 125**: 1-6

56. Y Ohmiya and HM Mehendale (1981) Pulmonary metabolism of imipramine in the rat and rabbit. Comparison with hepatic metabolism. *Pharmacology* **Vol. 22**: 172-182

57. RE Tynes, RM Philpot (1987) Tissue and species dependent expression of multiple forms of mammalian microsomal flavin-containing monooxygenase. *Mol. Pharmacol.* **Vol. 31**: 569-574

58. VL Burnett, MP Lawton and RM Philpot (1994) Cloning and sequencing of flavin-containing monooxygenases FMO3 and FMO4 from rabbit and characterisation of FMO3. *J. Biol. Chem.* **Vol. 269**: 14314-14322

59. LL Poulsen, K Taylor, DE Williams, BSS Masters and DM Ziegler (1986) Substrate specificity of the rabbit lung flavin-containing monooxygenase for amines: oxidation products of primary alkylamines. *Mol. Pharmacol.* **Vol. 30**: 680-685

60. J Ozols (1989) Liver microsomes contain 2 distinct NADPH-monooxygenases with NH_2 terminal segments homologous to the flavin-containing NADPH monooxygenase of *Pseudomonas fluorescenc. Arch. Biochem. Biophys.* **Vol. 163**: 49-55

61. W-X A Guo, LL Poulsen and DM Zeigler (1992) Use of thiocarbamides as selective substrate probes for isoforms of flavin-containing monooxygenases. *Biochem. Pharmacol.* **Vol. 44**: 2029-2037

62. KL Taylor, DM Ziegler (1987) Studies on substrate-specificity of the hog liver flavin-containing monooxygenase. Anionic organic sulfur compounds. *Biochem. Pharmacol.* **Vol. 36**: 141-146

63. Y Ohmiya, HM Mehendale (1983) *N*-oxidation of *N,N,*-dimethylaniline in the rabbit and rat lung. *Biochem. Pharmacol.* **Vol. 32**: 1281-1285

64. MV Lee, S Smiley, S Kadkhodayan, RN Hines, DE Williams (1995) Developmental regulation of flavin-containing monooxygenase (FMO) isoforms 1 and 2 in pregnant rabbit. *Chem. Biol. Interact.* **Vol. 96**: 75-85

65. GA Dannan, FP Guengerich (1982) Immunochemical comparison and quantitation of microsomal flavin-containing monooxygenase in various hog, mouse, rat, rabbit, dog and human tissues. *Mol. Pharmacol.* **Vol. 22**: 787-794

66. A Lemoine, DE Williams, T Cresteil, JP Leroux (1991) Hormanal regulation of microsomal flavin-containing monooxygenase: tissue-dependent expression and substrate specificity. *Mol. Pharmacol.* **Vol. 40**: 211-217

67. SL. Ripp, K Itagaki, RM. Philpot, and AA. Elfarra (1999) Species and Sex differences in Expression of Flavin-Containing Monooxygenase Form 3 in Liver and Kidney Microsomes. *Drug Metab. Disp.* **Vol. 27**: 46-52

68. BSS Masters and DM Ziegler (1984) The distinctive nature and function of NADPH-dependent mixed function amide oxidase by *N*-1(1-methylcyclopropyl)-benzylamine. *Biochemistry* **Vol. 23**: 1322-1338

69. JG Falls, BL Blake, Y Cao, PE Levi and E Hodgsen (1995) Gender differences in hepatic expression of flavin-containing monooxygenase isoforms (FMO1, FMO3 and FMO5) in mice. *J. Biochem. Toxicol.* **Vol. 10**: 171-177

70. MV Lee, JE Clark and DE Williams (1993) Induction of flavin-containing monooxygenase (FMOB) in rabbit lung and kidney by sex steroids and glucocorticoids. *Arch. Biochem. Biophys.* **Vol. 302**: 332-336

71. S Coecke, G Debast, IR Phillips, A Vercruysse, EA Shephard and V Rogiers (1998) Hormonal regulation of microsomal flavin-containing monooxygenase activity by sex steroids and growth hormone in co-cultured adult male rat hepatocytes. *Biochem. Pharmacol.* **Vol. 56**: 1047-1051

72. JI Brodfuehrer, VG Zannoni (1986) Ascorbic acid deficiency and the flavin-containing monooxygenases. *Biochem. Pharmacol.* **Vol. 35**: 637-644

73. JI Brodfuehrer and VG Zannoni (1987) Flavin-containing monooxygenase and ascorbic acid deficiency. Qualitative and quantitative difference. *Biochem. Pharmacol* **Vol. 36**: 3161-3167

74. PJ Wirth and SS Thorgeirsson (1978) Amine oxidase in mice: sex differences and developmental aspects. *Biochem. Pharmacol.* **Vol. 27**: 601-603

75. MW Duffel, JM Graham and DM Ziegler (1981) Changes in dimethylaniline N-oxidase activity of mouse liver and kidney induced by steroid sex hormones. *Mol. Pharmacol.* **Vol. 19**: 134-139

76. TR Devereux and JR Fouts (1975) Effects of pregnancy or treatment with certain steroids on *N,N*-dimethylaniline demethylation and *N*-oxidation by rabbit liver or lung microsomes. *Drug Metab. Dispos.* **Vol. 3**: 254-258

77. DE Williams, SE Hale, AS Muerhoff and BSS Masters (1985) Rabbit lung flavin-containing monooxygenase: purification, characterisation and induction during pregnancy. *Mol. Pharmacol.* **Vol. 28**: 381-390

78. JG Falls, DY Ryu, Y Cau, PE Levi and E Hodgson (1997) Regulation of mouse liver flavin-containing monooxygenases 1 and 3 by sex steroids. *Arch. Biochem. Biophys.* **Vol. 342**: 212-223

79. TG Osimitz and AP Kulkarni (1982) Oxidative metabolism of xenobiotics during pregnancy: significance of microsomal flavin-containing monooxygenase. *Biochem. Biophys. Res. Commun.* **Vol. 109**: 1164-1171

80. P Skett (1987) Hormonal regulation and sex differences of xenobiotic metabolism. *Prog. Drug Metab.* **Vol. 10**: 85-140

81. RK Kaderlik, E Weser and DM Ziegler (1991) Selective loss of liver flavin-containing monooxygenase in rats on chemically defined diets. *Prog. Pharmacol. Clin. Pharmacol.* **Vol. 8**: 95-103

82. S Larsen-Su and DE Williams (1996) Dietary indole-3-carbinol inhibits FMO activity and the expression of flavin-containing monooxygenase form 1 in rat liver and intestine. *Drug Metab. Dispos* **Vol. 24**: 927-931

83. DE Williams, DM Ziegler, DJ Nordin, SE Hale and BSS Masters (1984) Rabbit lung flavin-containing monooxygenase is immunochemically and catalytically distinct from the liver enzyme. *Biochem. Biophys. Res. Commun.* **Vol. 125**: 116-122

84. RE Tynes and RM Philpot (1987) Tissue and species dependent expression of multiple forms of mammalian flavin-containing monooxygenase. *Mol. Pharmacol.* **Vol. 31**: 569-574

85. Y Ohmiya and HM Mehendale (1982) Metabnolism of chlorpromazine by pulmonary microsomal enzymes in the rat and rabbit. *Biochem. Pharmacol.* **Vol. 31**: 157-162

86. Y Ohmiya and HM Mehendale (1984) Species differences in pulmonary *N*-oxidation of chlorpromazine and imipramine. *Pharmacology* **Vol. 28**: 289-295

87. TR Devereux, RM Philpot and JR Fouts (1977) The effects of Hg^{2+} on rabbit hepatic and pulmonary solubilized, partially purified *N,N*-dimethylaniline *N*-oxidases. *Chem. Biol. Interact.* **Vol. 19**: 277-297

88. Y Ohmiya and HM Mehendale (1981) Pulmonary metabolism of imipramine in the rat and rabbit. Comparison with hepatic metabolism. *Pharmacology* **Vol. 22**: 172-182

89. RE Tynes, PJ Sabourin, E Hodgson and RM Philpot (1986) Formation of hydrogen peroxide and *N*, hydroxylated amines catalysed by pulmonary flavin-containing monooxygenases in the presence of primary alkylamines. *Arch. Biochem. Biophys.* **Vol. 251**: 654-664

90. E Hodgson and PE Levi (1988) Species, organ and cellular variation in the flavin-containing monooxygenases. *Drug Metab. Drug Interact.* **Vol. 6**: 219-233

91. E Atta-Asafo-Adjei, MP Lawton, RM Philpot (1991) Cloning aand sequences of a cDNA encoding a third flavin-containing monooxygenase in rabbits. FASEB *J*: **5**, (A 843).

92. DM Ziegler (1980) Microsomal flavin-containing monooxygenase :oxygenation of nucleophilic Nitrogen and Sulfur compounds . In *Enzymatic Basis of Detoxification* (ed) WB Jakoby pp201-277 Academic Press. New York.

93. DM Zeigler, LL Poulsen (1978) Hepatic microsomal mixed function amine oxidase. *Methods in Enzymology.* **Vol. 52**:142-151

94. J Ozols (1990) Covalent structure of liver microsomal flavin-containing monooxygenase form 1. *J. Biol. Chem.* **Vol. 265**:10289-10299

95. TR Deveroux and JR Fouts (1974) *N*-oxidation and demethylation of *N,N*-dimethylaniline by rabbit liver and lung microsomes.Effects of age and metabolism. *Chem. Biol. Interact.* **Vol. 8**: 91-105

96. MK Wyatt, RM Philpot, G Carver, MP Lawton and KN Nikbakht (1996) Sturctural characteristics of the flavin-containing monooxygenase genes one and two (*FMO1* and *FMO2*). *Drug Metab. Dispos.* **Vol. 24**: 1320-1327

97. A Kubo, S Itoh, K Itoh and T Kamataki (1997) Determination of FAD-binding domains in flavin-containing monooxygenase 1 (FMO1). *Arch. Biochem. Biophys.* **Vol. 345**: 271-277

98. AE Rettie, BD Bogucki, I Lim and GP Meier (1990) Sterioselective sulfoxidation of a series of alkyl *p*-tolyl sulfides by microsomal and purified flavin-containing monooxygenases. *Mol. Pharmacol.* **Vol. 37**: 643-651

99. CT Dolphin, DJ Beckett, A Janmohamed, TE Cullingford, RL Smith, EA Shephard and IR Phillips (1998) The Flavin-containing Monooxygenase 2 Gene (FMO2) of Humans, but Not of Other Primates, Encodes a Truncated, Nonfunctional Protein. *J Biol Chem.* **Vol. 273:** p30599-30607

100. M Yueh, SK Krueger and DE Williams (1997) Pulmonary flavin-containing monooxygenase (FMO) in rhesus macaque: expression of FMO2 protein, mRNA and analysis of the cDNA. *Biochem Biophys Acta.* **Vol. 1350**: 267-271

101. S Larsen-Su, SK Krueger, MF Yueh, MY Lee, SE Shehin, RN Hines and DE Williams (1999) Flavin-containing monooxygenase isoform 2: developmental expression in fetal and neonatal rabbit lung. *J Biochem Mol Toxicol* **Vol. 13**: 187-93

102. J Ozols (1991) Multiple forms of liver microsomal flavin-containing monooxygenase: complete covalent structure of form 2. *Arch. Biochem. Biophys.* **Vol. 290**: 103-115

103. RL Haining, AP Hunter, AJM Sadeque, RM Philpot and AE Rettie (1997) Baculovirus-mediated expression and purification of human FMO3. Catalytic, immunochemical and structural characterisation. *Drug Metab. Dispos.* **Vol. 25**: 790-797

104. A Brunelle, Yi-AN BI, J Lin, B Russel, L Luy, C Berkish and J Cashman (1997). Escherichia *Coli* as maltose binding protein fusions. *Drug Metab. Dispos.* **Vol. 25**: 1001-1007

105. JG Falls, NJ Cherrington, KM Clements, RM Philpot, PE Levi, RL Rose and E Hodgson (1997) Molecular cloning, sequencing and expression in *E.coli* of mouse flavin-containing monooxygenase 3 (FMO3): Comparison with the human isoforms. *Arch. Biochem.Biophys.* **Vol. 347**: 9-18

106. LH Overby, GC Carver and RM Philpot (1997) Quantitation and kinetic properties of hepatic microsomal and recombinant flavin-containing monooxygenases 3 and 5 from humans. *Chemico. Biol. Interact.* **Vol. 106**: 29-45

107. CT Dolphin, EA Shephard, S Povey, RL Smith and IR Phillips (1992) Cloning, primary sequence and chromosomal localisation of FMO2, a new member of the flavin-containing monooxygenase family. *Biochem. J.* **Vol. 287**: 261-267

108. V Burnett, MP Lawton and RM Philpot (1992) Cloning and sequencing of rabbit flavin-containing monooxygenases 1D1 and 1E1. *FASEB J.* **6** (A5258)

109. RL Haining, AP Hunter, AJM Sadeque, RM Philpot and AE Rettie (1997) Baculovirus-mediated expression and purification of human FMO3, catalytic, immunochemical and structural characterisation. *Drug Metab. Dispos.* **Vol. 25**: 790-797

110. Z Luo and RN Hines (1996) Identification of multiple rabbit flavin-containing monooxygenase form 1 (FMO1) gene promoters and observation of tissue specific DNase 1 hypersensitive sites. *Arch. Biochem .Biophys.* **Vol. 336**: 251-260

111. K Itagaki, G Carver and RM Philpot (1996) Expression and characterisation of a modified flavin-containing monooxygenase 4 (FMO4) from humans. *J. Biol. Chem.* **Vol. 271**: 20102-20107

112. EAA Adjei, MP Lawton and RM Philpot (1993) Cloning, sequencing, distribution and expression in *Escherichia Coli* of flavin-containing monooxygenase 1C1. Evidence for a third gene subfamily in rabbits. *J. Biochem.* **Vol. 268**: 9687-9689

113. LH Overby, GC Carver and RM Philpot (1997) Quantitation and kinetic properties of hepatic microsomal and recombinant flavin-containing monooxygenases 3 and 5 from humans. *Chem. Biol. Interact.* **Vol. 106**: 29-45

114. N Lomri, Z Yang and JR Cashman (1993) Regio- and sterio- selective oxygenations by adult human liver flavin-containing monooxygenase 3. Comparison with forms 1 and 2. *Chem. Res. Toxicol.* **Vol. 6**: 800-807

115. AJM Sadeque, KE Thummel and AE Rettie (1993) Purification of macaque liver flavin-containing monooxygenase: A form of the enzyme related immunochemically to an isozyme expressed selectively in adult human liver. *Biochem. Biophys. Acta.* **Vol. 1162**: 127-134

116. N Lomri, Q Gu and JR Cashman (1992) Molecular cloning of the flavin-containing monooxygenase (form II) cDNA from adult human liver. *Proc. Natl. Acad. Sci. USA* **Vol. 89**: 1685-1689

117. LH Overby, AR Buckpitt, MP Lawton, AAE Atta, J Schulze and RM Philpot (1995) Charcaterisation of flavin-containing monooxygenase 5 (FMO5) cloned from human and guinea pig: evidence that the unique catalytic properties of FMO5 are not confined to the rabbit ortholog. *Arch. Biochem. Biophys.* **Vol. 317**: 275-284

118. IR Phillips, CT Dolphin, P Clair, MR Hadley, AJ Hutt, RR M^{c}Combie, RL Smith and EA Shephard (1995) The molecular biology of the flavin-containing monooxygenases of man. *Chemico. Biol. Inter.* **Vol. 96**: 17- 32

119. The Sanger Centre Data Base (1999) . Evidence of a sixth form of FMO (FMO6) in genomic sequence www.sanger.ac.uk/

120. EA Shephard, CT Dolphin, S Povey, R Smith and IR Phillips (1991) The genes encoding the flavin-containing monooxygenases FMO1 and FMO2 are located on human chromosome 1q. *Cytogenet. Cell Genet.* **Vol. 58**: 1863-1869

121. EA Shephard, CT Dolphin, MF Fox, S Povey, R Smith and IR Phillips (1993) Localisation of genes encoding three distinct flavin-containing monooxygenases to human chromosome 1q. *Genomics* **Vol. 16**: 85-89

122. RR McCombie, CT Dolphin, S Povey, IR Phillips and EA Shephard (1996) Localization of human flavin-containing monooxygenase genes FMO2 and FMO5 to chromosome 1q. *Genomics* **Vol. 34**: 426-429

122a. K Itoh, T Kimura, T Yokoi, S Itoh and T Kamataki (1993) Rat liver flavin-containing monooxygenase (FMO): cDNA cloning and expression in yeast. *Biochem Biophys Acta.* **Vol. 1173**: 165-171

123. M P Lawton, J R Cashman, T Cresteil, C T Dolphin, A A Elfarra, R N Hines, E Hodgson, T Kimuva, J Ozols, I R Phillips, R M Philpot, L L Poulson, A E Rettie, E A Shephard, D E Williams and D M Ziegler (1994) A nomenclature for mammalian flavin-containing monooxygenase gene family based on amino acid sequence identity. *Archives of Biochem. and Biophysics* **Vol. 308**: 254-257

124. NJ Cherrington, Y Cao, JW Cherrington, RL Rose and E Hodgson (1998) Physiological factors affecting protein expression of flavin-containing monooxygenases 1, 3 and 5. *Xenobiotica* **Vol. 7**:673-82

125. AJM Sadeque, AC Eddy, GP Meier and AE Rettie (1992) Stereoselective sulfoxidation by human flavin-containing monooxygenase: catalytic diversity between hepatic, fetal and renal forms. *Drug Metab. Dispos.* **Vol. 20**: 832-839

126. MP Lawton and RM Philpot (1993). Molecular genetics of the flavin-dependent monooxygenases. *Pharmacogentics* **Vol. 3**: p40-44

127. CT Dolphin, TE Cullingford, EA Shephard, RL Smith and IR Phillips (1996) Differential development and tissue specific regulation of expression of the genes encoding three members of the flavin-containing monooxygenase family of man, FMO1, FMO3 and FMO4. *Eur. J. Biochem.* **Vol. 235**: 683-689

128. ML Das and DM Ziegler (1970) Rat liver oxidative *N*-dealkylase and *N*-oxidase activities as a function of animal age. *Archives. Biochem. and Biophysics* **Vol. 140**: 300-306

129. CT Dolphin, EA Shephard, S Povey, CN Palmer, DM Ziegler, R Ayesh, RL Smith and IR Phillips (1991) Cloning, primary sequence and chromosomal mapping of a human flavin-containing monooxygenase (FMO1). *J. Biol. Chem.* **Vol. 266**: 12379-12385

130. A Janmohamed (1998) The characterisation of the flavin-containing monooxygenase family of man. PhD Thesis .University of London UCL.

131. M Al-Waiz, SC Mitchell, JR Idle and RL Smith (1987) The metabolism of ^{14}C-labelled trimethylamine and its *N*-oxide in man. *Xenobiotica* **Vol. 17**: 551-558

132. AQ Zhang, SC Mitchell and RL Smith (1996) Discontinuous distribution of *N*-oxidation of dietary-derived trimethylamine in a British population. *Xenobiotica* **Vol. 26**: 957-961

133. CT Dolphin, JH Riley, RL Smith, EA Shephard and IR Phillips (1997) Structural organisation of the human flavin-containing monooxygenase 3 gene (*FMO3*), the favoured candidate for fish odour syndrome, determined directly from genomic DNA. *Genomics*. **Vol. 46**: 260-267

134. M Al-Waiz, R Ayesh, SC Mitchell, JR Idle and RL Smith (1987) Trimethylaminuria (fish odour syndrome): and inborn error of oxidative metabolism. *The Lancet* **1**: 634-635

135. M Al-Waiz, M Ayesh, R Mitchell, SC Idle and RL Smith (1989) Trimethylaminuria: the detection of carriers using a trimethylamine load test. *J. Inherit. Metab. Dispos.* **Vol. 12**: 80-85

136. JA Humbert, KB Hammond and WE Hathaway (1970) Trimethylaminuria: the fish odour syndrome. *The Lancet* **2**: 770-771

137. M Al-Waiz, M Ayesh, R Mitchell, SC Idle and RL Smith (1987) A genetic polymorphism of the *N*-oxidation of trimethyamine in humans. *Clin. Pharmacol. Ther*. **Vol. 42**: 588-594

138. R Ayesh, SC Mitchell, A Zhang and RL Smith (1993) The fish odour syndrome: biochemical, familial and clinical aspects. *BMJ*. **Vol. 307**: 655-657

139. CT Dolphin, A Janmohamed, RL Smith, EA Shephard and IR Phillips (1997) Missense mutation in flavin-containing monooxygenase 3 gene (*FMO3*), underlies fish odour syndrome. *Nat. Genet*. **Vol. 17**: 491-494

140. EP Treacy, BR Akerman, LML Chow, R Youil, C Bibeau, J Lin, AG Bruce, M Knight, DM Danks, JR Cashman and SM Forrest (1998) Mutations of the flavin-containing monooxygenase gene (FMO3) cause trimethylaminuria, a defect in detoxication. *Hum Mol Genet* **Vol. 7**: 839-45

141. DH Lang, CK Yeung, RM Peter, C Ibarra, R Gasser, K Itagaki, RM Philpot and AE Rettie (1998) Isoform specificity of trimethylamine *N*-oxygenation by human flavin-containing monooxygenase (FMO) and P450 enzymes: selective catalysis by FMO3. *Biochem Pharmacol* **Vol. 56**: 1005-12

142. C Mani and D Kupfer (1991) Cytochrome P-450-mediated activation and irreversible binding of the antiestrogen tamoxifen to proteins in rat and human liver: possible involvement of flavin-containing monooxygenases in tamoxifen activation. *Cancer Res*. **Vol. 51**: 6052-6058

143. PC Ruenitz and X Bai (1995) Acidic metabolites of tamoxifen. Aspects of formation and fate in the female rat. *Drug Metab Dispos*. **Vol. 23**: 993-998

144. C Mani, E Hodgson and D Kupfer (1993) Metabolism of the antimammary cancer antiestrogenic agent tamoxifen. II. Flavin-containing monooxygenase-mediated *N*-oxidation. *Drug Metab Dispos*. **Vol. 21**: 657-661

145. MA England and J Wakely (1991) Brain and Spinal Cord. An introduction to normal neuroanatomy. Wolfe Publishing Ltd.. London England.

146. PL M^{c}Geer, JC Eccles and EG M^{c}Geer (1987) Molecular Neurobiology of the mammalian brain (2nd edn.) Plenum Press (NY).

147. AM Graybiel (1990) Neurotransmitters and neuromodulators in the basal ganglia. *Trends Neurosci.* **Vol. 13**: 44-254

148. AR Crossman (1987) Primate models of dyskinesia: the experimental approach to the study of basal ganglia related involuntary movement disorders. *Neuroscience* **Vol. 21**: 1-40

149. RL Albin, AB Young and JB Penny (1989) The functional anatomy of basal ganglia disorders. *Trends Neurosci.* **Vol. 12**: 366-375

150. DJ Selkoe (1991) The molecular pathology of Alzheimers disease. *Neuron.* **Vol. 6**: 487-498

151. CD Marsden (1990) Parkinson's Disease. *Lancet.* **Vol. 335**: 948-952

152. IJ Mitchell, AJ Cross, MA Sambrook and AR Crossman (1985) Sites of the neurotoxic action of 1-methyl-4-phenyl-1,2,3,6-tetrahydropyridine in the macaque monkey include the ventral tegmental area and the locus coeruleus. *Neurosci. Lett.* **Vol. 61**: 195-200

153. MR DeLang (1990) Primate models of movement disorders of basal ganglia origin. *Trends Neurosci.* **Vol. 13**: 281-185

154. GE Alexander MR DeLong and PL Strick (1986) Parallel organisation of functionally segregated circuits linking basal ganglia and cortex. *Annual Rev. Neurosci.* **Vol. 9**: 357-381

155. I J Kopin (1993). The pharmacology of Parkinsons disease therapy: An update. *Ann. Rev. Pharmacol. Toxicol.* **Vol. 32**: p467-495

156. HE Lowndes, CM Beiswanger, MA Philbert and KR Reuhl (1994) Substrates for neural metabolism of xenobiotics in adult and developing brain. *Neurotoxicology.* **Vol. 15**: 61-74

157. MW Duffel, SG Gillespie (1984) Microsomal flavin-containing monooxygenase activity in rat corpus striatum. *J Neurochem.* **Vol. 42**: 1350-1353

158. A Kawaji, T Miki and E Takabatake (1995) Partial purification and substrate specificity of flavin-containg monooxygenase from rat brain microsomes. *Biol. Pharm. Bull.* **Vol. 18**: 1657-1659

159. S Bhamre and V Ravindranath (1991) Presence of flavin-containing monooxygenase in rat brain. *Biochem. Pharmacol.* **Vol. 42**: 442-444

160. S Bhamre, SV Bhagwat, SK Shankar and V Ravindranath (1993) Cerebral flavin-containing monooxygenase mediated metabolism of antidepressants in brain : Immunochemical properties and Immunocytochemical localisation J. *Pharm. Exp. Ther.* **Vol. 267**: 555-559

161. C Kohler, LG Eriksson, T Hansson, M Warner and J Ake-Gustafsson (1988) Immunohistochemical localisation of cytochrome P450 in the rat brain. *Neuroscience Letters* **Vol. 84**: 109-114

162. V Ravindranath (1995) Xenobiotic metabolism in brain. *Toxicol. Letts.* **Vol. 82/83**: 633-638

163. S Bhamre, SV Bhagwat, SK Shankar, MR Boyd and V Ravindranath (1995) Flavin-containing monooxygenase mediated metabolism of psychoactive drugs by human brain microsomes. *Brain Res.* **Vol. 672**: 276-280

164. A Kawaji, K Ohara and E Takabatake (1994) Determination of flavin-containing monooxygenase activity in rat brain microsomes with benzydamine *N*-oxidation. *Biol. Pharm. Bull.* **Vol. 17**: 603-606

165. V Ravindranath, HK Anandatheerthavarada and SK Shankar (1989) Xenobiotic metabolism in human brain: presence of cytochrome P450 and associated monooxygenases. *Brain Res.* **Vol. 496**: 331-335

166. SV Bhagwat, S Bhamre, MR Boyd and V Ravindranath (1996) Cerebral metabolism of imipramine and a purified flavin-containing monooxygenase from human brain. *Neuropsychopharmacology.* **Vol. 15**: 133-142

167. SV Bhagwat, BC Leelavathi, SK Shankar, MR Boyd and V Ravindranath (1995) Cytochrome P450 and associated monooxygenase activities in the rat and human spinal cord: induction, immunological characterisation and immunocytochemical localisation. *Neuroscience.* **Vol.68**: 593-601

168. BL Blake, RM Philpot, PE Levi and E Hodgson (1996) Xenobiotic biotransforming enzymes in the central nervous system: an isoform of flavin-containing monooxygenase (FMO4) is expressed in rabbit brain. *Chemico. Biol. Interact.* **Vol. 99**: 253-261

169. JR Cashman and DM Zeigler (1986) Contribution of *N*-oxygenation to the metabolism of MPTP (1-methyl-4-phenyl-1,2,3,6-tetrahydropyridine) by various liver preparations. *Molecular Pharmacol.* **Vol. 29**: 163-167

170. K Chiba, LA Peterson, KP Castagnoli, AJ Trevor and A Castagnoli Jr. (1985) Studies on the molecular mechanism of biotransformation of the selective nigostriatal toxin 1-methyl-4-phenyl-1,2,3,6-tetrahydropyridine. *Drug Metab. Dispos.* **Vol. 13**: 342-347

171. JW Langston, P Ballard, JW Tetrudand I Irwin (1983) Chronic parkinsonism in humans due to a product of meperidine-analog synthesis. *Science* **Vol. 219**: 979-980

172. RS Burns, CC Chiueh, SP Markey, MH Ebert, DM Jacobowitz and IJ Kopin (1983) A primate model of parkinsonism: selective destruction of dopaminergic

neurons in the pars compacta of the substantia nigra by *N*-methyl-4-phenyl-1,2,3,6-tetrahydropyridine. *Proc. Natl. Acad. Sci. USA.* **Vol. 80**: 4546-4550

173. JW Langston, LS Forno, CS Rebert and I Irwin (1985) Selective nigral toxicity after systematic administration of 1-methyl-4-phenyl-1,2,3,6-tetrahydropyridine (MPTP) in the squirrel monkey. *Brain Res.* **Vol. 292**: 390-394

174. JS Fowler, ND Volkow, GJ Wang, N Pappas, J Logan, R MacGregor, D Alexoff, C Shea, D Schlyer, AP Wolf, D Warner, I Zezulkova and R Cilento (1996) Inhibition of monoamine oxidase B in the brains of smokers. *Nature* **Vol. 379**: 733-737

175. I Irwin (1986) The neurotoxin1-methyl-4-phenyl-1,2,3,6-tetrahydropyridine (MPTP), a key to Parkinsons disease ? *Pharm. Res.* **Vol. 3**: p7-11

176. J W Langston and I Irwin (1993) Pyridine toxins, *in* Drugs for the treatment of Parkinsons disease. Handbook of Experimental Pharmacology **Vol. 88** Edited by D B Calne, pp205-226. Springer-Verlag

177. IJ Kopin (1992). Mechinisms of 1-methyl-4-phenyl-1,2,3,6-tetrahydropyridine induced destruction of dopaminergic neurons, *in* Selective Neurotoxicity Edited by H Herken and F Hucho, pp333-356. Springer-Verlag

178. K Chiba, H Horii, E Kubota, T Ishizaki and Y Kato (1990) Effects of *N*-methylmercaptoimidazole on the disposition of MPTP and its metabolities in mice. *Euro. J Pharmacol.* **Vol. 180**: 59-67

179. K Chiba, E Kubota, T Miyakawa, Y Kato and T Ishizaki (1998) Characterization of hepatic microsomal metabolism as an in vivo detoxication pathway of 1-methyl-4-phenyl-1,2,3,6-tetrahydropyridine in mice. *J Pharmacol Exp Ther* **Vol. 246**: 1108-15

180. J Hoe, DG Kim, Hye Ryun Bahng and Jin-SOO Kim (1995) Dimethylthiourea prevents MPTP-induced decreas in [^{3}H] dopamine uptake in rat striatal slices. *Brain Res.* **Vol. 671**: p321-324

181. RE Hekkila, L Manzino, FS Cabbat and RS Duvoisin (1984) Protection against the dopaminergic neurotoxicity of 1-methyl-4-phenyl-1,2,3,6-tetrahydropyridine (MPTP) by monoamine oxidaseinhibitors. *Nature* **Vol. 311**: 467-469

182. KF Tipton and TP Singer (1993) Advances in our understanding of the mechanisms of the neurotoxicity of MPTP and related compounds. *J Neurochem.* **Vol. 61**: 1191-1206

183. DA Di-Monte, EY Wu, I Irwin, LE Delanney and JW Langston (1991) Biotransformation of 1-methyl-4-phenyl-1,2,3,6-tetrahydropyridine (MPTP) in primary culturres of mouse astrocytes. *J Pharmacol. Exp. Ther.* **Vol. 258**: 594-510

184. JW Tetrud and JW Langston (1989) The effect of deprenyl on the natural history of Parkinson's disease. *Science* **Vol. 245**: 519-522

185. W Birkmayer, P Riederer, L Ambrozi and MBH Youdim (1977) Implications of combined treatment with "Mardopar" and L-deprenyl in Parkinson's disease. A long term therapy. *Lancet i*, : 439-443

186. RM Wu, DL Murphy and CC Chiueh (1994) Protection of nigral neurons against MPP+-induced oxidative injury by deprenyl (selegilene), U-78517F, and DMSO. *Trends Clin. Neuropharmacol.* **Vol. 8**: 187-188

187. RM Wu, CC Chiueh, A Pert and DL Murphy (1993) Apparent antioxidant effect of L-deprenyl on hydroxyl radical formation and nigral injury elicited by MPP+ in vivo. *Euro. J. Pharmacol.* **Vol. 243**: 241-247

188. NA Simonian and JT Coyle (1996) Oxidative stress in neurodegenerative diseases. *Annu. Rev. Pharmacol. Toxicol.* **Vol.36**: 83-106

189. AHV Schapira, J Cooper, D Dexter, P Jenner and JB Clark (1989) Mitochondrial complex I deficiency in Parkinson's disease. *J. Neurochem.* **Vol. 54**: 823-827

190. JZ Fields, RR Albores, EJ Neafsey and MA Collins (1998) Inhibition of mitochondrial succinate oxidation. Similarities and differences between *N*-methylated β-carbolines and MPP. *Arch.Biochem.Biophys.* **Vol. 249**: 539-543

191. T Nagatsu and M Yoshida (1988) An endogenous substance of the brain, tetrahydroisoquinoline, produces parkinsonism in primates with decreased dopamine, tyrosine hydroxylase and biopterin in the nigostriatal regions. *Neurosci. Lett.* **Vol. 87**: 178-182

192. T Niwa, N Takeda, H Yoshizumi, A Tatematsu, M Yoshida, P Dostert, M Naoi and T Nagatsu (1991) Presence of 2-methyl-6,7-dihydroxy-1,2,3,4- tetrahydroisoquinoline and 1,2-dimethyl-6,7-dihydroxy-1,2,3,4-tetrahydroisoquinoline, novel endogenous amines, in parkinsonian and normal human brains. *Biochem. Biophys. Res. Commun.* **Vol. 177**: 603-609

193. Y Kotake, M Yoshida, M Ogawa, Y Tasaki, M Hirobe and S Ohta (1996) Chronic administration of 1-benzyl-1,2,3,4-tetrahydroisoquinoline, an endogenous amine in the brain, induces parkinsonism in a primate. *Neurosci Lett* **Vol. 217**: 69-71

194. T Yamakawa and S Ohta (1999) Biosynthesis of a parkinsonism-preventing substance, 1-methyl-1,2,3,4 tetrahydroisoquinoline, is inhibited by parkinsonism-inducing compounds in rat brain mitochondrial fraction. *Neurosci Lett* **Vol. 259**:157-160

195. Y Kotake, Y Tasaki, M Hirobe and S Ohta (1998) Deprenyl decreases an endogenous parkinsonism-inducing compound, 1-benzyl-1,2,3,4-tetrahydroisoquinoline in mice: in vivo and in vitro studies. *Brain Res* **Vol. 787**: 341-343

196. K Itoh, K Nakamura, T Kimura, S Itoh and T Kamataki (1997) Molecular cloning of mouse liver flavin containing monooxygenase (FMO1) cDNA and characterization of the expression product: metabolism of the neurotoxin, 1,2,3,4-tetrahydroisoquinoline (TIQ). *J Toxicol Sci* **Vol. 22**: 45-56

197 JR. Cashman , Y N. Xiong, L Xu and A Janowsky (1999) *N*-Oxygenation of Amphetamine and Methamphetamine by the Human Flavin-Containing Monooxygenase (Form 3): Role in Bioactivation and Detoxication1 *J Pharmacol Exp Ther* **Vol. 288**: 1251-60

198. J Williamson (1984) Drug-induced Parkinsons disease. *BMJ* **Vol. 288**: 145-147

199. J Sambrook, RF Fritsch and R Maniatis Molecular Cloning: a laboratory manual. Cold Spring Harbor Laboratory, Cold Spring Harbor, New York (1989)

200. D Hanahan (1983) Studies on transformation of Escherichia coli with plasmids. *J Mol. Biol.* **Vol. 166**: 557-580

201. C Yannish-Perrom, J Viera and J Messing (1985) Improved M13 phage cloning vectors and host strains: nucleotide sequences of the M13mp18 and pUC19 vectors. *Gene* **Vol.33**: 103-119

202. T A Brown (Ed.) Essential Molecular Biology: A practical approach **Vol. 1**. Oxford University Press (1991)

203. JC Alwine, DJ Kemp and GR Stark (1977). Method for detection of specific RNAs in agarose gels by transfer to diazobenzyloxymethyl-paper and hybridisation with DNA probes. *Proc.Nat. Acad. Sci. USA*, **Vol. 74**: 5350-5354

204. A Lonstaff and P Revest (Ed.) Methods in molecular biology (13). Protocols in molecular neurobiology. Humana Press. Totowa, New Jersey (1992)

205. DG Wilkinson (Ed.) *In-situ* hybridisation. IRL Press at Oxford University Press (1993)

206. OH Lowry, NJ Rosenberg, AL Farr and RJ Randal (1951) Protein measurement with the Folin phenol reagent. *J Biol. Chem.* **Vol.193**: 265-275

207. H Towbin, T Staehelin and J Gordon (1979) Electrophoretic transfer of proteins from polyacrylamide gels to nitrocellulose sheets: procedure and some applications. *Proc.Nat.Acad. Sci. USA* **Vol. 76**: 4350-4354

208 . JM Graham and D Billington in Gel Electrophoresis: Proteins (1993) (Ed.) MJ Dunn. Bios scientific Publishers Ltd. Oxford U.K.

209. KB Mullis and F Faloona (1987) Specific synthesis of DNA in vitro via a polymerase-catalyzed chain reaction. Methods in Enzymology **Vol. 155** :335-350

210. HG Griffin and AM Griffin (Ed) PCR technology : current innovations (1994) CRC Press Inc. Boca Raton, Florida USA

211. RA Gibb, JS Chamberlain and CT Caskey in PCR technology: principles and applications for DNA amplification (1991). (Ed.) HA Erlich. WH Freeman and Company, New York , USA

212. EM Southern (1975) Detection of specific sequences among DNA fragments separated by gel electrophoresis. *J Mol.Biol.* **Vol. 98**: 503-517

Appendix 1.

List of Companies

Amersham Pharmacia Biotec Ltd.	Amersham Place Little Chalfont Buckinghamshire HP7 9NA
BDH Lab Supplies	Poole, Dorset, BH15 1TD U.K
BIO 101 Inc.	P.O. Box 2284, La Jolla, CA 92038-2284 U.S.A.
Bioline UK Ltd.	
BioRad Laboratories	2000 Alfred Nobel Drive, Hercules, CA 94547 U.S.A.
Biotecx Laboratories Inc.	12 Thorney Leys Park, Witney, Oxon. OX8 7GE U.K.
Boehringer-Mannheim	Bell Lane, Lewes East Sussex, BN7 1LG U.K.
Calibiochem	10394 Pacific Centre Court, San Diego, CA 92121 U.S.A.
Clontech Laboratories Inc.	4030 Fabian Way, Palo Alto, CA 94303-4607 U.S.A.
Du Pont Company (Europe)	GmbH, NEN D-6072 Dreiech, West Germany 401240
Fisons	Bishop Meadow Road, Loughborough LE11 ORG U.K.
GibcoBRL Life Technologies Inc.	Paisley, Scotland U.K.
Invitrogen	De Schelp 12, 9351 NV Leek, The Netherlands
Kodak Company	IBI Ltd. 36 Clifton Road, Cmbridge CB1 4ZR U.K.
Merck Ltd.	Merck House, Poole, Dorset BH15 1TD U.K.
Millipore	The Boulevard, Blackmoor Lane, Watford WD1 8YW U.K.
Molec. Bio. Prods.	San Diego, CA 92121 U.S.A.
New England Biolabs (U.K.) Ltd.	Knowl Piece, Wilbury Way, Hitchin, Herts, SG4 0TY U.K.
Perkin Elmer	Kelvin Close, Birchwood Science Park, Cheshire WA3 7PB
Promega Corporation (U.K.)	Delta House, Enterprise Road, Southampton SO16 7NS
Qiagen Ltd.	Boundary Court, Gatwick Road, Crawley RH10 2AX U.K.
Sigma Chemicals	P.O. box 14508, St. Louis, MO 63178 U.S.A.
Stratagene Ltd.	Cambridge Science Park, Milton Road, Cambridge CB4 4GF
Vector Laboratories Inc.	16 Wulfric Square, Bretton, Peterborough PE3 8RF U.K.
Whatman International Ltd.	St Leonard's Road, 20/20 Maidstone Kent ME16 OLS
.	.